WAKE ISLAND PASSAGE FLUX EXPERIMENT DATA BOOK

WAKE ISLAND PASSAGE FLUX EXPERIMENT DATA BOOK

Hiroshi Uchida (JAMSTEC),
Hirofumi Yamamoto (JAMSTEC),
Kaoru Ichikawa (Kyushu Univ./JAMSTEC),
Masaki Kawabe (The Univ. of Tokyo),
Masao Fukasawa (JAMSTEC)

WAKE ISLAND PASSAGE FLUX EXPERIMENT DATA BOOK

31, March, 2009 Published
Hiroshi Uchida (JAMSTEC), Hirofumi Yamamoto (JAMSTEC),
Kaoru Ichikawa (Kyushu University/JAMSTEC), Masaki Kawabe (The University of Tokyo),
and Masao Fukasawa (JAMSTEC)

Published by © JAMSTEC, Yokosuka, Kanagawa, 2009
Japan Agency for Marine-Earth Science and Technology
2-15 Natsushima, Yokosuka, Kanagawa 237-0061, Japan
Phone +81-46-867-9474, Fax +81-46-867-9455

Printed by Aiwa Printing Co., Ltd.
3-22-4 Takanawa, Minato-ku, Tokyo 108-0074, Japan

Contents

Preface

The primary focus of Wake Island Passage Flux Experiment (WIFE) is the quantification of transport of Deep Western Boundary Current (DWBC) in the North Pacific. Transport of the DWBC for the South Pacific was quantified at two sites by moored current meter observations during the World Ocean Circulation Experiment (WOCE) in the 1990s. For the North Pacific, however, mooring observations in Wake Island Passage were proposed but did not occur in WOCE. Moreover, Wake Island Passage was an observational gap in the WOCE Hydrographic Programme (WHP). During WIFE from 2003 to 2005, mooring array observations and repeated hydrographic surveys were carried out along a line across a deep passage just south of Wake Island Passage. By conducting not only traditional current measurements but also density measurements by moored CTDs, horizontally and vertically integrated geostrophic transport could be evaluated throughout the deep passage. Our hope is that this dataset and transport estimates of the transport reference site will contribute to oceanographic and climate studies.

Hiroshi Uchida
Yokosuka, Kanagawa, Japan

Hirofumi Yamamoto
Yokosuka, Kanagawa, Japan

Kaoru Ichikawa
Kasuga, Fukuoka, Japan

Masaki Kawabe
Nakano-ku, Tokyo, Japan

Masao Fukasawa
Yokosuka, Kanagawa, Japan

Acknowledgments

The success of WIFE was dependent upon the cooperation of Captain Masaharu Akamine and the crew of the R/V Mirai cruises MR03-K02 and MR05-05 leg 2, Captain Syouichi Suzuki and the crew of the R/V Hakuho-maru cruise KH04-4 leg 2, and scientists, students and technicians who participated in the cruises. We are grateful to Drs. Ikuo Kaneko (Japan Meteorological Agency), Takeshi Kawano [Institute of Observational Research for Global Change (IORGC), Japan Agency for Marine-Earth Science and Technology (JAMSTEC)], and Yasushi Yoshikawa (Mutsu Institute for Oceanography, JAMSTEC) for putting in enormous support to carry on the project. KI acknowledges the support of Drs. Hiroshi Ichikawa (IORGC, JAMSTEC) and Hirohiko Nakamura (Kagoshima University) for the current meter observations.

1 Wake Island Passage Flux Experiment (WIFE)

1.1 Introduction

The abyssal waters of the Pacific Ocean are renewed by flow from the Southern Ocean; there is no abyssal source in the North Pacific Ocean. The northward abyssal flow plays an important role in the earth's climate as a part of meridional overturning circulation. The northward abyssal flow for the South Pacific was quantified at two sites by moored current meter observations during the World Ocean Circulation Experiment (WOCE) in the 1990s. East of the Tonga-Kermadec Ridge (at 30.5°S), the transport was evaluated as 15.8 ± 1.4 Sv (1 Sv = 10^6 m^3 s^{-1}) (Whitworth et al., 1999; Hogg, 2001). In the Samoa Passage and adjacent regions (10°S), the transport was evaluated as 10.6 ± 1.7 Sv (Roemmich et al., 1996). For the North Pacific, however, mooring observations of the northward abyssal flow in Wake Island Passage were proposed but did not occur in WOCE (Hogg, 2001).

Wake Island Passage (near 18°N, 169°E) connects the Central Pacific Basin with the Northwest Pacific Basin (Fig. 1.1.1). Through Wake Island Passage, the coldest, saltiest, most oxygen-rich and silicate-poor bottom water is supplied to area north of Wake Island Passage from its southern source. Transports of Wake Island Passage abyssal flow were estimated in two recent studies. One estimate is based on conductivity-temperature-depth (CTD) with oxygen observation in 1999 across Wake Island Passage (Kawabe et al., 2003). The other is based on 1-year (from 1999 to 2000) moored current meter observations in Wake Island Passage (Kawabe et al., 2005). Kawabe et al. (2005) provided the first estimates of 1-year mean volume transport (3.6 Sv ± 1.3 Sv). However, the mooring data did not quantify a transport in an additional western passage, which was estimated from a single observation to be about 1 Sv northward (Kawabe et al., 2003).

1.2 Objectives and Methods

To clarify water mass characteristics and to quantify accurately the temporal mean and variations of volume transport of the abyssal water into Wake Island Passage, the Wake Island Passage Flux Experiment (WIFE) was carried out from 2003 to 2005, which consisted of repeated shipboard hydrographic surveys and mooring array observations along a line across a deep passage just south of Wake Island Passage. Water mass characteristics of the abyssal water in the deep passage were investigated by using the WIFE shipboard hydrographic data in 2003, 2004, and 2005 to determine the extent and volume of the northward flowing abyssal water (Uchida et al., 2007b). Temporal mean and short-term variability of the volume transport were evaluated by means of geostrophic calculations from density measurements by moored CTDs. Velocity measurements by moored current meters were also used as reference velocities for the geostrophic calculation. The average transport for the 2.5-year mooring period from May 2003 to December 2005 was estimated to be 2.9 ± 0.8 Sv. (H. Uchida et al., manuscript in preparation, 2009).

The WIFE shipboard hydrographic observations and mooring array observations are described in detail in section 2 and section 3, respectively.

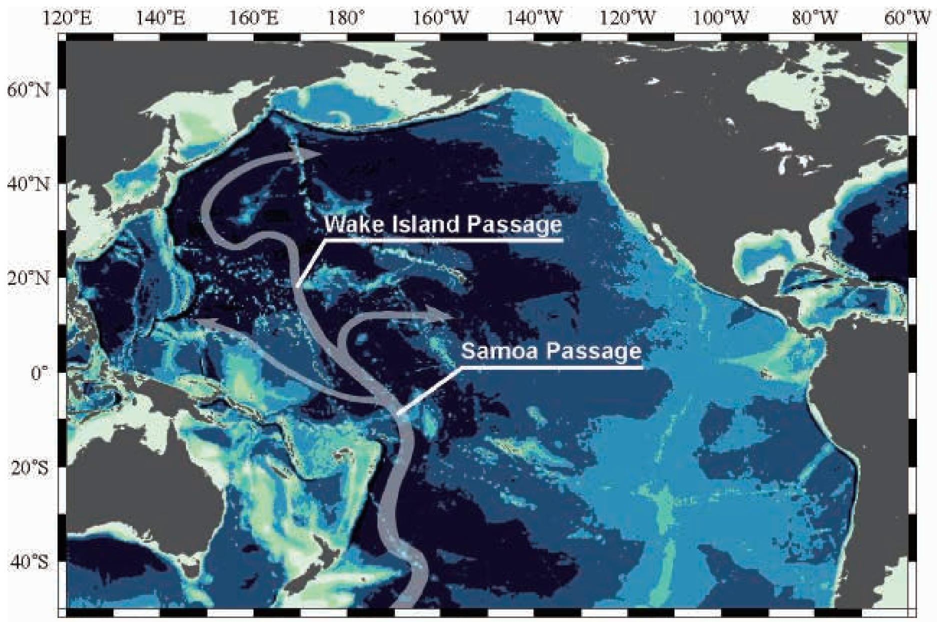

Figure 1.1.1. Schematic flow patterns of deep circulation superimposed over bottom topography. Location of the Samoa Passage and Wake Island Passage is also shown.

2 Shipboard Hydrographic Observations

2.1 Overview

A total of three full-depth hydrographic sections were obtained from 2003 to 2005. First, a total of 9 CTD stations were occupied on the R/V Mirai cruise MR03-K02 from 27 to 30 May 2003. Second, a total of 11 CTD stations were occupied on the R/V Hakuho-maru cruise KH04-4 leg 2 from 13 to 18 October 2004, adding a station on each sidewall of the passage to the nine stations from 2003. Finally, a total of 11 CTD stations were occupied on the R/V Mirai cruise MR05-05 leg 2 from 16 to 19 December 2005. An acoustic Doppler current profiler (ADCP) was lowered along with the CTD at all stations to obtain current profiles.

During the WIFE cruises, continuous profiles of conductivity, temperature, and dissolved oxygen were made with an SBE-9/11*plus* CTD system equipped with an SBE-43 dissolved oxygen sensor (Sea-Bird Electronics, Inc., Bellevue, Washington, USA) from the surface to within 10 m above the bottom in 2003 and 2005, and to within 20 m of the bottom in 2004. In addition, a novel optode-based oxygen sensor (Aanderaa Data Instruments AS, Bergen, Norway) was also used in 2005. Water samples were collected using either 24 (2004) or 36 (2003 and 2005) 12-L Niskin bottles mounted on an SBE-32 Carousel water sampler (Sea-Bird Electronics, Inc.). Samples were collected at 250 dbar intervals below 2000 dbar (500 dbar intervals between 2000 and 3500 dbar in 2004). Accurate temperature measurements were made at the same time as the water samplings using an SBE-35 reference thermometer (Sea-Bird Electronics, Inc.). All water samples were analyzed for salinity, dissolved oxygen, and nutrients (nitrate, nitrite, silicate, and phosphate).

Salinity (practical salinity units) of water samples was measured with a salinometer (Autosal model 8400B; Guildline Instruments Ltd., Ontario, Canada), which was standardized with IAPSO standard seawater from batches P141, P144, and P145 for the cruises in 2003, 2004, and 2005, respectively. The salinity offset for the batches from the average of recent batches (P130–P145; Kawano et al., 2006) is –0.0003 (P141), –0.0005 (P144), and –0.0008 (P145; the value is revised from Kawano et al. 2006, T. Kawano, 2009, personal communication). Dissolved oxygen in water samples was measured with two sets of automatic photometric titrators (model DOT-01; Kimoto Electronic Co. Ltd., Osaka, Japan). Nutrients were measured with an autoanalyzer (TRAACS 800 system; BRAN+LUEBBE, Norderstedt, Germany). Reference Material for Nutrients in Seawater (RMNS; The General Environmental Technos Co. Ltd., Osaka, Japan) were measured on each cruise to establish comparability of nutrient analyses between the cruises (Aoyama et al., 2007). Analyses of CO_2-system parameters [dissolved inorganic carbon (DIC), total alkalinity, and pH], stable carbon isotope ($\delta^{13}C$), and radiocarbon ($\Delta^{14}C$) were performed in 2003. Analyses of chlorofluorocarbons were also performed at the three southernmost stations in 2005, although no chlorofluorocarbons were observed above the detection limits (0.02 pmol kg^{-1} for CFC-11 and 0.01 pmol kg^{-1} for CFC-12) below a depth of 1000 m. The variability in data from water samples is summarized in Table 2.1.1. The silicate data from 2003 was corrected using the results of the RMNS measurements from the three cruises (Uchida et al., 2007b).

The CTD pressure sensors were calibrated before each cruise against a dead-weight piston gauge (Budenberg Gauge Co. Ltd, Manchester, United Kingdom), and time drift for each pressure sensor during the cruise was checked with the pressure measurements on the ship's deck. The accuracy of the pressure data was estimated to be within 2 dbar, based on calibration results from the dead-weight piston gauge against laboratory reference standards for effective area, pressure, and mass, traceable to the National Institute of Standards & Technology, USA. The CTD temperature data were corrected using the in situ reference temperature (Uchida et al., 2007a). Both accuracy and precision of the CTD temperature data were evaluated as 0.4 mK. The CTD salinity and dissolved oxygen data were corrected using the in situ water sample data. In 2005, high-quality CTD oxygen data was obtained from the optode-based oxygen sensor. The variability of the CTD salinity and oxygen data is summarized in Table 2.1.1.

Details of the measurement techniques and calibrations are described in the cruise report (http://www.jamstec.go.jp/cruisedata/mirai/e/MR03-K02.html) for the cruise MR03-K02 and the data book of WHP P03 revisit (Kawano and Uchida, 2007) for the cruise MR05-05 leg 2. The data book is also available through the web site (http://www.jamstec.go.jp/iorgc/ocorp/data/p03rev_2005/). For the cruise KH04-4 leg 2, the measurement techniques and calibrations are described in brief in section 2.2.

Table 2.1.1. The quality (reproducibility) of water sample and CTD data obtained from the WIFE cruises, including standard deviations for standard seawater measurements and replicate samples of salinity, oxygen, silicate, nitrate, phosphate, DIC, total alkalinity, pH, $\delta^{13}C$ and $\Delta^{14}C$ measured during the cruises. Standard deviations of the differences between the CTD and water sample data for depths below 2000 dbar from the WIFE stations are also listed. The number of samples is shown in brackets.

Year (cruise number) Parameter	2003 (MR03-K02)	2004 (KH04-4_2)	2005 (MR05-05_2)
Salinity (standard seawater)	0.0002 [12]	0.0005 [56]	0.0002 [109]
Salinity (replicates)	0.0003 [48]	0.0004 [244]	0.0002 [665]
Oxygen (replicates) (μmol kg^{-1})	0.13 [63]	0.24 [400]	0.08 [493]
Silicate (replicates) (μmol kg^{-1})	0.26 [248]	0.13 [1373]	0.13 [4084]
Nitrate (replicates) (μmol kg^{-1})	0.07 [217]	0.07 [1381]	0.05 [4044]
Phosphate (replicates) (μmol kg^{-1})	0.008 [282]	0.006 [1396]	0.005 [4084]
DIC (replicates) (μmol kg^{-1})	1.1 [32]	not sampled	not sampled
Alkalinity (replicates) (μmol kg^{-1})	2.6 [34]	not sampled	not sampled
pH (replicates)	0.0012 [20]	not sampled	not sampled
$\delta^{13}C$ (replicates) (‰)	0.017 [8]	not sampled	not sampled
$\Delta^{14}C$ (replicates) (‰)	3.3 [11]	not sampled	not sampled
CTD salinity – water sample salinity	0.0003 [132]	0.0008 [113]	0.0003 [161]
CTD oxygen – water sample oxygen (μmol kg^{-1})	0.41 [138]	0.61 [128]	0.08 [162]

2.2 Measurement Techniques and Calibrations for the Cruise KH04-4 Leg 2

(1) Salinity

Conductivity of water samples was measured with a salinometer (Guildline Instruments Ltd., Autosal model 8400B, S/N 66183), which was modified by addition of a peristaltic-type sample intake pump (Ocean Scientific International Ltd., Hampshire, United Kingdom). The salinometer was standardized by IAPSO standard seawater (Ocean Scientific International Ltd.) of batch P144 (K_{15}=0.99987). The Standard Seawater was measured every 30 samples. Also sub-standard seawater, which was deep-sea water filtered by pore size of 0.45 micrometer and stored in two 20 liter cubitainers made of polyethylene and stirred for all the time, was measured every 15 samples. The measurement was done in the air-conditioned laboratory 5, in which air-temperature was kept around 22 °C, at the salinometer bath temperature of 24 °C.

(2) Dissolved oxygen

Dissolved oxygen of water samples was measured with two automatic photometric titrators (Kimoto Electronic Co. Ltd., DOT-01, S/N 134351001 and 134351002) and two automatic burettes (Kimoto Electronic Co. Ltd., APB-510, S/N NUC14584 and NUC14589) with controlling software (Kimoto Electronic Co. Ltd., DOT controller version 2.1.1). We also used two automatic burettes (Metrohm AG, Herisau, Switzerland, Model 725 and 765 Dosimat, S/N 15104 and 05135) for standardization and determination of the blank. Temperature of sampled water taken from a Niskin bottle into a calibrated clear glass bottle (ca. 100 cm^3) was measured with a digital thermometer (Sato Keiryoki Mfg. Co., Ltd., Tokyo, Japan, SK-1250MCIII) in order to correct volume of the bottle and to calculate density of sampled water. Two reagent solutions (pickling reagent I and II) of 0.5 cm^3 each were added into the sample bottle with glass dispensers (Fortuna Optifix 2410-1). To secure traceability on dissolved oxygen analysis, CSK standard solution of potassium iodate (Wako Pure Chemical Industries Ltd., Osaka, Japan, Lot TCK8677, 0.001667M) was measured three times during the cruise.

Reagents used in this cruise were as follows: Pickling reagent I, Manganous chloride solution (3M); Pickling reagent II, Sodium hydroxide (8M) / sodium iodide solution (4M); Sulfuric acid solution (5M); Sodium thiosulfate (0.025M), Wako Pure Chemical Industries Ltd.; Potassium iodate (0.001667M), Lot KLR3004, Wako Pure Chemical Industries Ltd.

(3) Nutrients

Nutrients of seawater samples were measured with continuous-flow analysis systems (BRAN+LUEBBE, TRAACS 800 systems, S/N 9503973 and 9504201), which have 4-channel analyzing systems for nitrate, nitrite, silicate and phosphate. Samples were drawn into two of virgin 10 ml polyacrylates vials that were rinsed three times before sampling without sample drawing tubes. All regents were of very high purity such as “Analytical Grade”, “Analyzed Reagent Grade” and others. And assay of nitrite was determined according JISK8019 and assays of nitrite salts was 99.0%. That value was used to adjust the weights taken. For the silicate standards solution, commercial available silicon standard solution for atomic absorption spectrometry of 1000 mg/L was used. The standard solutions were measured every 12–13 samples and were used to evaluate precision of nutrients analysis during the cruise. Three concentrations of reference material for nutrients in seawater, RMNS (The General Environmental Technos Co. Ltd., lots AS, AT and AU), were also used for all runs to secure traceability on nutrient analysis throughout the cruise. The measurement was done in the air-conditioned laboratory 5, in which air-temperature was kept around 22 °C.

Results of the RMNS measurements are listed in Table 2.2.1. Results of the measurements of the standard solutions are also listed in Table 2.2.2.

Table 2.2.1. Results of the RMNS measurements.

	Nitrate	Nitrite	Silicate	Phosphate
RMNS-AU (number of samples: 72)				
Average (μmol kg^{-1})	29.96	0.01	68.16	2.18
SD (μmol kg^{-1})	0.068	0.004	0.106	0.006
RMNS-AT (number of samples: 36)				
Average (μmol kg^{-1})	7.48	0.01	18.32	0.58
SD (μmol kg^{-1})	0.025	0.004	0.046	0.007
RMNS-AS (number of samples: 36)				
Average (μmol kg^{-1})	0.08	0.01	1.61	0.07
SD (μmol kg^{-1})	0.023	0.004	0.047	0.009

Table 2.2.2. Results of the measurements of the standard solutions.

	Nitrate + Nitrite	Nitrite	Silicate	Phosphate
Average (%)	0.15	0.2	0.08	0.13
Maximum (%)	0.20	0.32	0.11	0.22
Concentration (μmol kg^{-1})	54.9	1.18	172	3.74

(4) CTD/O_2 measurements

The CTD/O_2 was an SBE-9/11*plus* CTD system equipped with an SBE-43 dissolved oxygen sensor (Sea-Bird Electronics, Inc.; SBE-9*plus*, S/N 12545-0400; SBE-3*plus*, S/N 4378; SBE-4, S/N 2496 at stations C094–C95 and S/N 518 at stations C096–C104; SBE-43, S/N 0628; SBE-5T, S/N 51267). Pressure sensor (S/N 60965) was calibrated with a dead-weight piston gauge (Budenberge Gauge model 480DA, S/N 23906) on 27 April 2004 by Marine Works Japan Ltd., Kanagawa Japan. Calibration coefficients for the sensor drift correction were determined as an offset (0.0517 dbar) at all pressure and a change of span slope (0.9999207).

A deep ocean standards thermometer (Sea-Bird Electronics Inc., SBE-35, S/N 0022) was used with the SBE-9/11*plus* CTD system to calibrate the SBE-3 thermometer of the CTD. The SBE-35 was standardized against Triple Point of Water and Gallium Melt Point cells on 2 July 2004 by Sea-Bird Electronics Inc. Like standards-grade platinum resistance thermometers (SPRT), the slow time drift of the SBE-35 was adjusted by a slope (1.000038) and an offset (0.000258 °C) correction to the basic non-linear calibration equation. The SBE-35 was used with the SBE-32 Carousel Water Sampler and SBE-9/11*plus* CTD system. The SBE-35 makes a temperature measurement each time a bottle fire confirmation is received. The time required for one measurement cycle of the SBE-35 was 1.1 s, and four measurement cycles were taken and averaged at each samples.

At the WIFE hydrographic stations, the water sample bottle was closed 30 s after the stop for pressure ≥ 2000 dbar and without stopping for pressure < 2000 dbar. The CTD data sampled at a rate of 24 Hz were averaged for the same duration (4.4 s) as the SBE-35 sample and compared with the SBE-35 data.

(5) Post-cruise calibration of the CTD/O_2

The SBE-35 was calibrated against Triple Point of Water and Gallium Melt Point cells (a slope, 1.000020; an offset, 0.000161°C) on 19 November 2004 by Sea-Bird Electronics Inc. Offset of the SBE-35 data from the pre-cruise calibration was estimated to be smaller than 0.2 mK for temperature lower than 4.5 °C. So the post-cruise correction for the SBE-35 temperature data was not deemed necessary for the SBE-35.

The SBE-3 was calibrated with the SBE-35 in accordance with a method by Uchida et al. (2007a). The calibrated SBE-3 temperature (T_c) was expressed as: $T_c = T - (c_0 + c_1 P)$, where T is the SBE-3 temperature, P is pressure and c_0 and c_1 are the calibration coefficients. Result of the in situ calibration is shown in Fig. 2.2.1. Standard deviation for the difference (188 data points) between the in situ calibrated SBE-3 and the SBE-35 was 0.33 mK.

The CTD salinity data was calibrated with the water sample data by using the same method as that for the cruise MR05-05 leg 2 (Kawano and Uchida, 2007). The calibrated CTD salinity (S_c) was expressed as: $S_c = S - (d_0 \times P + d_1 \times C + d_2 \times C \times P + d_3)$, where S is CTD salinity, C is conductivity, and $d_0 \sim d_3$ are the calibration coefficients. The calibration coefficients were determined for two groups: stations from C073 to C095 and stations from C096 to C119. Result of the in situ calibration is shown in Fig. 2.2.2 and Table 2.1.1.

The CTD oxygen data was also calibrated with the water sample data by using the same method as that for the cruise MR05-05 leg 2 (Kawano and Uchida, 2007). The calibrated CTD oxygen (O_c) was expressed as: $O_c = \mathrm{Soc} \times (V + \mathrm{Offset}) \times exp\{(\mathrm{Tcor}) \times T_c + (\mathrm{Pcor}) \times P\} \times \mathrm{Oxsat}(T_c, S_c)$, where V is the raw sensor data in volts, Oxsat is the oxygen saturation value, and Soc, Offset, Tcor, and Pcor are the calibration coefficients. The calibration coefficients were determined for four groups: stations from C094 to C095, stations from C096 to C097, stations from C098 to C101, and stations from C102 to C105. Result of the in situ calibration is shown in Fig. 2.2.3 and Table 2.1.1.

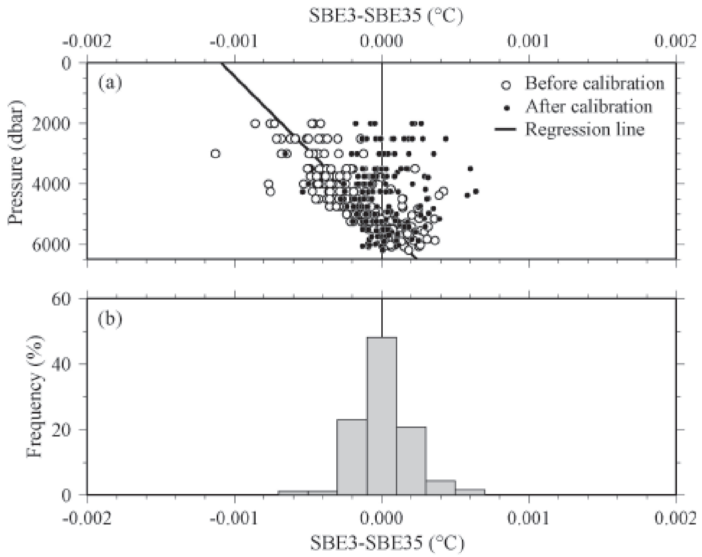

Figure 2.2.1. Difference between temperature from the in situ calibrated SBE-3 data and the SBE-35 data: (a) vertical distribution, (b) histogram.

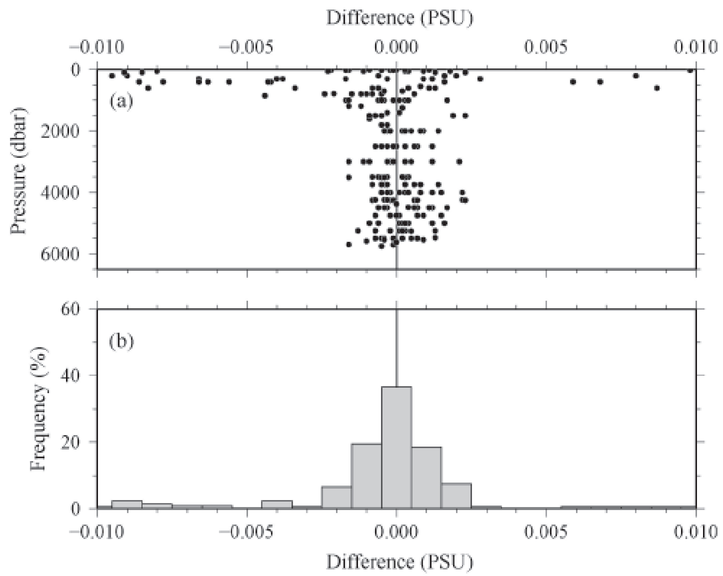

Figure 2.2.2. Difference between salinity from the in situ calibrated CTD data and the water sample data: (a) vertical distribution, (b) histogram.

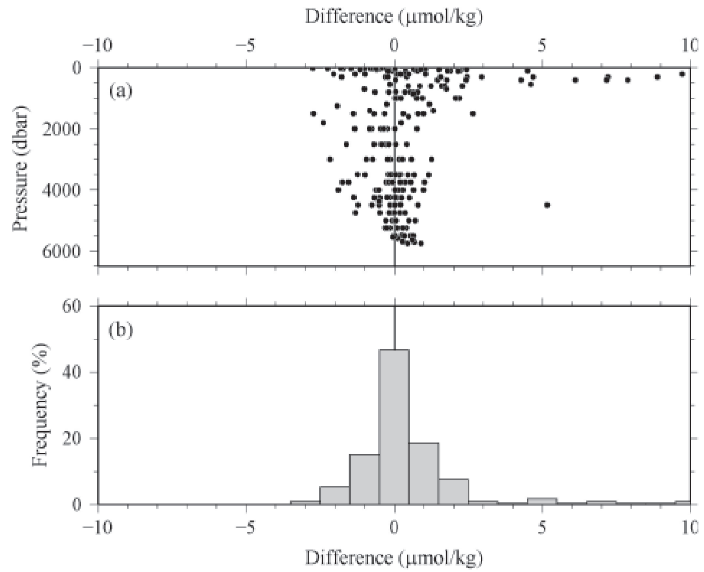

Figure 2.2.3. Difference between oxygen from the in situ calibrated CTD oxygen data and the water sample data: (a) vertical distribution, (b) histogram.

3 Mooring Array Observations

3.1 Overview

(1) Design of the mooring systems

Five moorings were deployed at the cruise MR03-K02 in May 2003, replaced at the cruise KH04-4 leg 2 in October 2004, and recovered at the cruise MR05-05 leg 2 in December 2005 (Figs. 3.1.1 and 3.1.2). Each mooring had five attached CTDs at 500-m intervals and three attached current meters at 1000-m intervals between about 3400-m and 5400-m depths. For the second mooring period, CTDs were attached at 500-m intervals between 3400-m and 4400-m depths, at 250-m intervals between 4400-m and 5400-m depths, and to near the bottom (for stations WM2, WM3, and WM4). Moreover, oxygen optode sensors were attached to near the bottom for each mooring for the second mooring period. To detect top depth of the mooring line from the ship, an acoustic transponder (model XT-6000; Teledyne Benthos, Inc., North Falmouth, Massachusetts, USA) was attached to the top of each mooring. Depth of the transponder during deployment was monitored using an acoustic navigation system on the R/V Mirai and the decent rate of the moorings was estimated to be 0.96 to 1.26 m s^{-1}. To recover the moorings as securely as possible, two (parallel) acoustic releasers (model L and/or L II; Nichiyu Giken Kogyo Co., Ltd., Toshima-ku, Tokyo, Japan) were used for each mooring. The releaser applies gas-generation mechanism to free a hock.

Bathymetry along the WIFE observation line was measured by multinarrow beam echo sounding system on the R/V Mirai in the cruises MR03-K02 and MR05-05 leg2. Details of bathymetry around the mooring stations are shown in Figs. 3.1.3–3.1.7.

(2) Problems encountered in the mooring observations

At station WM1 in the first mooring period, six glass buoys installed on the middle of the mooring line broke just after the mooring deployment. Therefore, the mooring line tilted more than the other mooring lines and the maximum deepening of the top of the mooring line was about 90 m, although the deepening of the other mooring lines was usually smaller than 10 m. Moreover, at station WM5 in the second mooring period, six glass buoys installed on the bottom of the mooring line also broke at between 20:00 and 20:30, May 22, 2005 (UTC). Therefore, the instruments were deepened about 2 m on average after the break.

Two transponders (WM1 and WM2) leaked during the second mooring period.

Six CTDs leaked during the mooring observations and one CTD leaked during the in situ calibration after the mooring recovery. Moreover, for 20 CTDs, pressure and conductivity data were not available because of a failure of the pressure sensor occurred during the mooring observation period (see section 3.3 for detail).

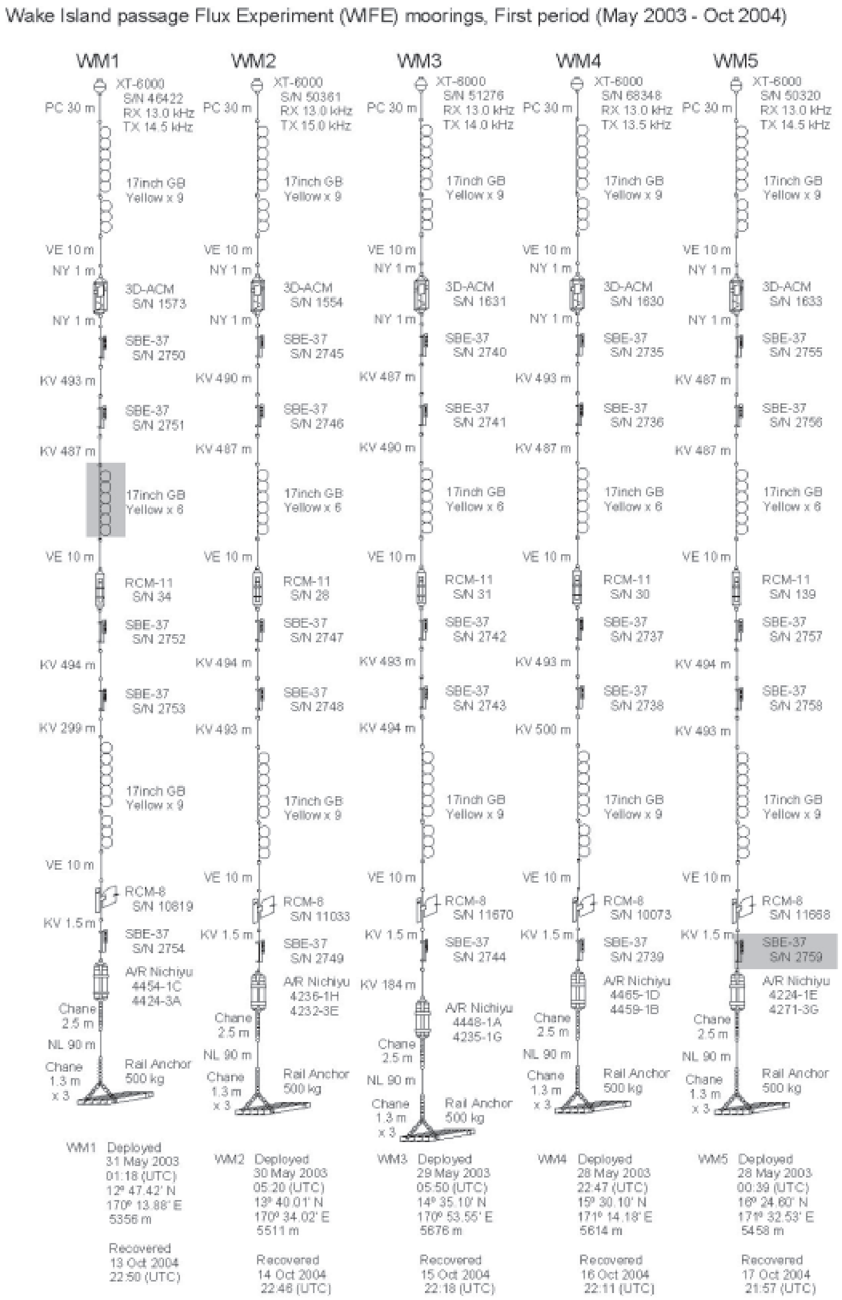

Figure 3.1.1. Schematic illustration of the WIFE mooring system for the first mooring period. Instruments leaked or broken during the mooring observations are shaded.

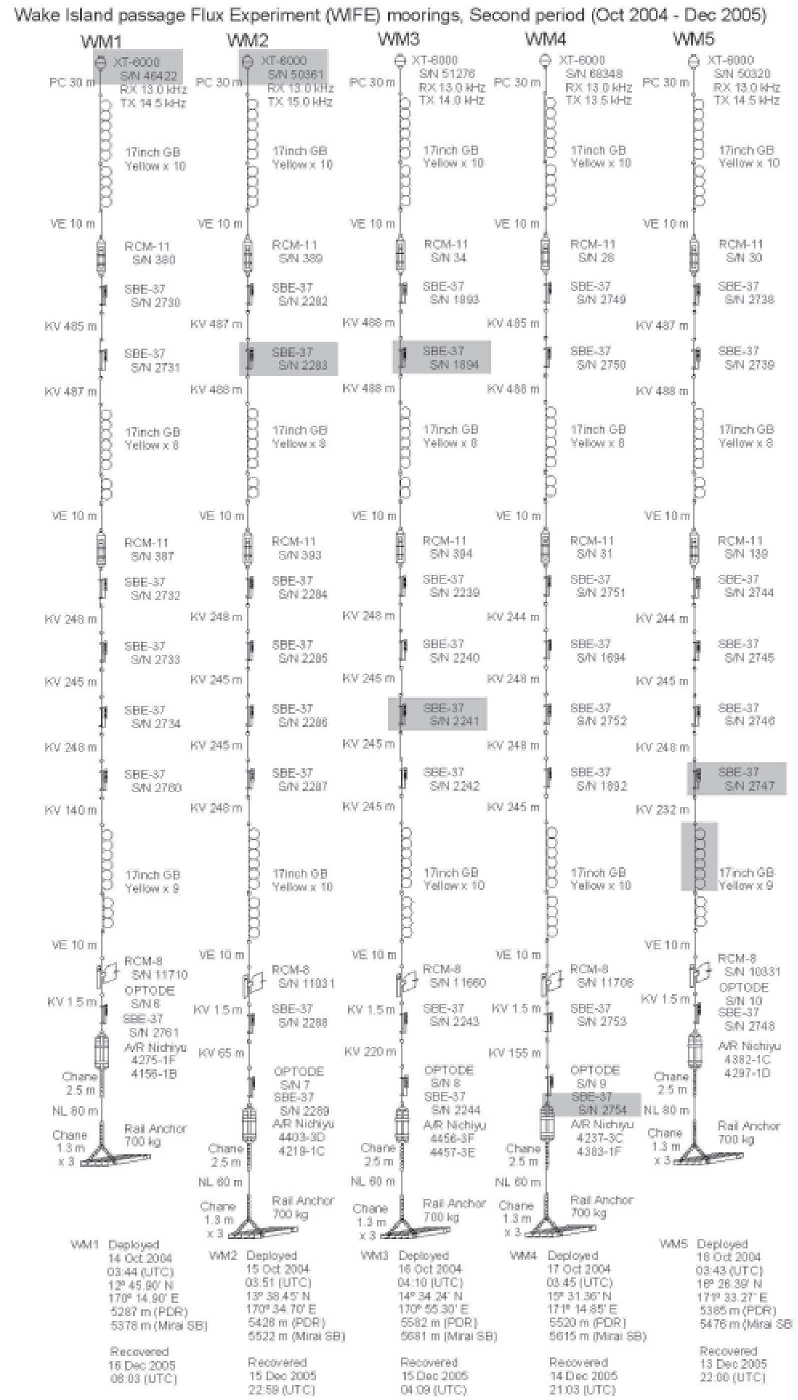

Figure 3.1.2. Same as Fig. 3.1.1 but for the second mooring period.

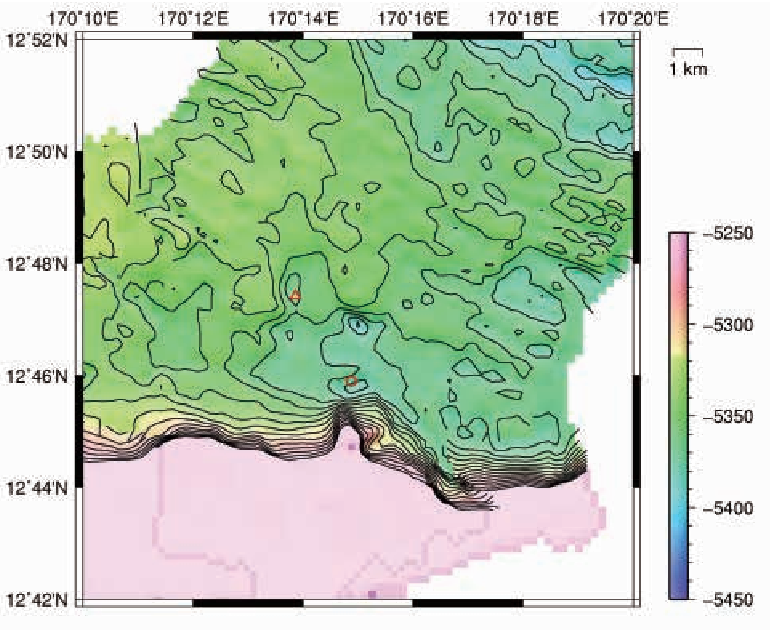

Figure 3.1.3. Bathymetry (in m) around the mooring station WM1. Triangle indicates the station location for the first mooring period and circle indicates the station location for the second mooring period. Bathymetry measured by multinarrow beam echo sounding system is shown. Bathymetry measured in the cruise MR05-05 leg 2 is superimposed over the bathymetry measured in the cruise MR03-K02. Contour interval is 10 m.

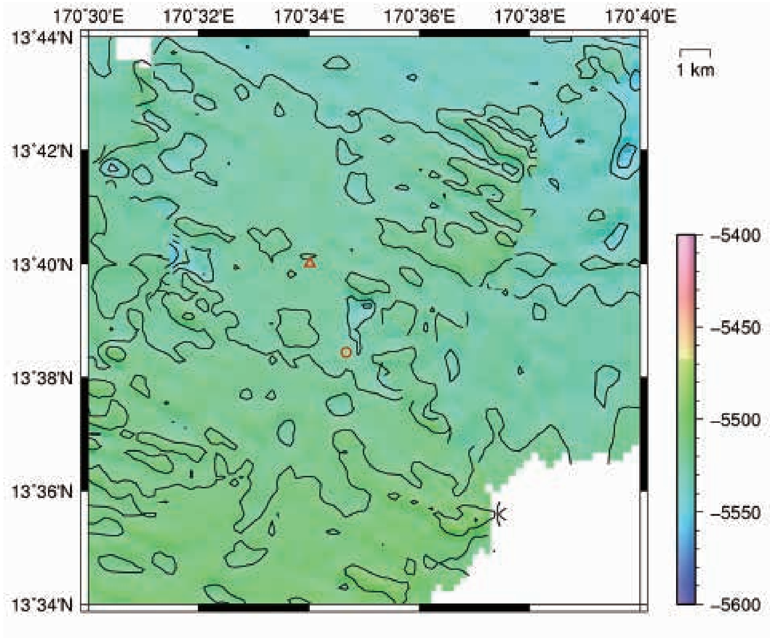

Figure 3.1.4. Same as Fig. 3.1.3 but around the mooring station WM2.

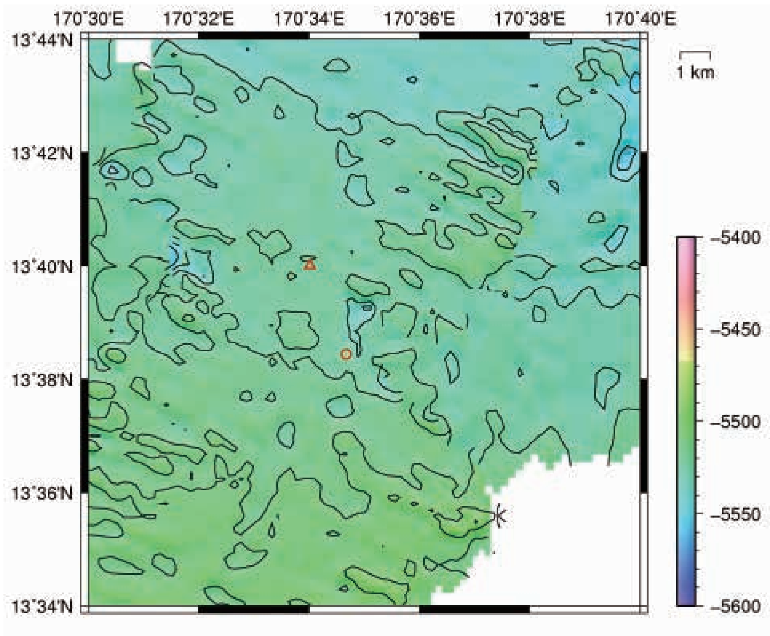

Figure 3.1.5. Same as Fig. 3.1.3 but around the mooring station WM3.

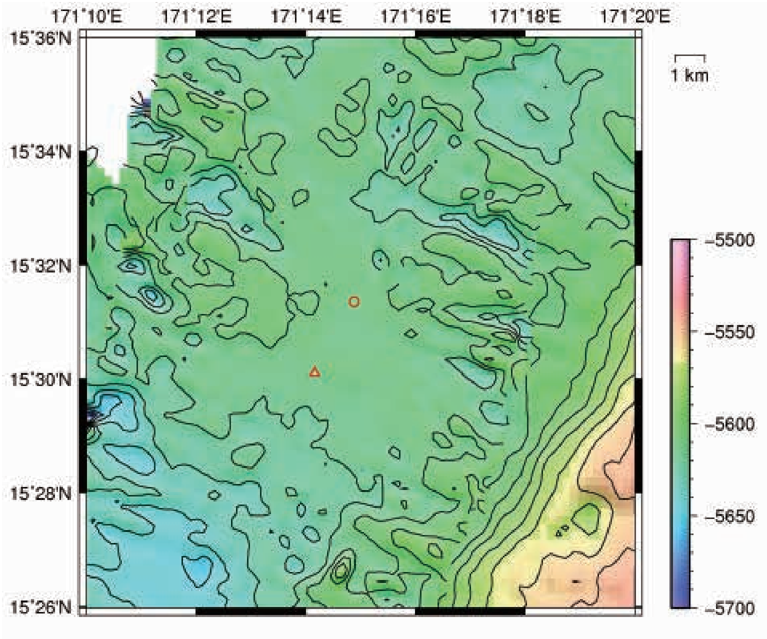

Figure 3.1.6. Same as Fig. 3.1.3 but around the mooring station WM4.

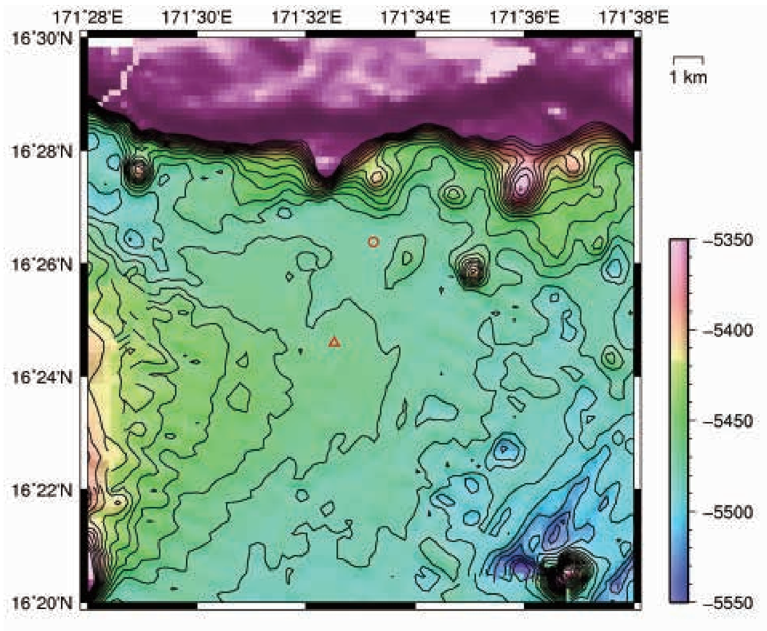

Figure 3.1.7. Same as Fig. 3.1.3 but around the mooring station WM5.

3.2 Current Meters

(1) Instruments and methods

During WIFE, three types of current meters were used. For the 3400 m layer in the first mooring period, three-dimensional acoustic current meters, 3D-ACM (Falmouth Scientific Inc., Cataumet, Massachusetts, USA), were used. For the 3400 m layer in the second mooring period and for the 4400 m layer, acoustic Doppler current meters, RCM-11 (Aanderaa Data Instruments AS, Bergen, Norway), were used. For the 5400 m layer, recording vector averaging current meters, RCM-8 (Aanderaa Data Instruments AS), were used. Setup parameters for the current meters are listed in Table 3.2.1.

For RCM-11 and RCM-8 current meters, the data storing unit, DSU 2990E, was used except for three RCM-8s (WM1, WM2, and WM3) used in the first mooring period. For the three RCM-8s, the DSU 2990 was used with the same setup parameters as the other RCM-8, and therefore the data of the last three months of the mooring period were not recorded due to small capacity of the data storing unit.

(2) Data processing and corrections

The azimuth values relative to the magnetic north were corrected with respect to the true north. The declinations were estimated from the 10th Generation International Geomagnetic Reference Field (http://www.ngdc.noaa.gov/IAGA/vmod/igrf.html) at each mooring location in the middle of the mooring period. The correction range was 7.5–7.9°.

The RCM-8 cannot measure velocities lower than 1.1 cm s^{-1} and the data were recorded as 1.1 cm s^{-1}. Therefore, the data whose speed was 1.1 cm s^{-1} were conservatively replaced to 0.0 cm s^{-1}.

Two 3D-ACMs showed strange velocity distributions like a doughnut shape (Fig. 3.2.1). The cause of these strange distributions has not been determined, despite a close examination of the sensor by the manufacturer. These questionable data were simply corrected by subtracting 4.5 cm s^{-1} and 0.5 cm s^{-1} from the measured speed of the 3D-ACM serial no. 1630 (WM4) and 1633 (WM5), respectively.

Table 3.2.1. Setup parameters for the current meters.

Instrument	Sampling interval	Sampling rate (mode)	Averaging time
3D-ACM	1-hour	2 Hz	1 minute
RCM-11	1-hour	2.5 Hz (Burst)	1 minute
RCM-8	1-hour	50/3600 Hz	1 hour

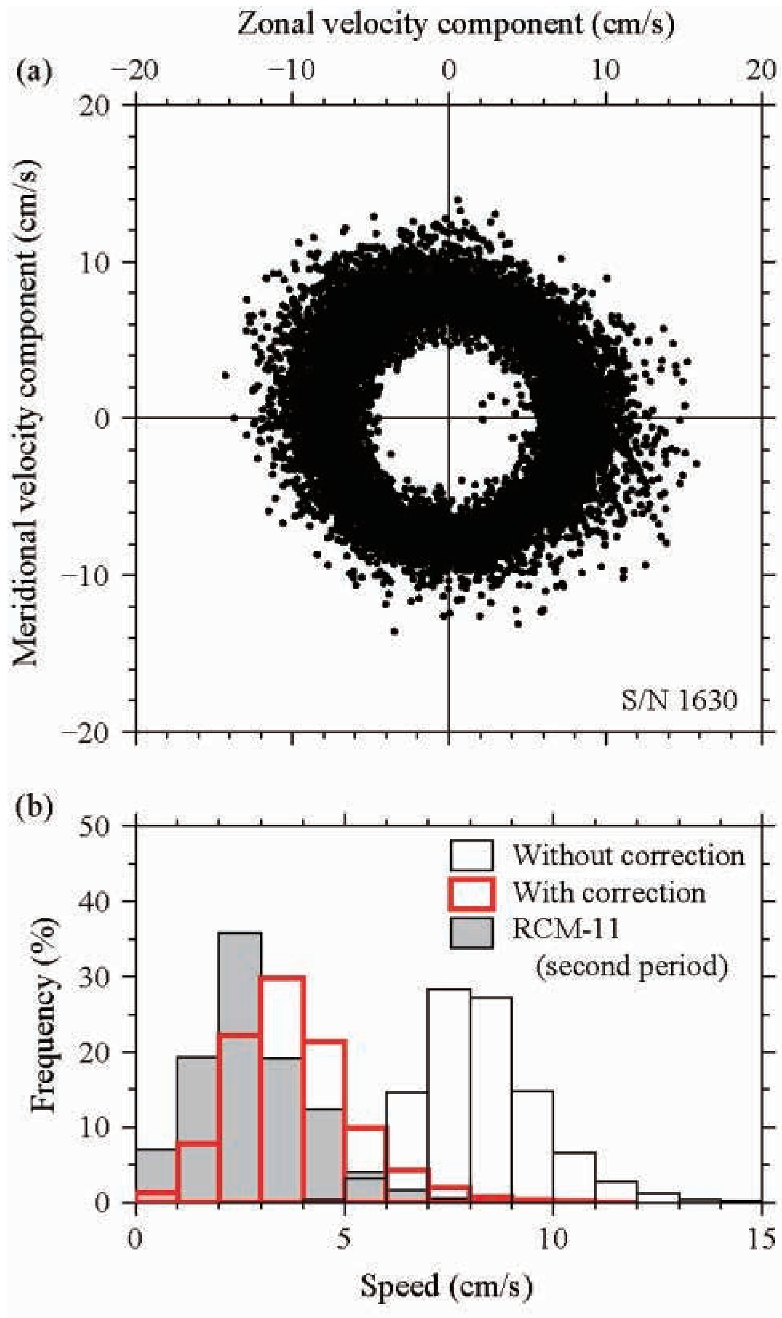

Figure 3.2.1. An example of the strange velocity distributions of the 3D-ACM: (a) scatter plot and (b) histogram. Offset (–4.5 cm s^{-1}) corrected data is similar in histogram to the RCM-11 data obtained at the same location in the different mooring period.

3.3 Moored CTDs

(1) Instruments and methods

During WIFE, high-accuracy conductivity and temperature recorders, SBE-37SM MicroCAT (Sea-Bird Electronics, Inc.), were used. The SBE-37s used had no pump, but included an optional pressure sensor with a measurement range of 7000 dbar, developed by Druck, Ltd., Leicester, United Kingdom. The SBE-37s were attached to a water-sampling frame during shipboard hydrographic casts before mooring deployment and after mooring recovery to obtain data from both the SBE-37s and the well-calibrated shipboard CTD. The SBE-37s were calibrated in situ by comparing these simultaneously measured CTD data (Uchida et al., 2008a). The time required for one measurement cycle (pressure, temperature, and conductivity) was 1.6 s. A sampling interval was set to 6 s for in situ calibration and was set to 30 minutes for mooring observation. Twenty-five SBE-37s out of a total of 50 were used for the first set of mooring observations (from May 2003 to October 2004) and 36 SBE-37s were used for the second set of mooring observations (from October 2004 to December 2005).

(2) Problems encountered in the mooring observations

Six SBE-37s leaked during the mooring observations (one is in the first mooring period and five is in the second mooring period; Figs 3.1.1 and 3.1.2) and therefore the data could not be retrieved. One SBE-37 attached at 3400 m layer of WM2 in the second mooring period also leaked a little. After cleaning inside of the instrument and replacing the battery, the data could be retrieved except for last four hours of the mooring period. However, this SBE-37 leaked during the post-recovery in situ calibration and the data for the in situ calibration could not be retrieved.

For 20 SBE-37s, a failure of the Druck pressure sensor occurred during the mooring observation period (Fig. 3.3.1). The nature of the failure was an internal short to the Druck transducer body, and the failure appears randomly in a significant number of sensors for serial numbers below 4550 (Sea-Bird Electronics, Inc., 2004, personal communication). The Druck transducer body was grounded to seawater via the SBE-37 housing. When the pressure sensor fails, the current can flow from the housing through seawater to the conductivity sensor's ground electrode (Sea-Bird Electronics, Inc., 2005, personal communication). This caused an uncorrectable error in the conductivity data. In addition, for 4 SBE-37s, the pressure data showed relatively large time drift probably due to the same reason as the failure.

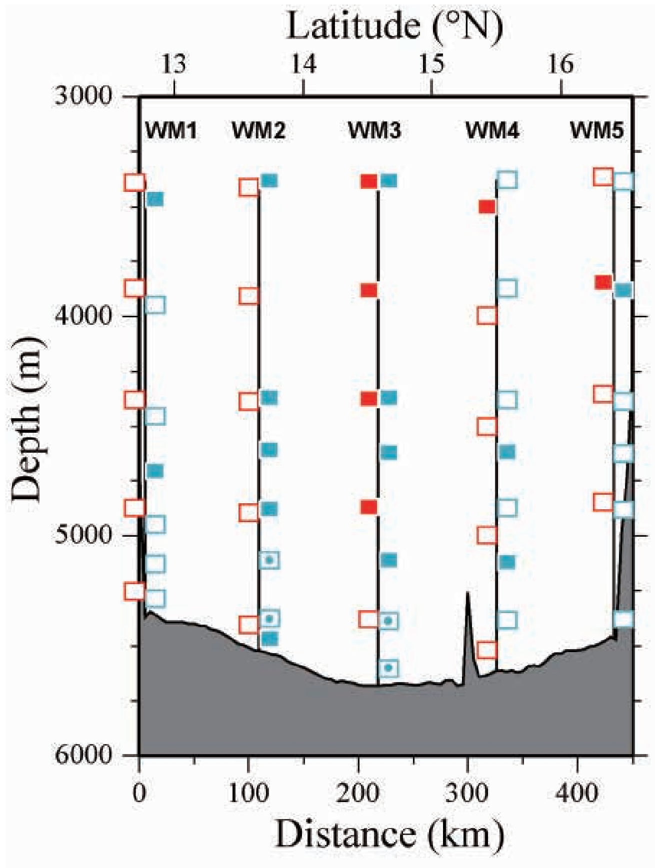

Figure 3.3.1. Locations of the SBE-37s for the first set (red: from May 2003 to October 2004) and the second set (blue: from October 2004 to December 2005) of the mooring observations. Closed squares indicate that the failure of the Druck pressure sensor occurred during the mooring observation period. Open squares with dots indicate that the pressure data showed large time drift.

(3) In situ calibration

For in situ calibration during hydrographic casts, up to 10 SBE-37s were attached to the water-sampling frame at about the same height as the shipboard CTD (Table 3.3.1; see also section 3.7). In situ calibration method and results of the in situ calibration are described in detail by Uchida et al. (2008a). The standard seawater batch correction was not applied to the shipboard CTD salinity data since maximum batch-to-batch difference of standard seawater for batches P141, P144, and P145 is small (0.0005). Mean salinity offset of the in situ calibrated SBE-37 data from the average of recent batches (P130–P145; Kawano et al., 2006) is estimated to be –0.0005.

Table 3.3.1. CTD casts for the in situ calibration of the SBE-37s before mooring deployment and after mooring recovery.

CTD cast	Serial number	Note
MR03-K02		
WC9	2735, 2736, 2737, 2738, 2739	WM4_1_pre
	2755, 2756, 2757, 2758, 2759	WM5_1_pre
WC8	2740, 2741, 2742, 2743, 2744	WM3_1_pre
	2745, 2746, 2747, 2748, 2749	WM2_1_pre
WC7	2750, 2751, 2752, 2753, 2754	WM1_1_pre
KH04-4 leg 2		
C095	2730, 2731, 2732, 2733, 2734, 2760, 2761	WM1_2_pre
C096	2282, 2283, 2284, 2285, 2286, 2287, 2288, 2289	WM2_2_pre
C097	1893, 1894, 2239, 2240, 2241, 2242, 2243, 2244	WM3_2_pre
C099	1694, 1892	WM4_2_pre
	2750, 2751, 2752, 2753, 2754	WM1_1_post, WM4_2_pre
	2749	WM2_1_post, WM4_2_pre
C101	2745, 2746, 2747, 2748	WM2_1_post, WM5_2_pre
	2744	WM3_1_post, WM5_2_pre
	2742, 2743	WM3_1_post
C102	2740, 2741	WM3_1_post
	2738, 2739	WM4_1_post, WM5_2_pre
	2735, 2736 2737	WM4_1_post
C103_3	2755, 2756, 2757, 2758	WM5_1_post
MR05-05 leg 2		
WC1	2730, 2731, 2732, 2733, 2734, 2760, 2761	WM1_2_post
WC3	2738, 2739, 2744, 2745, 2746, 2748	WM5_2_post
WC4	1694, 1892, 2749, 2750, 2751, 2752, 2753	WM4_2_post
WC5	1893, 2239, 2240, 2242, 2241, 2242, 2243, 2244	WM3_2_post
WC7	2282*, 2284, 2285, 2286, 2287, 2288, 2289	WM2_2_post

* In situ calibration data could not be retrieved due to leaking during the CTD cast.

(4) Data processing

The SBE-37 CTD data during mooring observations were processed as follows:

1) Spikes were manually removed from the SBE-37 data, and the data gap in temperature were linearly interpolated in time.
2) Time drift of the pressure data was estimated from the best-fitting curves of a second-order polynomial and was removed from the pressure data for the following SBE-37s: WM3_2743 and WM4_2739 of the first mooring period, and WM2_2286, WM2_2287, WM2_2288, WM3_2244, WM5_2738, and WM5_2739 of the

second mooring period. If the in situ calibration data of conductivity after the mooring recovery were not available, the conductivity data were re-calculated by using the drift-corrected pressure data.

3) Pressure, temperature, and conductivity data of the SBE-37 were calibrated by using the results of the in situ calibration (Uchida et al., 2008a). Time drift of the pressure data was not removed from the following SBE-37s: WM3_2743 and WM4_2739 of the first mooring period, and WM2_2286, WM2_2287, WM2_2288, WM3_2244, and WM5_2738 of the second mooring period, since time drift of the pressure data was already corrected by using the second-order polynomial.

4) Bad conductivity data judged by temperature–salinity diagram were deleted for the following SBE-37s: WM3_2741 (time > 29 August 2003), WM4_2735 (time > 20 July 2003), WM4_2739 (time > 27 November 2003) of the first mooring period, and WM1_2731 (time > 20 May 2005), WM1_2733 (time > 04:00, 19 May 2005), WM4_2749 (time > 11 November 2004) of the second mooring period.

5) Time drift of the conductivity data was estimated from temperature–conductivity diagram, if the in situ calibration data of conductivity after the mooring recovery were not available, for the following SBE-37s: WM1_2751, WM3_2740, WM3_2741, WM3_2742, WM3_2743, WM4_2735, WM4_2737, WM4_2739, and WM5_2756 of the first mooring period, and WM1_2730, WM1_2731, WM1_2733, WM2_2286, WM2_2289, WM4_2749, and WM5_2739 of the second mooring period. A linear drift was estimated by minimizing residual from a regression line of the temperature–conductivity relation.

6) Missing data of pressure were estimated from a nearby SBE-37 pressure data (Table 3.3.2). High-frequency tidal signal and low-frequency variability were estimated separately. The tidal signal was estimated by using a harmonic analysis. The low-frequency variability was estimated by subtracting the tidal signal from the pressure data and by multiplying an appropriate factor (Table 3.3.2)

7) Missing data of conductivity were estimated from the temperature–conductivity relation taking conductivity change corresponding to pressure change into account

8) Time drift of the salinity data was corrected by using the shipboard CTD data (Uchida et al., 2008a).

Table 3.3.2. Serial number of the SBE 37 whose pressure data were estimated.

Mooring period	Serial number	Serial number used for estimation of tidal signal	Serial number used for estimation of variability	Factor
1	WM3_2743	WM3_2743	WM3_2744	3.70
1	WM3_2740	WM3_2740	WM3_2743	1.54
1	WM3_2741	WM 3_2741	WM3_2743	1.54
1	WM3_2742	WM 3_2742	WM3_2743	1.22
1	WM4_2735	WM 4_2735	WM4_2736	1.00
1	WM5_2756	WM 5_2756	WM5_2755	1.00
2	WM1_2730	WM1_2731	WM1_2731	1.00
2	WM1_2733	WM1_2733	WM1_2732	0.69
2	WM2_2282	WM2_2286	WM2_2288	6.25
2	WM2_2284	WM2_2286	WM2_2288	5.00
2	WM2_2285	WM2_2286	WM2_2288	4.55
2	WM2_2286	WM2_2286	WM2_2287	1.72
2	WM2_2289	WM2_2289	WM2_2288	1.00
2	WM3_1893	WM3_2243	WM3_2243	6.25
2	WM3_2239	WM3_2243	WM3_2243	5.00
2	WM3_2240	WM3_2243	WM3_2243	4.55
2	WM3_2242	WM3_2243	WM3_2243	2.22
2	WM4_1694	WM4_2751	WM4_2751	0.89
2	WM4_1892	WM4_2752	WM4_2752	0.58
2	WM5_2739	WM5_2739	WM5_2738	1.00

3.4 Oxygen Optodes

(1) Instruments and methods

Oxygen optode sensors (Oxygen Optode model 3830; Aanderaa Data Instruments AS, Bergen, Norway) are based on the oxygen luminescence quenching of a platinum porphyrine complex. The optode sensor was attached to a datalogger with an internal battery and memory in a titanium housing designed for mooring observation (Compact-Optode; Alec Electronics Co., Ltd., Kobe, Japan). The optode sensors were used in the second WIFE mooring period (October 2004 to December 2005) and their serial numbers are listed in Table 3.4.1. Data were sampled at 1-hour intervals. Ten data measured at 1-second intervals were averaged at each sampling. From the internally-calculated oxygen and temperature data, raw phase shift data were back calculated. Oxygen concentration from the phase shift data of the optode sensors were calculated on the basis of the Stern–Volmer equation according to a method by Uchida et al. (2008b). For the in situ calibration, data were sampled at 1-second intervals.

(2) In situ calibration

The optode sensors were calibrated in situ by using high-quality oxygen data obtained with discrete water samples measured by means of the Winkler titration method according to a method by Uchida et al. (2008b). The optode sensors were attached to the water sampling frame at CTD casts before mooring deployment in the cruise KH04-4 leg 2 and after mooring recovery in the cruise MR05-05 leg 2 to collect the calibration data (Table 3.4.1). The optode oxygen data were calibrated by using the optode data at the water sampling layers and the Winkler oxygen data. Data obtained from the CTD cast after mooring recovery were used since the optode data were drifted in time during the mooring period. Data collected for depths deeper than 450 dbar were used for the calibration. Mean difference between the in situ calibrated optode data and the Winkler oxygen data was 0.16 μmol kg^{-1}. For the optode temperature data, mean temperature offsets were estimated by comparing with the CTD temperature data obtained from the CTD casts before mooring deployment and after mooring recovery (Table 3.4.1).

(3) Data processing

Necessary temperature compensation for calculation of the oxygen data during the mooring period was performed using the optode temperature data. Necessary pressure and salinity compensations were performed using mean values at the moored locations. The mean values were estimated from the shipboard CTD data obtained in the cruises MR03-K02, KH04-4 leg 2, and MR05-05 leg 2 (Table 3.4.1). Unfortunately, the data were obtained only for the first 2.5 months because of a failure of Alec Electronics's firmware.

The in situ calibrated optode oxygen data were drifted in time during the mooring period, probably due to a slow time-dependent, pressure-induced effect. Therefore, the time drift was estimated by fitting an exponential-linear curve (Fig. 3.4.1). Data for the first 0.5–2.5 days were excluded since the data were largely deviated from the fitting curve. Oxygen anomalies from the fitting curve were only available for the analysis (Fig. 3.4.2).

Table 3.4.1. Nominal depth and salinity used for the calculation of oxygen from optode data. Temperature offsets which were added to the optode temperature data are also shown. CTD casts for the in situ calibration before mooring deployment and after mooring recovery are also shown.

Serial no. of datalogger	Serial no. of sensor	Pressure (dbar)	Salinity	Temperature offset (°C)	CTD casts for the in situ calibration before deployment / after recovery
6	385	5348	34.703	0.00	C095 (WC1) / WC8
7	466	5525	34.704	–0.01	C096 (WC2) / WC8
8	472	5688	34.704	0.00	C097 (WC3) / WC8
9	474	5625	34.703	0.00	C101 (WC7) / WC8
10	475	5461	34.703	–0.01	C102 (WC8) / WC8

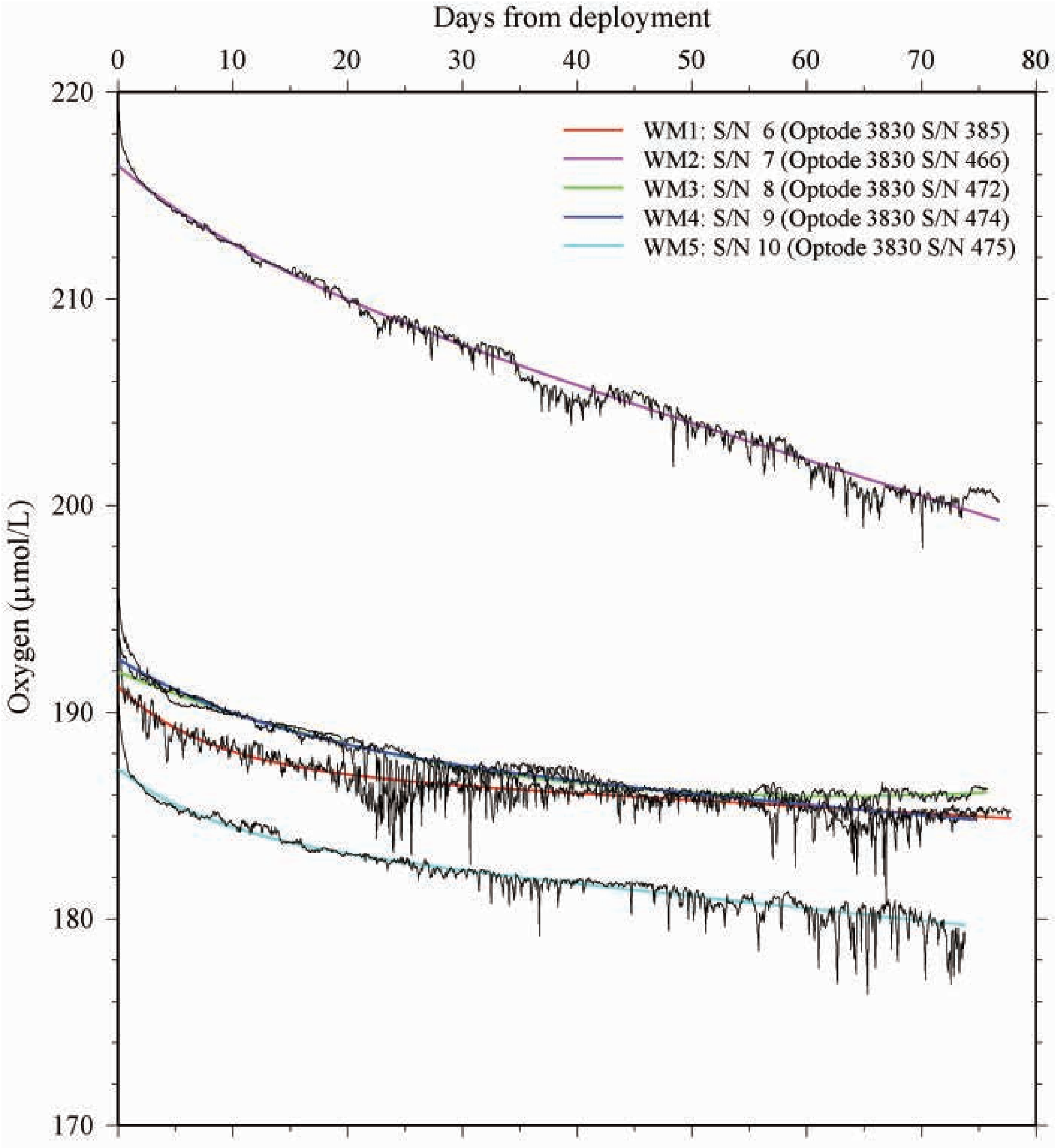

Figure 3.4.1. Time series of dissolved oxygen. Hourly data obtained from 5 optodes are shown. The lines represents the best fitting exponential-linear curves.

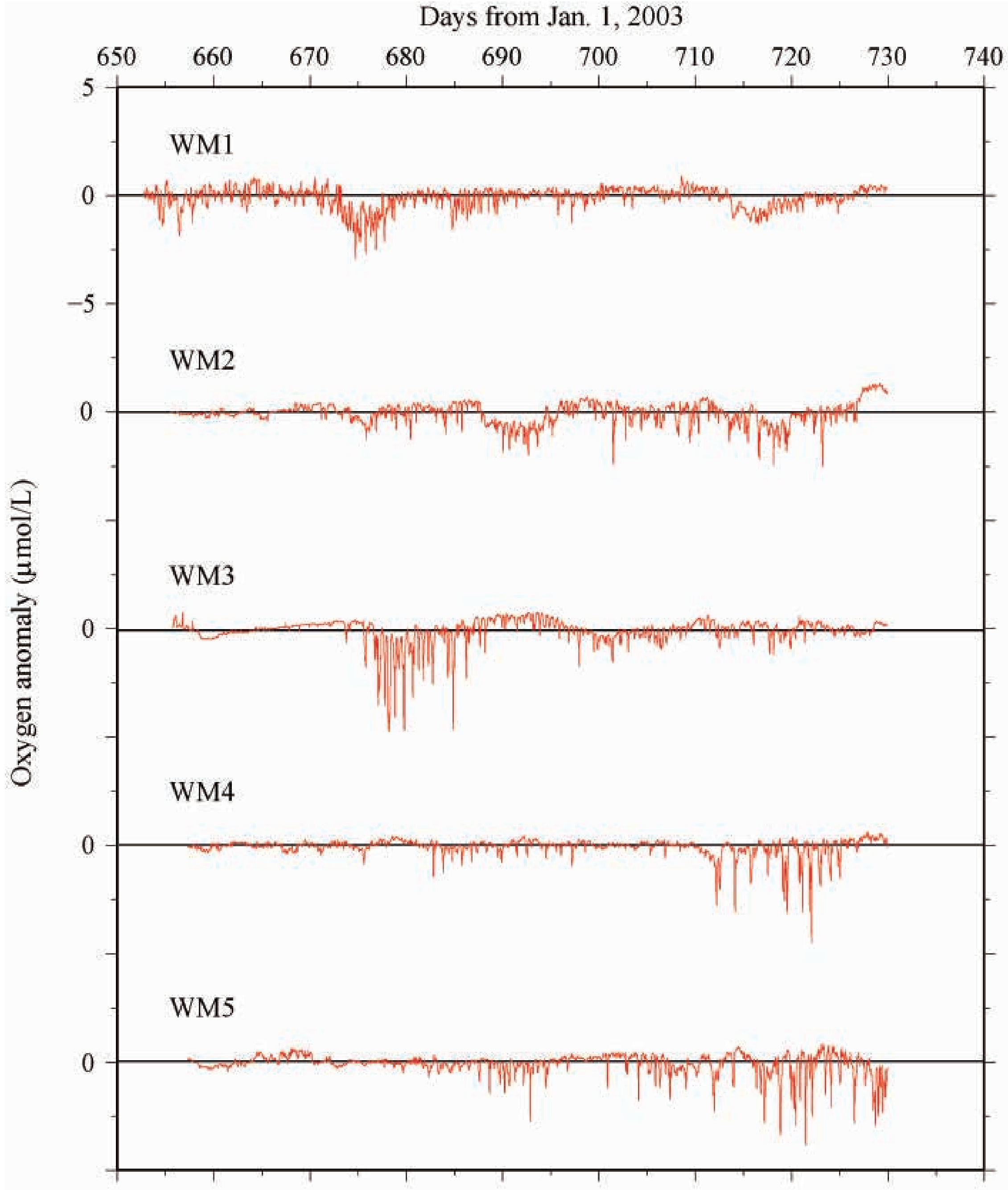

Figure 3.4.2. Time series of dissolved oxygen anomalies from the best fitting exponential-linear curves.

3.5 Gridding of the Moored CTD and Current Meter Data

(1) Smoothing and re-sampling of the data

In order to remove short-term fluctuation associated with tidal currents and inertial oscillation (period of 1.8–2.3 days at the mooring locations), the moored CTD data sampled at 30-minute intervals and the current meter data sampled at 1-hour intervals were low-pass-filtered with a half power gain at 5 days of the third order bi-directional (forward and backward) Butterworth filter (Fig. 3.5.1), and the data were re-sampled at 1-day intervals.

(2) Extrapolation of temperature and salinity data near the bottom

The WIFE is designed to estimate transport of the abyssal water through the deep passage by means of geostrophic calculations from density measurements by moored CTDs referred to velocity measurements by current meters. To calculate geostrophic velocities near the bottom, temperature and salinity near the bottom were estimated for three locations before gridding of the data (Table 3.5.1). Mean temperature and salinity were estimated from the shipboard CTD data obtained at those mooring stations just before and after the mooring period. Fluctuation component of temperature and salinity were estimated for WM3 and WM4 by using empirical relations. For WM3, a linear relation between fluctuation components of temperature at 5688 and 5454 dbar was estimated from the moored CTD data in the second mooring period. Fluctuation component of temperature at 5688 dbar for the first period was estimated from the fluctuation component of temperature at 5465 dbar multiplied by a factor of 0.69. Fluctuation component of conductivity was estimated by using the estimated temperature and a temperature-conductivity relationship at that depth obtained from the shipboard CTD data. Salinity was calculated from the estimated temperature and conductivity. For WM4, fluctuation components of temperature and salinity were similarly estimated. A linear relation between fluctuation components of temperature at 5625 and 5458 dbar was estimated from the moored CTD data at WM2 (5450 and 5524 dbar) and WM3 (5454 and 5688 dbar) in the second mooring period. Fluctuation component of temperature at 5625 dbar for the second period was estimated from the fluctuation component of temperature at 5458 dbar multiplied by a factor of 0.71. For WM5, fluctuation components of temperature and salinity were not estimated since the fluctuations were estimated to be small from the data in the second period and the available moored CTD data at the station in the first period was relatively distant (> 500 dbar) from the bottom.

(3) Interpolation of the data

At each mooring station, the moored CTD and current meter data were vertically interpolated at 2 dbar intervals. A linear interpolation was used for the current meter data and a piecewise cubic Hermite spline interpolation (de Boor, 2001) was used for the CTD data. For the CTD data, potential temperature and salinity data were interpolated, and then temperature data was back calculated by using the potential temperature, salinity and pressure data. Data gap between the first and second mooring periods was linearly interpolated in time.

Error of the interpolated temperature and salinity data were estimated by using the shipboard CTD data. Temperature and salinity profiles for depths from 3400 to 5400 dbar were compared with the interpolated profiles calculated from discrete data sub-sampled at 500-dbar intervals (Fig. 3.5.2). Mean differences were almost zero (mean ± SD was 0.1 ± 1.4 m°C for temperature and was –0.02 ± 0.09 mPSU for salinity) and considerably smaller than the results obtained by using a linear interpolation method (mean ± SD was 1.9 ± 1.3 m°C for temperature and was 0.1 ± 1.4 mPSU for salinity) (Fig. 3.5.3).

Table. 3.5.1. Estimated mean temperature and salinity near the bottom.

Station no.	Pressure (dbar)	Mooring period	Mean temperature (°C)	Mean salinity	Fluctuation component of temperature and salinity
WM3	5688	First	1.4013	34.7035	estimated
WM5	5458	First	1.3815	34.7029	–
WM4	5625	Second	1.4007	34.7033	estimated

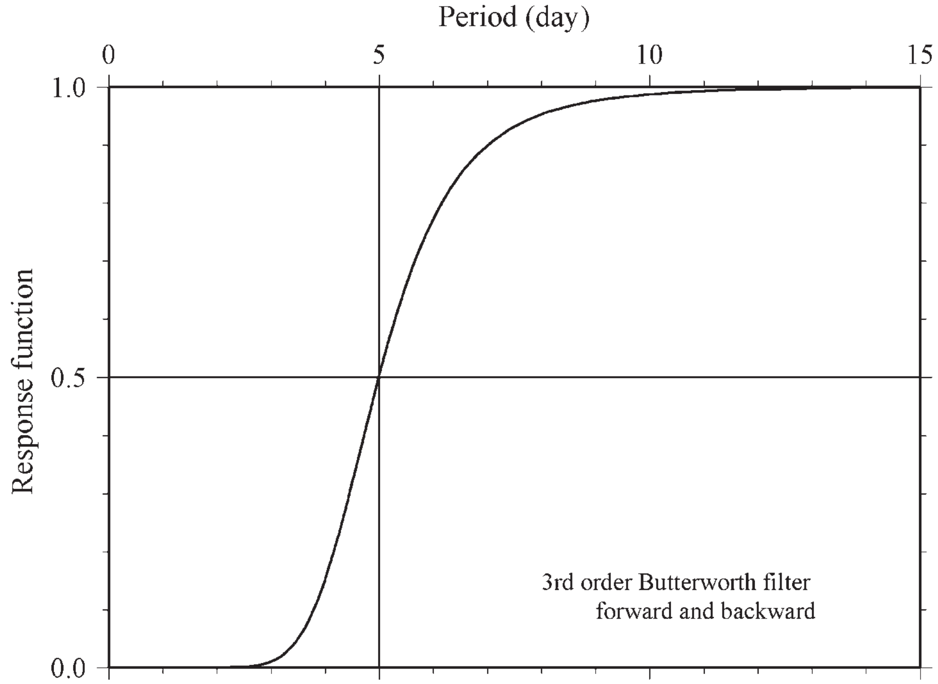

Figure 3.5.1. Response function of the third order bi-directional (forward and backward) Butterworth low-pass filter.

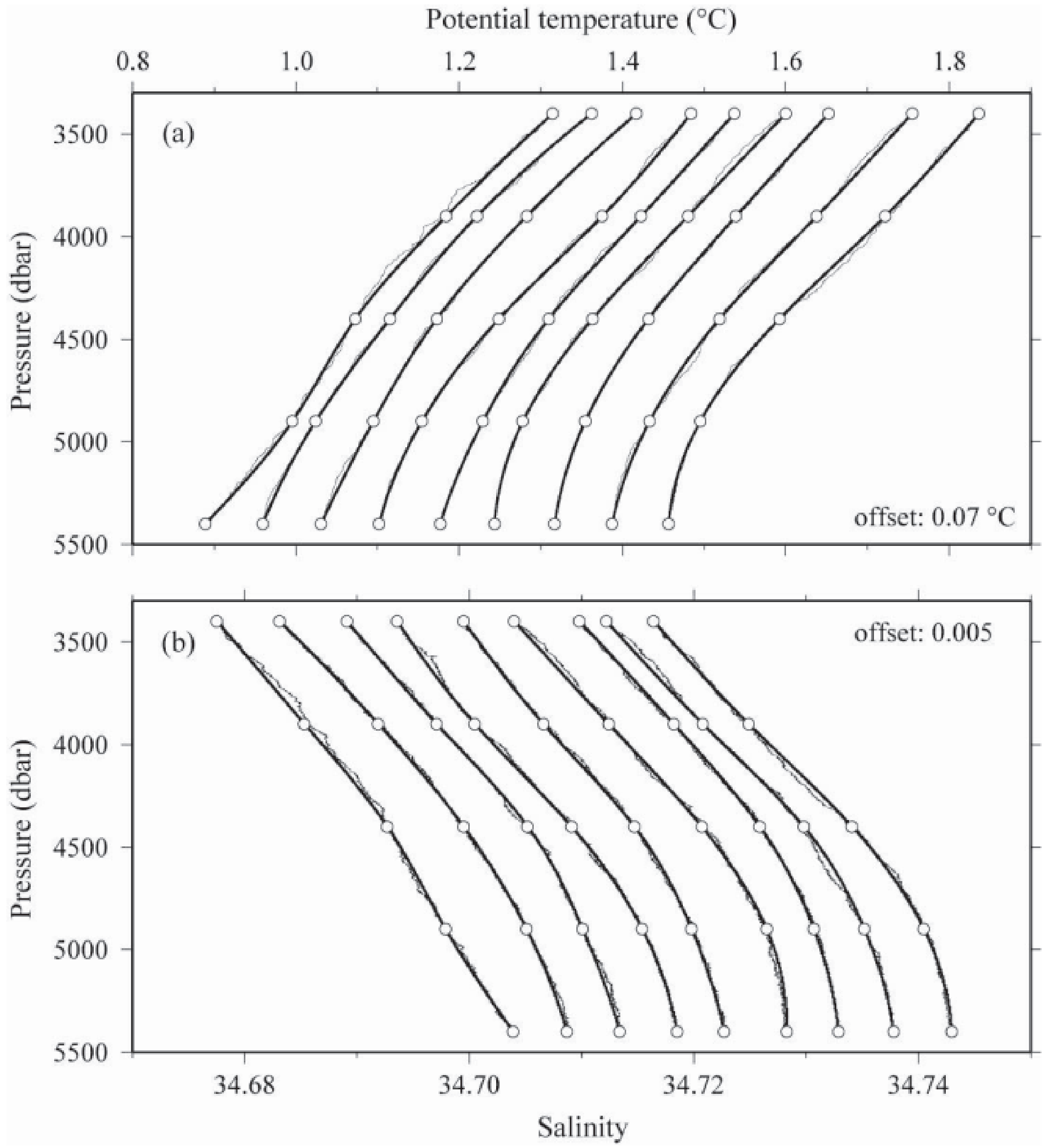

Figure 3.5.2. Comparison between observed profiles (thin lines) and estimated profiles (thick lines) for (a) temperature and (b) salinity for depths from 3400 to 5400 dbar. Data sub-sampled at 500-dbar intervals (circles) are used for the estimation and are vertically interpolated at 2-dbar intervals by a piecewise cubic Hermite spline interpolation. Nine CTD profiles obtained in the cruise MR03-K02 are shown.

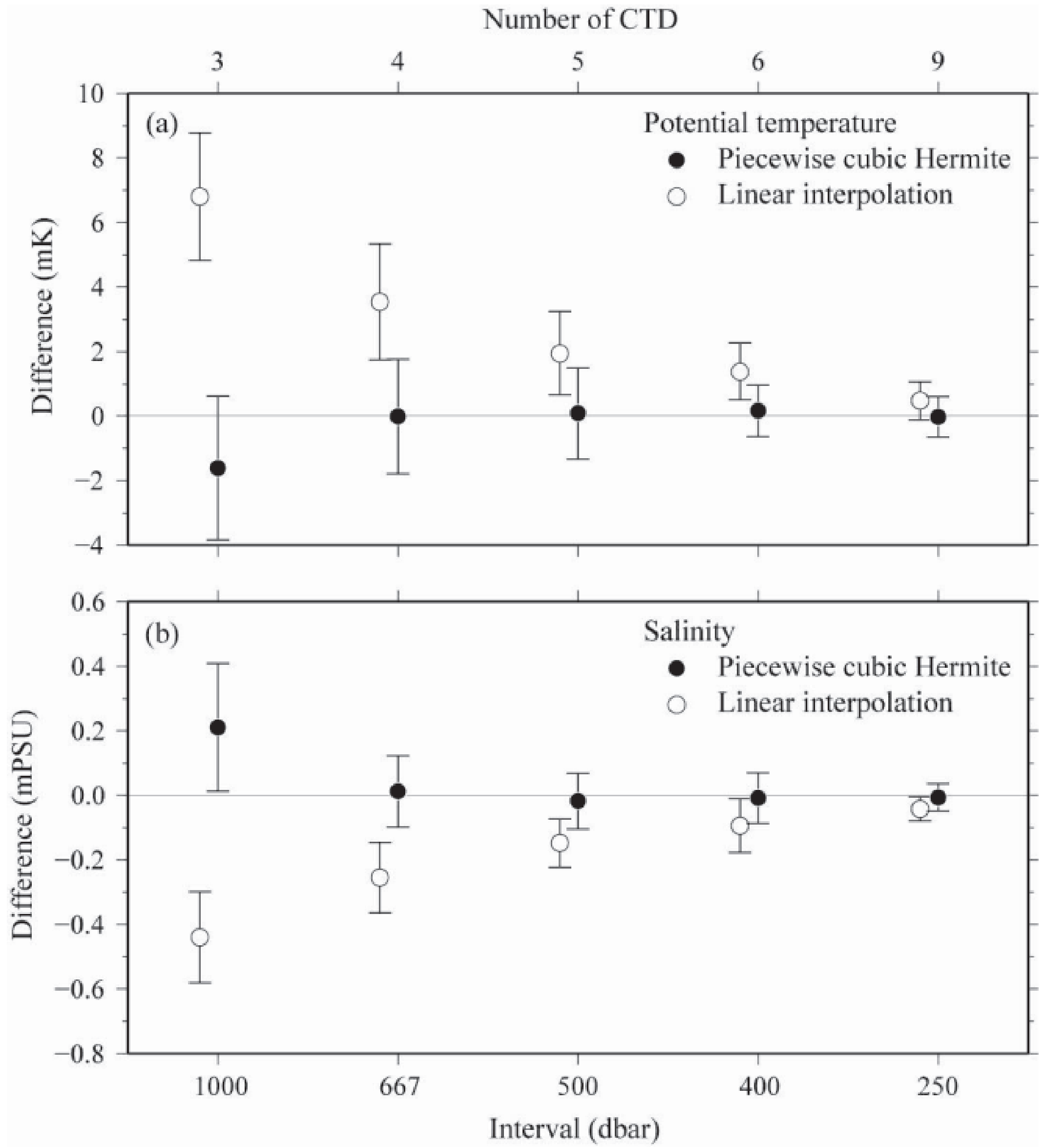

Figure 3.5.3. Mean difference in (a) temperature and (b) salinity between observed and estimated vertical profiles for depths between 3400 and 5400 dbar. Results obtained from the data sub-sampled at 1000, 667, 500, 400, and 250 dbar intervals are shown. Twenty-seven CTD profiles obtained in the cruises MR03-K02, KH04-4 leg 2, and MR05-05 leg 2 are used. Vertical bars show their standard deviations.

Statistics of current meter records

Instrument depth (m)	Record length (days)	Mean velocity: Magnitude (cm s^{-1})	Mean velocity: Direction (°T)	Mean velocity: Stability (%)	Standard error: Major (cm s^{-1})	Standard error: Direction (°T)	Std. error ratio Min./Maj. (%)	Time scale: Major (days)	Time scale: Minor (days)	$\langle u \rangle$ (cm s^{-1})	$\langle v \rangle$ (cm s^{-1})	$\langle u'v' \rangle$ (cm^2 s^{-2})	$\langle u'^2 \rangle$ (cm^2 s^{-2})	$\langle v'^2 \rangle$ (cm^2 s^{-2})	K_E (cm^2 s^{-2})	K_M (cm^2 s^{-2})	Standard error: u (cm s^{-1})	Standard error: v (cm s^{-1})	Time scale: u (days)	Time scale: v (days)
WM1: Latitude, 12.77765 N; Longitude, 170.23980 E; Depth, 5367 m, 3 June 2003 - 14 December 2005																				
3413	926	0.72	277	25	0.72	251	22.9	24.8	7.5	-0.71	0.09	2.46	8.73	2.51	5.62	0.26	0.87	0.24	39.7	10.8
4410	926	0.04	266	2	0.39	262	22.4	16.7	4.0	-0.04	0.00	0.44	4.20	0.96	2.58	0.00	0.39	0.09	16.9	4.3
5272	833*	0.26	244	7	0.59	269	24.0	8.6	3.9	-0.23	-0.12	0.21	17.18	2.14	9.66	0.03	0.59	0.14	8.5	4.0
*Data gap (93 days) from 16 July to 16 October, 2004																				
WM2: Latitude, 13.65380 N; Longitude, 170.57265 E; Depth, 5516 m, 2 June 2003 - 13 December 2005																				
3389	926	1.74	299	65	0.36	009	72.5	15.1	15.2	-1.51	0.86	0.31	2.15	3.96	3.05	1.51	0.26	0.36	14.7	15.2
4386	926	1.56	314	53	0.41	339	83.1	15.1	16.0	-1.12	1.08	-0.62	3.63	4.96	4.30	1.22	0.38	0.40	18.2	14.9
5398	832*	2.20	337	55	0.80	341	57.7	19.9	14.2	-0.85	2.04	-2.16	6.95	12.53	9.74	2.43	0.53	0.76	16.9	19.2
*Data gap (94 days) from 16 July to 17 October, 2004																				
WM3: Latitude, 14.57785 N; Longitude, 170.90710 E; Depth, 5678 m, 1 June 2003 - 13 December 2005																				
3382	927	0.14	249	6	0.31	340	106.4	14.3	18.4	-0.13	-0.05	-0.12	2.78	3.07	2.93	0.01	0.32	0.32	16.6	15.0
4380	927	0.69	297	30	0.38	356	70.8	14.6	13.6	-0.62	0.32	-0.13	2.41	4.46	3.44	0.24	0.26	0.38	13.4	14.7
5388	832*	1.55	295	43	0.61	347	65.7	12.5	10.6	-1.41	0.64	-1.33	6.60	12.00	9.30	1.20	0.40	0.61	10.2	12.7
*Data gap (95 days) from 16 July to 18 October, 2004																				
WM4: Latitude, 15.51220 N; Longitude, 171.24190 E; Depth, 5614 m, 1 June 2003 - 12 December 2005																				
3439	926	0.25	034	12	0.35	111	71.2	14.7	14.8	0.14	0.20	-0.63	3.55	2.14	2.85	0.03	0.36	0.24	16.6	12.2
4437	926	1.06	082	46	0.33	102	66.6	14.1	10.7	1.04	0.15	-0.29	3.42	2.10	2.76	0.56	0.33	0.22	14.8	10.2
5452	926	2.22	082	57	0.55	076	56.6	11.8	6.5	2.20	0.31	1.14	11.37	7.04	9.21	2.47	0.52	0.34	11.0	7.5
WM5: Latitude, 16.42490 N; Longitude, 171.54835 E; Depth, 5467 m, 31 May 2003 - 11 December 2005																				
3374	926	0.55	263	26	0.36	239	44.8	14.0	9.5	-0.55	-0.07	1.35	3.55	2.09	2.82	0.15	0.32	0.24	13.0	12.9
4370	926	1.27	257	46	0.44	246	32.6	11.8	6.5	-1.24	-0.29	2.28	6.49	2.50	4.49	0.81	0.40	0.24	11.2	10.3
5373	926	1.74	275	47	0.73	262	18.2	13.8	2.1	-1.74	0.15	1.82	17.55	4.09	10.82	1.52	0.71	0.20	13.2	4.4

Standard error was estimated following Dickson et al. (1985) and time scale is the integral time scale. Stability is the directional stability defined by the ratio of vector mean velocity to scalar mean velocity. *u* and *v* denote eastward and northward respectively. Data are low-pass filtered to remove periods lower than 2 days. K_E is the eddy kinetic energy per unit mass and K_M is the kinetic energy per unit mass of the mean flow.

Photos of moored instruments and shipboard CTD used in the WIFE

3D-ACM

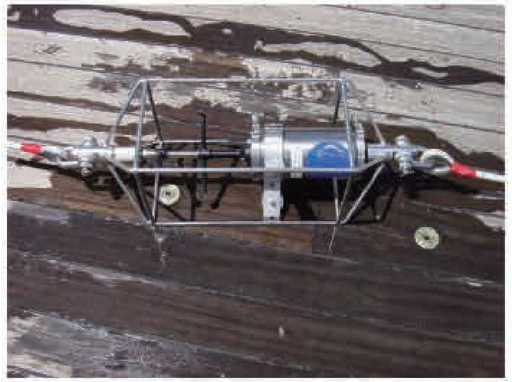

RCM-11

RCM-8

SBE-37SM

Compact-OPTODE

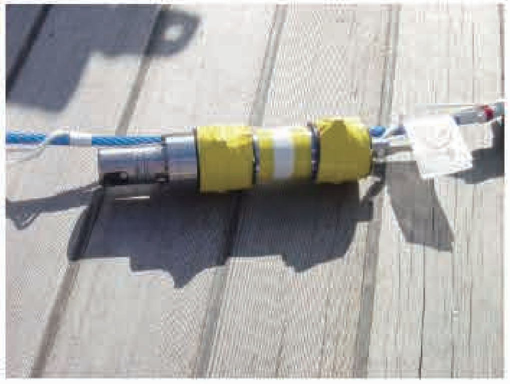

Transponder XT-6000

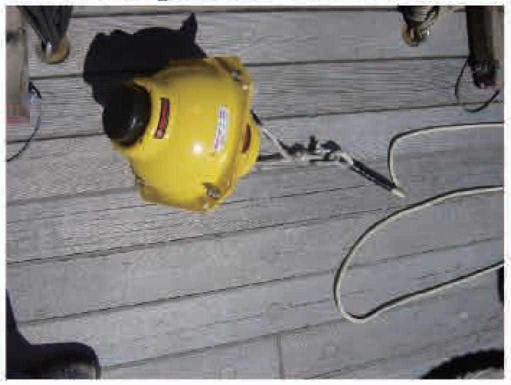

Acoustic Releasers, Model-L

17-inch Glass Buoys

Rail Anchor

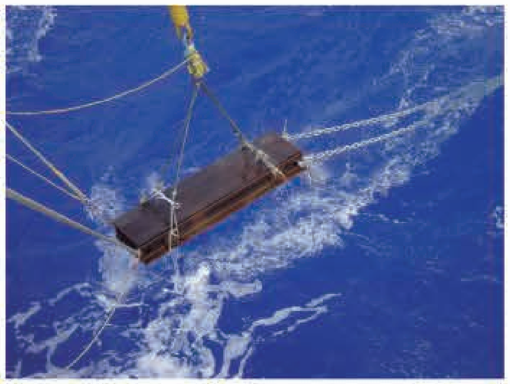

SBE-9*plus* CTD with SBE-35

SBE-9*plus* with Moored CTDs and OPTODEs

R/V Mirai

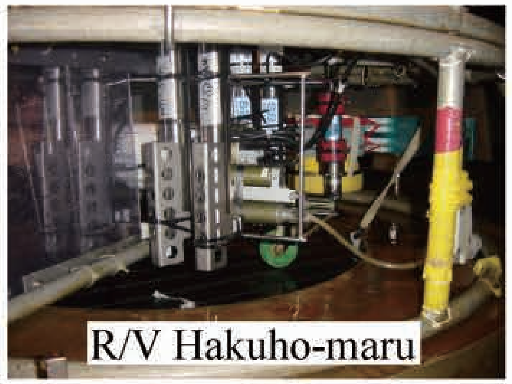

R/V Hakuho-maru

WIFE cruises station summary files

WIFE R/V MIRAI CRUISE MR03-K02

SHIP/CRS EXPOCODE	SECT	STNNBR	CASTNO	CAST TYPE	DATE	UTC TIME	EVENT CODE	POSITION LATITUDE	LONGITUDE	NAV	UNC DEPTH	COR DEPTH	HT ABOVE BOTTOM	WIRE OUT	MAX PRESS	NO. OF BOTTLES	PARAMETERS	COMMENTS
49MR03K02_1	WIFE	WC9	1	ROS	052703	1550	BE	16 25.04 N	171 34.98 E	GPS	-9	5471						LADCP
49MR03K02_1	WIFE	WC9	1	ROS	052703	1714	BO	16 25.13 N	171 34.87 E	GPS	-9	5471	8	5466	5562	36	1-8,12,13,23,24,26	WITH SMALL VANE
49MR03K02_1	WIFE	WC9	1	ROS	052703	1920	EN	16 25.34 N	171 34.59 E	GPS	-9	5474						#16 NOT CONFIRMED
49MR03K02_1	WIFE	WM5	1	MOR	052703	2328	BE	16 24.41 N	171 30.43 E	GPS	-9	5446						TRANSPONDER TX 14.5KHZ, RX 13.0KHZ
49MR03K02_1	WIFE	WM5	1	MOR	052803	0039	DE	16 24.60 N	171 32.53 E	GPS	-9	5458						NY A/R 4224-1E, 4271-3G
49MR03K02_1	WIFE	WC8	1	ROS	052803	0404	BE	15 57.65 N	171 24.84 E	GPS	-9	5532						LADCP
49MR03K02_1	WIFE	WC8	1	ROS	052803	0534	BO	15 58.23 N	171 24.76 E	GPS	-9	5538	5	5531	5625	36	1-8,13,23,24	WITH SMALL VANE
49MR03K02_1	WIFE	WC8	1	ROS	052803	0749	EN	15 58.77 N	171 24.91 E	GPS	-9	5538						
49MR03K02_1	WIFE	WC7	1	ROS	052803	1208	BE	15 30.26 N	171 15.09 E	GPS	-9	5612						LADCP
49MR03K02_1	WIFE	WC7	1	ROS	052803	1345	BO	15 30.97 N	171 15.08 E	GPS	-9	5614	7	5636	5703	36	1-8,12,13,23,24,26	WITH SMALL VANE, WIRE SPEED 1M/S
49MR03K02_1	WIFE	WC7	1	ROS	052803	1601	EN	15 30.97 N	171 14.92 E	GPS	-9	5606						#16 NOT CONFIRMED
49MR03K02_1	WIFE	WM4	1	MOR	052803	2146	BE	15 30.54 N	171 11.94 E	GPS	-9	5607						TRANSPONDER TX 13.5KHZ, RX 13.0KHZ
49MR03K02_1	WIFE	WM4	1	MOR	052803	2247	DE	15 30.10 N	171 14.18 E	GPS	-9	5614						NY A/R 4465-1D, 4459-1B
49MR03K02_1	WIFE	WM3	1	MOR	052903	0442	BE	14 35.00 N	170 51.61 E	GPS	-9	5676						TRANSPONDER TX 14.0KHZ, RX 13.0KHZ
49MR03K02_1	WIFE	WM3	1	MOR	052903	0550	DE	14 35.10 N	170 53.55 E	GPS	-9	5676						NY A/R 4448-1A, 4235-1G
49MR03K02_1	WIFE	WC5	1	ROS	052903	0648	BE	14 36.72 N	170 51.66 E	GPS	-9	5664						LADCP
49MR03K02_1	WIFE	WC5	1	ROS	052903	0814	BO	14 36.93 N	170 51.68 E	GPS	-9	5663	7	5654	5758	36	1-8,12,13,23,24,26	WITH TWO SMALL VANES
49MR03K02_1	WIFE	WC5	1	ROS	052903	1023	EN	14 37.17 N	170 51.76 E	GPS	-9	5663						#16 NOT CONFIRMED
49MR03K02_1	WIFE	WC6	1	ROS	052903	1320	BE	15 2.77 N	171 4.99 E	GPS	-9	5674						LADCP
49MR03K02_1	WIFE	WC6	1	ROS	052903	1446	BO	15 2.87 N	171 5.13 E	GPS	-9	5678	8	5667	5767	36	1-8,13,23,24	BETWEEN TWO SMALL SEA MONTAINS
49MR03K02_1	WIFE	WC6	1	ROS	052903	1705	EN	15 3.42 N	171 5.26 E	GPS	-9	5671						#16 NOT CONFIRMED
49MR03K02_1	WIFE	WC4	1	ROS	052903	2119	BE	14 7.43 N	170 44.95 E	GPS	-9	5625						LADCP
49MR03K02_1	WIFE	WC4	1	ROS	052903	2243	BO	14 7.61 N	170 44.78 E	GPS	-9	5625	7	5619	5719	36	1-8,13,23,24	WITH LAGE VANE
49MR03K02_1	WIFE	WC4	1	ROS	053003	0045	EN	14 7.77 N	170 44.84 E	GPS	-9	5625						
49MR03K02_1	WIFE	WM2	1	MOR	053003	0415	BE	13 40.03 N	170 32.37 E	GPS	-9	5513						TRANSPONDER TX 15.0KHZ, RX 13.0KHZ
49MR03K02_1	WIFE	WM2	1	MOR	053003	0520	DE	13 40.01 N	170 34.02 E	GPS	-9	5511						NY A/R 4236-1H, 4232-3E
49MR03K02_1	WIFE	WC3	1	ROS	053003	0618	BE	13 37.66 N	170 33.30 E	GPS	-9	5512						LADCP
49MR03K02_1	WIFE	WC3	1	ROS	053003	0739	BO	13 37.84 N	170 33.00 E	GPS	-9	5506	7	5507	5601	36	1-8,12,13,23,24,26	WITH SMALL VANE (OPPOSITE SIDE AS WC9)
49MR03K02_1	WIFE	WC3	1	ROS	053003	0945	EN	13 38.35 N	170 32.89 E	GPS	-9	5511						#25 MISS FIRED
49MR03K02_1	WIFE	WC2	1	ROS	053003	1232	BE	13 12.47 N	170 25.01 E	GPS	-9	5403						LADCP
49MR03K02_1	WIFE	WC2	1	ROS	053003	1354	BO	13 12.47 N	170 24.99 E	GPS	-9	5403	7	5429	5487	36	1-8,13,23,24,26	WITH LARGE VANE
49MR03K02_1	WIFE	WC2	1	ROS	053003	1616	EN	13 13.63 N	170 24.84 E	GPS	-9	5404						#16 NOT CONFIRMED, CABLE DISORDERED AT 670M
49MR03K02_1	WIFE	WC1	1	ROS	053003	1832	BE	12 45.97 N	170 14.83 E	GPS	-9	5361						LADCP
49MR03K02_1	WIFE	WC1	1	ROS	053003	2004	BO	12 46.26 N	170 14.87 E	GPS	-9	5369	8	5364	5449	36	1-8,12,13,23,24,26	WIRE SPEED 1M/S
49MR03K02_1	WIFE	WC1	1	ROS	053003	2231	EN	12 47.06 N	170 14.60 E	GPS	-9	5364						#16 NOT CONFIRMED
49MR03K02_1	WIFE	WM1	1	MOR	053103	0019	BE	12 46.92 N	170 12.36 E	GPS	-9	5344						TRANSPONDER TX 14.5KHZ, RX 13.0KHZ
49MR03K02_1	WIFE	WM1	1	MOR	053103	0118	DE	12 47.42 N	170 13.88 E	GPS	-9	5356						NY A/R 4454-1C, 4424-3A

Parameter number:

1=SALNTY, 2=OXYGEN, 3=SILCAT, 4=NITRAT, 5=NITRIT, 6=PPHSPHT, 7=CFC-11, 8=CFC-12, 12=DELC14, 13=DELC13, 23=TCARBN, 24=ALKALI, 26=PH, 27=CFC113

WIFE R/V HAKUHO-MARU CRUISE KH04-4 LEG 2

SHIP/CRS EXPOCODE	SECT	STNNBR	CASTNO	CAST TYPE	DATE	UTC TIME	EVENT CODE	POSITION LATITUDE	LONGITUDE	NAV	UNC DEPTH	COR DEPTH	HT ABOVE BOTTOM	WIRE OUT	MAX PRESS	NO. OF BOTTLES	PARAMETERS	COMMENTS
49HH044_2	WIFE	C094	1	ROS	101304	0957	BE	12 43.11 N	170 13.72 E	GPS	5042	-9						LADCP, WIFE WC0
49HH044_2	WIFE	C094	1	ROS	101304	1120	BO	12 43.12 N	170 13.58 E	GPS	-9	-9	19	4422	4488	24	1-6	SBE9P400 CTDO
49HH044_2	WIFE	C094	1	ROS	101304	1255	EN	12 43.13 N	170 13.31 E	GPS	4138	-9						
49HH044_2	WIFE	C095	1	ROS	101304	1609	BE	12 45.90 N	170 13.99 E	GPS	5282	-9						LADCP, WIFE WC1
49HH044_2	WIFE	C095	1	ROS	101304	1752	BO	12 45.98 N	170 13.75 E	GPS	-9	-9	18	5344	5437	21	1-6	SBE9P400 CTDO
49HH044_2	WIFE	C095	1	ROS	101304	1947	EN	12 46.35 N	170 13.52 E	GPS	5273	-9						
49HH044_2	WIFE	WM1	1	MOR	101304	2152	BE	12 47.50 N	170 13.57 E	GPS	5250	-9						1 3DACM, 1 RCM11, 1 RCM8, 5 MICROCAT
49HH044_2	WIFE	WM1	1	MOR	101304	2250	RE	12 47.36 N	170 12.62 E	GPS	5259	-9						TRANSPONDER 13.0KHZ/14.5KHZ, A/R 1C/1A
49HH044_2	WIFE	WM1	2	MOR	101404	0211	BE	12 45.80 N	170 12.51 E	GPS	5258	-9						2 RCM11, 1 RCM8, 7 MICROCAT, 1 OPTODE
49HH044_2	WIFE	WM1	2	MOR	101404	0344	DE	12 45.90 N	170 14.90 E	GPS	5287	-9						TRANSPONDER 13.0KHZ/14.5KHZ, A/R 1F/1B
49HH044_2	WIFE	C096	1	ROS	101404	0635	BE	13 12.48 N	170 24.59 E	GPS	5319	-9						LADCP, WIFE WC2
49HH044_2	WIFE	C096	1	ROS	101404	0813	BO	13 12.58 N	170 24.35 E	GPS	-9	-9	19	5377	5471	23	1-6	SBE9P400 CTDO
49HH044_2	WIFE	C096	1	ROS	101404	1002	EN	13 12.66 N	170 24.19 E	GPS	5317	-9						
49HH044_2	WIFE	C097	1	ROS	101404	1241	BE	13 38.77 N	170 33.36 E	GPS	5426	-9						LADCP, WIFE WC3
49HH044_2	WIFE	C097	1	ROS	101404	1430	BO	13 38.91 N	170 33.23 E	GPS	-9	-9	20	5492	5590	24	1-6	SBE9P400 CTDO
49HH044_2	WIFE	C097	1	ROS	101404	1651	EN	13 38.92 N	170 33.30 E	GPS	5426	-9						
49HH044_2	WIFE	WM2	1	MOR	101404	2144	BE	13 39.99 N	170 33.69 E	GPS	5426	-9						1 3DACM, 1 RCM11, 1 RCM8, 5 MICROCAT
49HH044_2	WIFE	WM2	1	MOR	101404	2246	RE	13 39.77 N	170 33.06 E	GPS	5430	-9						TRANSPONDER 13.0KHZ/15.0KHZ, A/R 1H/3E
49HH044_2	WIFE	WM2	2	MOR	101504	0224	BE	13 38.26 N	170 32.04 E	GPS	5425	-9						2 RCM11, 1 RCM8, 8 MicroCAT, 1 OPTODE
49HH044_2	WIFE	WM2	2	MOR	101504	0351	DE	13 38.45 N	170 34.70 E	GPS	5426	-9						TRANSPONDER 13.0KHZ/15.0KHZ, A/R 3D/1C
49HH044_2	WIFE	C098	1	ROS	101504	0646	BE	14 7.37 N	170 44.56 E	GPS	5536	-9						LADCP, WIFE WC4
49HH044_2	WIFE	C098	1	ROS	101504	0831	BO	14 7.44 N	170 44.38 E	GPS	-9	-9	19	5603	5705	23	1-6	SBE9P400 CTDO
49HH044_2	WIFE	098	1	ROS	101504	1025	EN	14 7.36 N	170 44.36 E	GPS	5534	-9						
49HH044_2	WIFE	C099	1	ROS	101504	1301	BE	14 33.93 N	170 54.57 E	GPS	5582	-9						LADCP, WIFE WC5
49HH044_2	WIFE	C099	1	ROS	101504	1448	BO	14 34.08 N	170 54.48 E	GPS	-9	-9	19	5655	5756	24	1-8	SBE9P400 CTDO
49HH044_2	WIFE	C099	1	ROS	101504	1705	EN	14 34.65 N	170 54.23 E	GPS	5584	-9						
49HH044_2	WIFE	WM3	1	MOR	101504	2105	BE	14 35.28 N	170 53.09 E	GPS	5586	-9						1 3DACM, 1 RCM11, 1 RCM8, 5 MICROCAT
49HH044_2	WIFE	WM3	1	MOR	101504	2218	RE	14 35.12 N	170 52.13 E	GPS	5584	-9						TRANSPONDER 13.0KHZ/14.0KHZ, A/R 1A/3G
49HH044_2	WIFE	WM3	2	MOR	101604	0227	BE	14 32.43 N	170 53.59 E	GPS	5578	-9						2 RCM11, 1 RCM8, 8 MICROCAT, 1 OPTODE
49HH044_2	WIFE	WM3	2	MOR	101604	0410	DE	14 34.24 N	170 55.30 E	GPS	5582	-9						TRANSPONDER 13.0KHZ/14.0KHZ, A/R 3F/3E
49HH044_2	WIFE	C100	1	ROS	101604	0717	BE	15 2.75 N	171 4.78 E	GPS	5579	-9						LADCP, WIFE WC6
49HH044_2	WIFE	C100	1	ROS	101604	0904	BO	15 2.94 N	171 4.34 E	GPS	-9	-9	20	5650	5747	24	1-6	SBE9P400 CTDO
49HH044_2	WIFE	C100	1	ROS	101604	1101	EN	15 3.03 N	171 4.03 E	GPS	5566	-9						
49HH044_2	WIFE	C101	1	ROS	101604	1354	BE	15 31.30 N	171 14.90 E	GPS	5518	-9						LADCP, WIFE WC7
49HH044_2	WIFE	C101	1	ROS	101604	1542	BO	15 31.37 N	171 14.50 E	GPS	-9	-9	19	5602	5694	24	1-6	SBE9P400 CTDO
49HH044_2	WIFE	C101	1	ROS	101604	1756	EN	15 31.39 N	171 13.99 E	GPS	5515	-9						
49HH044_2	WIFE	WM4	1	MOR	101604	2111	BE	15 30.23 N	171 13.63 E	GPS	5522	-9						1 3DACM, 1 RCM11, 1 RCM8, 5 MICROCAT
49HH044_2	WIFE	WM4	1	MOR	101604	2211	RE	15 29.91 N	171 12.83 E	GPS	5513	-9						TRANSPONDER 13.0KHZ/13.5KHZ, A/R 1D/1B
49HH044_2	WIFE	WM4	2	MOR	101704	0221	BE	15 29.72 N	171 13.93 E	GPS	5520	-9						2 RCM11, 1 RCM8, 8 MICROCAT, 1 OPTODE
49HH044_2	WIFE	WM4	2	MOR	101704	0345	DE	15 31.36 N	171 14.85 E	GPS	5520	-9						TRANSPONDER 13.0KHZ/13.5KHZ, A/R 3C/1F
49HH044_2	WIFE	C102	1	ROS	101704	0639	BE	15 57.66 N	171 24.65 E	GPS	5449	-9						LADCP, WIFE WC8
49HH044_2	WIFE	C102	1	ROS	101704	0822	BO	15 57.90 N	171 24.19 E	GPS	-9	-9	19	5536	5615	23	1-6	SBE9P400 CTDO

49HH044_2	WIFE	C102	1	ROS	101704	1014	EN	15	58.05	N	171	24.01	E	GPS	5450	-9							
49HH044_2	WIFE	C103	1	CTD	101704	1251	BE	16	25.95	N	171	32.75	E	GPS	5393	-9							LADCP, WIFE WC9
49HH044_2	WIFE	C103	1	CTD	101704	1325	BO	16	26.00	N	171	32.71	E	GPS	-9	-9	-9	1585	1550	0			SBE9P400 CTDO
49HH044_2	WIFE	C103	1	CTD	101704	1409	EN	16	26.00	N	171	32.67	E	GPS	5386	-9							
49HH044_2	WIFE	C103	2	ROS	101704	1553	BE	16	26.00	N	171	32.92	E	GPS	5389	-9							LADCP, WIFE WC9
49HH044_2	WIFE	C103	2	ROS	101704	1733	BO	16	26.03	N	171	32.89	E	GPS	-9	-9	19	5449	5546	23	1-6		SBE9P400 CTDO
49HH044_2	WIFE	C103	2	ROS	101704	1933	EN	16	26.28	N	171	32.60	E	GPS	5388	-9							
49HH044_2	WIFE	WM5	1	MOR	101704	2107	BE	16	24.51	N	171	32.24	E	GPS	5374	-9							1 3DACM, 1 RCM11, 1 RCM8, 5 MICROCAT
49HH044_2	WIFE	WM5	1	MOR	101704	2157	RE	16	24.29	N	171	31.72	E	GPS	5370	-9							TRANSPONDER 13.0KHZ/14.5KHZ, A/R 1E/3G
49HH044_2	WIFE	WM5	2	MOR	101804	0225	BE	16	24.69	N	171	31.81	E	GPS	5373	-9							2 RCM11, 1 RCM8, 7 MICROCAT, 1 OPTODE
49HH044_2	WIFE	WM5	2	MOR	101804	0343	DE	16	26.39	N	171	33.27	E	GPS	5385	-9							TRANSPONDER 13.0KHZ/14.5KHZ, A/R 1C/1D
49HH044_2	WIFE	C103	3	ROS	101804	0501	BE	16	24.69	N	171	32.42	E	GPS	5546	-9							LADCP, WIFE WC9
49HH044_2	WIFE	C103	3	ROS	101804	0648	BO	16	24.71	N	171	32.35	E	GPS	-9	-9	18	5440	5537	23	1-6		SBE9P400 CTDO
49HH044_2	WIFE	C103	3	ROS	101804	0843	EN	16	24.73	N	171	32.32	E	GPS	5375	-9							
49HH044_2	WIFE	C104	1	ROS	101804	1012	BE	16	33.02	N	171	32.40	E	GPS	4236	-9							LADCP, WIFE WC10
49HH044_2	WIFE	C104	1	ROS	101804	1133	BO	16	32.98	N	171	32.40	E	GPS	-9	-9	20	4314	4377	22	1-6		SBE9P400 CTDO
49HH044_2	WIFE	C104	1	ROS	101804	1307	EN	16	33.07	N	171	32.28	E	GPS	4243	-9							

Parameter number:

1=SALNTY, 2=OXYGEN, 3=SILCAT, 4=NITRAT, 5=NITRIT, 6=PPHSPHT

WIFE R/V MIRAI CRUISE MR05-05 LEG 2

SHIP/CRS EXPOCODE	SECT	STNNBR	CASTNO	CAST TYPE	DATE	UTC TIME	EVENT CODE	LATITUDE	LONGITUDE	NAV	UNC DEPTH	COR DEPTH	HT ABOVE BOTTOM	WIRE OUT	MAX PRESS	NO. OF BOTTLES	PARAMETERS	COMMENTS
49MR0505_2	WIFE	WM5	1	MOR	121305	2042	BE	16 26.41 N	171 32.88 E	GPS	5476	5475						RCM11, 1 RCM8, 7 SBE37, 1 OPTODE
49MR0505_2	WIFE	WM5	1	MOR	121305	2200	RE	16 26.78 N	171 31.04 E	GPS	5469	5471						6 GRASS BUOY BROKEN, 1 SBE37 BROKEN
49MR0505_2	WIFE	WM4	1	MOR	121405	1943	BE	15 31.28 N	171 14.50 E	GPS	5614	5611						2 RCM11, 1 RCM8, 8 SBE37, 1 OPTODE
49MR0505_2	WIFE	WM4	1	MOR	121405	2103	RE	15 31.75 N	171 14.60 E	GPS	5606	5606						1 SBE37 BROKEN
49MR0505_2	WIFE	WM3	1	MOR	121505	0258	BE	14 34.04 N	170 55.08 E	GPS	5673	5672						2 RCM11, 1 RCM8, 8 SBE37, 1 OPTODE
49MR0505_2	WIFE	WM3	1	MOR	121505	0409	RE	14 34.00 N	170 55.02 E	GPS	5678	5673						2 SBE37 BROKEN
49MR0505_2	WIFE	WM2	1	MOR	121505	2133	BE	13 38.40 N	170 34.19 E	GPS	-9	5525						2 RCM11, 1 RCM8, 8 SBE37, 1 OPTODE
49MR0505_2	WIFE	WM2	1	MOR	121505	2259	RE	13 38.28 N	170 33.84 E	GPS	5516	5519						TRANSPONDER BROKEN, 1 SBE37 BROKEN
49MR0505_2	WIFE	WM1	1	MOR	121605	0503	BE	12 45.89 N	170 14.60 E	GPS	5362	5364						2 RCM11, 1 RCM8, 7 SBE37, 1 OPTODE
49MR0505_2	WIFE	WM1	1	MOR	121605	0603	RE	12 45.64 N	170 13.58 E	GPS	5348	5352						TRANSPONDER BROKEN, ROTOR OF RCM8 LOST
49MR0505_2	WIFE	WC0	1	ROS	121605	0833	BE	12 43.32 N	170 13.59 E	GPS	4560	4563						
49MR0505_2	WIFE	WC0	1	BUC	121605	0841	UN	12 43.37 N	170 13.51 E	GPS	4545	4556					1,33	27.8C
49MR0505_2	WIFE	WC0	1	UNK	121605	0850	UN	12 43.43 N	170 13.45 E	GPS	4577	4576						AIR N2O SMPL
49MR0505_2	WIFE	WC0	1	ROS	121605	0947	BO	12 43.80 N	170 13.34 E	GPS	4658	4667	9	4625	4669	32	1-8,27	
49MR0505_2	WIFE	WC0	1	ROS	121605	1145	EN	12 44.73 N	170 12.96 E	GPS	5267	5267						
49MR0505_2	WIFE	WC1	1	ROS	121605	1359	BE	12 45.89 N	170 14.88 E	GPS	5369	5369						WITH 7 SBE37 (WM1)
49MR0505_2	WIFE	WC1	1	BUC	121605	1406	UN	12 45.98 N	170 14.85 E	GPS	5356	5365					1	27.8C
49MR0505_2	WIFE	WC1	1	ROS	121605	1524	BO	12 46.60 N	170 14.58 E	GPS	5369	5373	7	5426	5450	35	1-8,27	
49MR0505_2	WIFE	WC1	1	ROS	121605	1745	EN	12 47.35 N	170 14.24 E	GPS	5347	5351						
49MR0505_2	WIFE	WC2	1	ROS	121605	2032	BE	13 12.56 N	170 24.85 E	GPS	5406	5408						
49MR0505_2	WIFE	WC2	1	BUC	121605	2039	UN	13 12.63 N	170 24.72 E	GPS	5402	5402					1,33	27.8C
49MR0505_2	WIFE	WC2	1	UNK	121605	2048	UN	13 12.71 N	170 24.64 E	GPS	5406	5403						AIR N2O SMPL
49MR0505_2	WIFE	WC2	1	ROS	121605	2152	BO	13 13.10 N	170 24.54 E	GPS	5401	5403	9	5412	5483	35	1-8,27	#1 MISS TRIP
49MR0505_2	WIFE	WC2	1	ROS	121705	0007	EN	13 13.80 N	170 23.85 E	GPS	5406	5405						
49MR0505_2	WIFE	WC3	1	ROS	121705	0249	BE	13 38.37 N	170 34.54 E	GPS	5518	5516						WITH 6 SBE37 (WM5)
49MR0505_2	WIFE	WC3	1	BUC	121705	0256	UN	13 38.44 N	170 34.40 E	GPS	5525	5522					1,33	27.8C
49MR0505_2	WIFE	WC3	1	UNK	121705	0305	UN	13 38.55 N	170 34.31 E	GPS	5520	5519						AIR N2O SMPL
49MR0505_2	WIFE	WC3	1	ROS	121705	0415	BO	13 39.01 N	170 34.23 E	GPS	5518	5519	9	5540	5602	36	1-6	
49MR0505_2	WIFE	WC3	1	ROS	121705	0639	EN	13 39.95 N	170 33.68 E	GPS	5510	5510						
49MR0505_2	WIFE	WC4	1	ROS	121705	0934	BE	14 7.46 N	170 45.04 E	GPS	5627	5628						WITH 7 SBE37 (WM4)
49MR0505_2	WIFE	WC4	1	BUC	121705	0941	UN	14 7.53 N	170 44.98 E	GPS	5624	5625					1,33	27.7C
49MR0505_2	WIFE	WC4	1	UNK	121705	0950	UN	14 7.63 N	170 44.92 E	GPS	5627	5625						AIR N2O SMPL
49MR0505_2	WIFE	WC4	1	ROS	121705	1103	BO	14 8.19 N	170 44.86 E	GPS	5627	5629	9	5664	5721	36	1-6	
49MR0505_2	WIFE	WC4	1	ROS	121705	1326	EN	14 9.37 N	170 44.83 E	GPS	5658	5651						
49MR0505_2	WIFE	WC5	1	ROS	121705	1612	BE	14 34.23 N	170 55.24 E	GPS	5672	5673						WITH 6 SBE37 (WM3)
49MR0505_2	WIFE	WC5	1	BUC	121705	1619	UN	14 34.31 N	170 55.18 E	GPS	5674	5674					1,33	27.7C
49MR0505_2	WIFE	WC5	1	UNK	121705	1628	UN	14 34.38 N	170 55.14 E	GPS	5672	5674						AIR N2O SMPL
49MR0505_2	WIFE	WC5	1	ROS	121705	1739	BO	14 34.87 N	170 55.04 E	GPS	5674	5674	10	5716	5769	36	1-6	#8 MISS TRIP
49MR0505_2	WIFE	WC5	1	ROS	121705	2003	EN	14 35.77 N	170 54.57 E	GPS	5681	5683						
49MR0505_2	WIFE	WC6	1	ROS	121705	2258	BE	15 2.38 N	171 4.81 E	GPS	5673	5672						
49MR0505_2	WIFE	WC6	1	BUC	121705	2307	UN	15 2.45 N	171 4.72 E	GPS	5672	5672					1,33	27.9C
49MR0505_2	WIFE	WC6	1	UNK	121705	2316	UN	15 2.52 N	171 4.65 E	GPS	5702	5690						AIR N2O SMPL

49MR0505_2	WIFE	WC6	1	ROS	121805	0025	BO	15	3.13	N	171	4.30	E	GPS	5663	5670	8	5767	5768	36	1-6	
49MR0505_2	WIFE	WC6	1	ROS	121805	0246	EN	15	4.47	N	171	3.60	E	GPS	5383	5385						
49MR0505_2	WIFE	WC7	1	ROS	121805	0530	BE	15	31.30	N	171	14.83	E	GPS	5618	5618						WITH 7 SBE37 (WM2)
49MR0505_2	WIFE	WC7	1	BUC	121805	0537	UN	15	31.37	N	171	14.82	E	GPS	5606	5607					1,33	27.8C
49MR0505_2	WIFE	WC7	1	UNK	121805	0547	UN	15	31.43	N	171	14.74	E	GPS	5619	5618						AIR N2O SMPL
49MR0505_2	WIFE	WC7	1	ROS	121805	0656	BO	15	31.74	N	171	14.64	E	GPS	5608	5607	11	5623	5701	36	1-6	PRI SENSORS SHIFTED
49MR0505_2	WIFE	WC7	1	ROS	121805	0918	EN	15	32.73	N	171	14.42	E	GPS	5610	5609						1 SBE37 BROKEN
49MR0505_2	WIFE	WC8	1	ROS	121805	1215	BE	15	57.46	N	171	25.04	E	GPS	5538	5537						PRI OXYGEN SENSOR REPLACED, WITH 5 COMPACT-OPTODE
49MR0505_2	WIFE	WC8	1	BUC	121805	1222	UN	15	57.50	N	171	25.00	E	GPS	5539	5539					1,33	27.8C
49MR0505_2	WIFE	WC8	1	UNK	121805	1230	UN	15	57.56	N	171	24.93	E	GPS	5538	5538						AIR N2O SMPL
49MR0505_2	WIFE	WC8	1	ROS	121805	1340	BO	15	58.06	N	171	24.76	E	GPS	5537	5537	9	5578	5623	36	1-6	
49MR0505_2	WIFE	WC8	1	ROS	121805	1557	EN	15	59.32	N	171	24.25	E	GPS	5574	5574						
49MR0505_2	WIFE	WC9	1	ROS	121805	1839	BE	16	26.28	N	171	33.22	E	GPS	5473	5474						
49MR0505_2	WIFE	WC9	1	BUC	121805	1847	UN	16	26.34	N	171	33.19	E	GPS	5471	5472					1,33	27.7C
49MR0505_2	WIFE	WC9	1	UNK	121805	1856	UN	16	26.42	N	171	33.15	E	GPS	5472	5474						AIR N2O SMPL
49MR0505_2	WIFE	WC9	1	ROS	121805	2003	BO	16	26.90	N	171	32.95	E	GPS	5471	5471	8	5510	5561	36	1-6	
49MR0505_2	WIFE	WC9	1	ROS	121805	2218	EN	16	27.96	N	171	32.64	E	GPS	5327	5340						
49MR0505_2	WIFE	WC10	1	ROS	121805	2346	BE	16	32.92	N	171	32.30	E	GPS	4341	4351						
49MR0505_2	WIFE	WC10	1	BUC	121805	2353	UN	16	32.98	N	171	32.28	E	GPS	4296	4296					1,33	27.9C
49MR0505_2	WIFE	WC10	1	UNK	121905	0001	UN	16	33.04	N	171	32.24	E	GPS	4288	4287						AIR N2O SMPL
49MR0505_2	WIFE	WC10	1	ROS	121905	0055	BO	16	33.46	N	171	32.15	E	GPS	4528	4528	14	4434	4456	32	1-6	#8=#23 DUPL SMPLS (4000DB)
49MR0505_2	WIFE	WC10	1	ROS	121905	0246	EN	16	33.96	N	171	31.98	E	GPS	4468	4468						

Parameter number:

1=SALNTY, 2=OXYGEN, 3=SILCAT, 4=NITRAT, 5=NITRIT, 6=PPHSPHT, 7=CFC-11, 8=CFC-12, 12=DELC14, 13=DELC13, 27=CFC113, 33=N2O

References

Aoyama, M., S. Becker, M. Dai, H. Daimon, L. I. Gordon, H. Kasai, R. Kerouel, N. Kress, D. Masten, A. Murata, N. Nagai, H. Ogawa, H. Ota, H. Saito, K. Sato, T. Shimizu, H. Takano, A. Tsuda, K. Yokouchi, and A. Youenou (2007): Recent comparability of oceanographic nutrients data: Results of a 2003 intercomparison exercise using reference materials, *Analytical Science*, **23**, 1151–1154.

de Boor, C. (2001): *A practical Guide to Splines*, rev. ed., 346 pp., Springer, New York.

Dickson, R. R., W. J. Gould, T. J. Müller, and C. Maillard (1985): Estimates of the mean circulation in the deep (>2000m) layer of the eastern North Atlantic, Prog. Oceanogr., **14**, 103–127.

Hogg, N. G. (2001): Quantification of the deep circulation, in *Ocean Circulation and Climate*, *Observing and Modeling the Global Ocean*, edited by G. Siedler, J. Church, and J. Gould, pp. 259–270, Academic Press, San Diego.

Kawabe, M., S. Fujio, and D. Yanagimoto (2003): Deep-water circulation at low latitudes in the western North Pacific, *Deep-Sea Res.*, Part 1, **50**, 631–656.

Kawabe, M., D. Yanagimoto, S. Kitagawa, and Y. Kuroda (2005): Variations of the deep western boundary current in Wake Island Passage, *Deep-Sea Res.*, Part 1, **52**, 1121–1137.

Kawano, T., M. Aoyama, T. Joyce, H. Uchida, Y. Takatsuki, and M. Fukasawa (2006): The latest batch-to-batch difference table of standard seawater and its application to the WOCE onetime sections, *J. Oceanogr.*, **62**, 777–792.

Kawano, T., and H. Uchida eds. (2007): *WHP P03 Revisit Data Book*, 207 pp., JAMSTEC, Yokosuka, Kanagawa, Japan.

Roemmich, D., S. Hautala, and D. Rudnick (1996): Northward abyssal transport through the Samoa Passage and adjacent regions, *J. Geophys. Res.*, **101**(C6), 14,039–14,055.

Smith, W. H. F. and D. T. Sandwell (1997): Global seafloor topography from satellite altimetry and ship depth soundings, Science, **277**, 1956–1962.

Uchida, H., K. Ohyama, S. Ozawa, and M. Fukasawa (2007a): In situ calibration of the SeaBird 9*plus* CTD thermometer, *J. Atmos. Oceanic Technol.*, **24**, 1961–1967.

Uchida, H., H. Yamamoto, K. Ichikawa, I. Kaneko, M. Fukasawa, T. Kawano, and Y. Kumamoto (2007b): Flow of abyssal water into Wake Island Passage: Properties and transports from hydrographic surveys, *J. Geophys. Res.*, **112**, C04008, doi:10.1029/2006JC004000.

Uchida, H., T. Kawano, and M. Fukasawa (2008a): In situ calibration of moored CTDs used for monitoring abyssal water, *J. Atmos. Oceanic Technol.*, **25**, 1695–1702.

Uchida, H., T. Kawano, I. Kaneko, and M. Fukasawa (2008b): In situ calibration of optode-based oxygen sensors, *J. Atmos. Oceanic Technol.*, **25**, 2271–2281.

Whitworth, T., B. A. Warren, W. D. Nowlin, S. B. Rutz, R. D. Pillsbury, and M. I. Moore (1999): On the deep western-boundary current in the Southwest Pacific Basin, *Prog. Oceanogr.*, **43**, 1–54.

Figure captions

Figure 1 Station locations for Wake Island Passage Flux Experiment (WIFE) with bottom topography based on Smith and Sandwell (1997).

Figure 2 Bathymetry measured by multinarrow beam echo sounding system along the cruise track of MR05-05 leg 2, superimposed over bottom topography based on Smith and Sandwell (1997).

Figure 3 Potential temperature (°C) cross sections along the WIFE observation line for depths below 2000 m for the cruises (a) MR03-K02 in 2003, (b) KH04-4 leg 2 in 2004, and (c) MR05-05 leg 2 in 2005. Triangles indicate location of the shipboard CTD station. Bottom topography shown was obtained from the multinarrow beam echo sounder. Vertical exaggeration is 2000:1.

Figure 4 CTD salinity (psu) cross sections along the WIFE observation line for depths below 2000 m for the cruises (a) MR03-K02 in 2003, (b) KH04-4 leg 2 in 2004, and (c) MR05-05 leg 2 in 2005. Otherwise is the same as Figure 3.

Figure 5 Potential density anomaly (σ_4) (kg m^{-3}) cross sections along the WIFE observation line for depths below 2000 m for the cruises (a) MR03-K02 in 2003, (b) KH04-4 leg 2 in 2004, and (c) MR05-05 leg 2 in 2005. Otherwise is the same as Figure 3.

Figure 6 Dissolved oxygen (μmol kg^{-1}) cross sections along the WIFE observation line for depths below 2000 m for the cruises (a) MR03-K02 in 2003, (b) KH04-4 leg 2 in 2004, and (c) MR05-05 leg 2 in 2005. Dots indicate locations of the water sample data. Otherwise is the same as Figure 3.

Figure 7 Silicate (μmol kg^{-1}) cross sections along the WIFE observation line for depths below 2000 m for the cruises (a) MR03-K02 in 2003, (b) KH04-4 leg 2 in 2004, and (c) MR05-05 leg 2 in 2005. Dots indicate locations of the water sample data. Otherwise is the same as Figure 3.

Figure 8 Nitrate (μmol kg^{-1}) cross sections along the WIFE observation line for depths below 2000 m for the cruises (a) MR03-K02 in 2003, (b) KH04-4 leg 2 in 2004, and (c) MR05-05 leg 2 in 2005. Dots indicate locations of the water sample data. Otherwise is the same as Figure 3.

Figure 9 Phosphate (μmol kg^{-1}) cross sections along the WIFE observation line for depths below 2000 m for the cruises (a) MR03-K02 in 2003, (b) KH04-4 leg 2 in 2004, and (c) MR05-05 leg 2 in 2005. Dots indicate locations of the water sample data. Otherwise is the same as Figure 3.

Figure 10 Property cross sections along the WIFE observation line for depths below 2000 m: (a) dissolved inorganic carbon (DIC) (μmol kg^{-1}); (b) total alkalinity (μmol kg^{-1}); and (c) pH. All properties were sampled in the cruise MR03-K02 in 2003. Dots indicate locations of the water sample data. Otherwise is the same as Figure 3.

Figure 11 Property cross sections along the WIFE observation line for depths below 2000 m: (a) stable carbon isotope (δ^{13}C) (‰); and (b) radiocarbon (Δ^{14}C) (‰). All properties were sampled in the cruise MR03-K02 in 2003. Dots indicate locations of the water sample data. Otherwise is the same as Figure 3.

Figure 12 Locations of the instruments [CTD, current meter (CM), and oxygen optode] for the first set (red: from May 2003 to October 2004) and the second set (blue: from October 2004 to December 2005) of the mooring observations. Bottom topography shown was obtained from the multinarrow beam echo sounder. Vertical exaggeration is 2000:1.

Figure 13 Velocity stick vector at the five mooring stations (positive y-axis pointing north). Data were low-pass-filtered with a half power gain at 5 days and resampled at 3-day intervals.

Figure 14 Potential temperature (°C) plotted against salinity at the five mooring stations. Contour lines indicate the potential density anomaly (σ_4) (kg m^{-3}). Black lines indicate shipboard CTD data from the cruises MR03-K02 in 2003, KH04-4 leg 2 in 2004, and MR05-05 leg 2 in 2005. Red and blue lines indicate moored CTD data for the first set (from May 2003 to October 2004) and for the second set (from October 2004 to December 2005) of the mooring observations, respectively.

Figure 15 Daily mean (a) potential temperature (°C) and (b) salinity at the five mooring stations. Depths below the bottom are shaded.

Figure 16 Daily mean velocity anomaly components (cm s^{-1}) (a) along and (b) normal to the WIFE observation line at depths of 3600, 4400, and 5300 dbar. Anomalies from the temporal mean of the mooring observation period are shown. Dots indicate location of mooring station.

Figure 17 Daily mean (a) potential temperature (°C) and (b) salinity anomalies at depths of 3600, 4400, and 5300 dbar. Anomalies from the temporal mean of the mooring observation period are shown. Dots indicate location of mooring station.

Figure 18 Mean velocity vectors of the mooring observation period at the three instrumented depths with bottom topography based on Smith and Sandwell (1997).

Figure 19 Cross sections of mean and standard deviation (SD) of velocity components (cm s^{-1}) along (U) and normal (V) to the WIFE observation line. The mean velocities were calculated from the current meter data for the mooring observation period. Triangles indicate location of mooring station. Vertical exaggeration is 2000:1.

Figure 20 Cross sections of mean and standard deviation (SD) of potential temperature (°C) and salinity. The mean values were calculated for the mooring observation period. Otherwise is the same as Figure 19.

Figure 1
Station locations

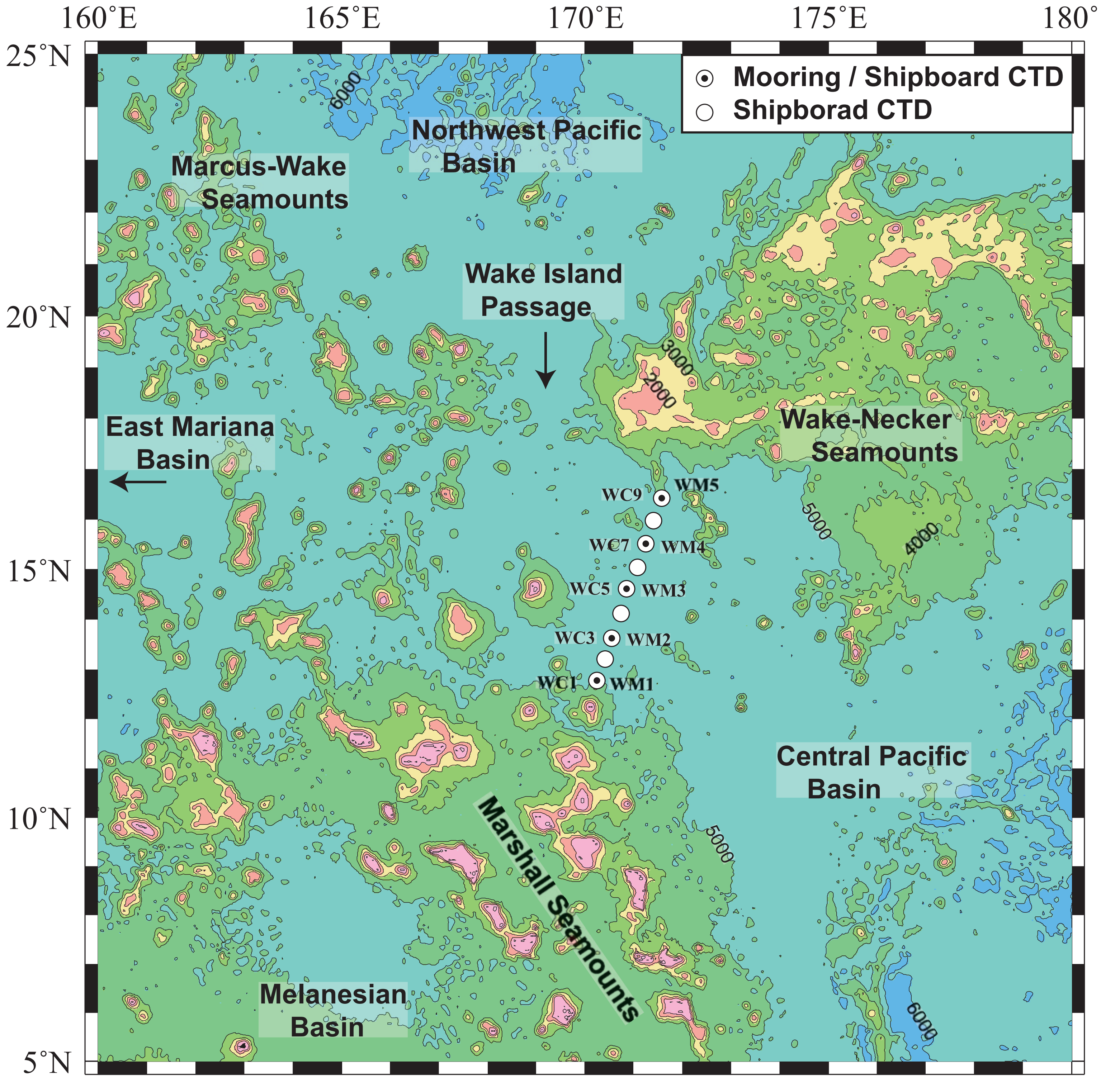

Figure 2
Bathymetry

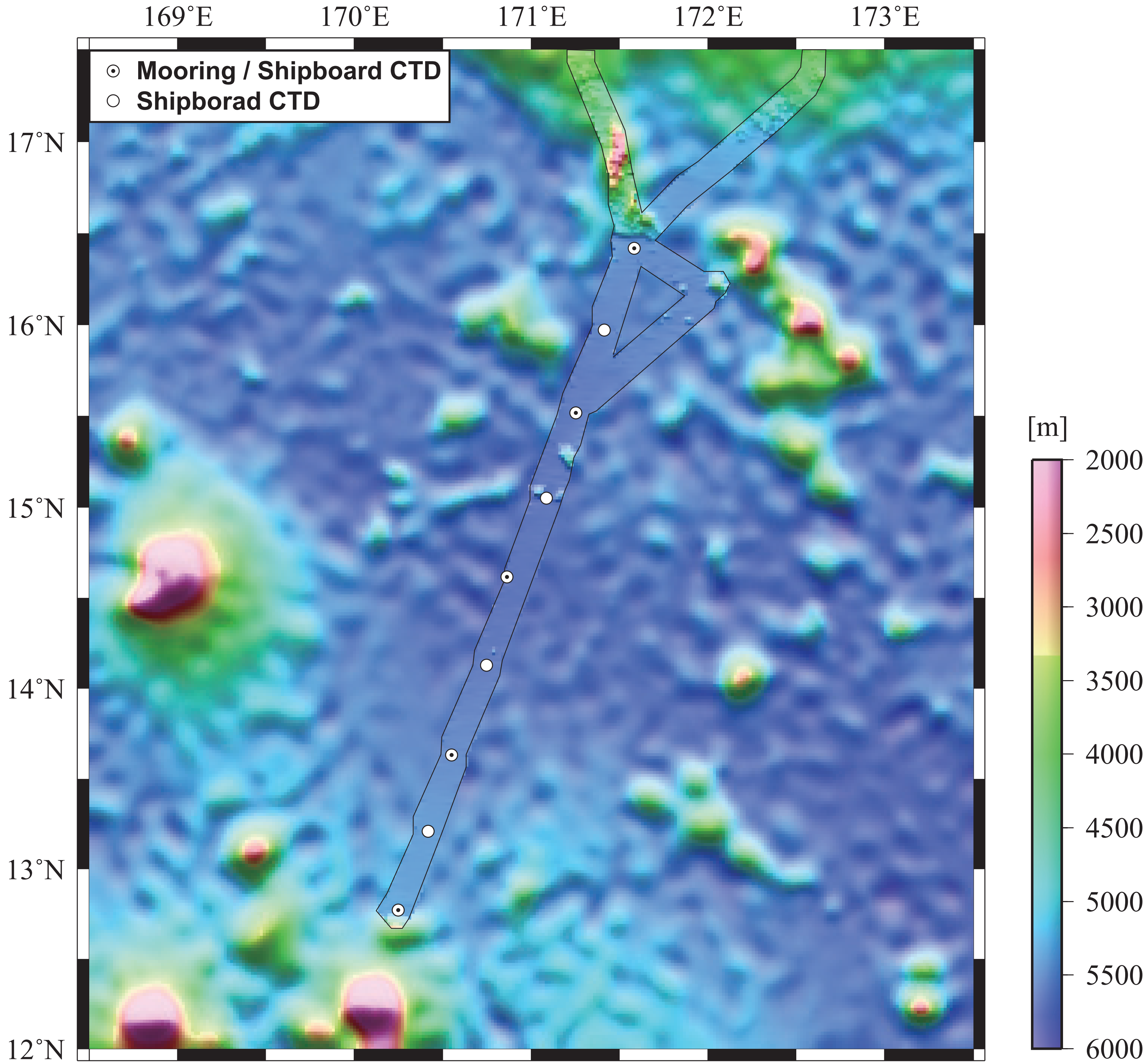

Figure 3
Potential temperature (°C)

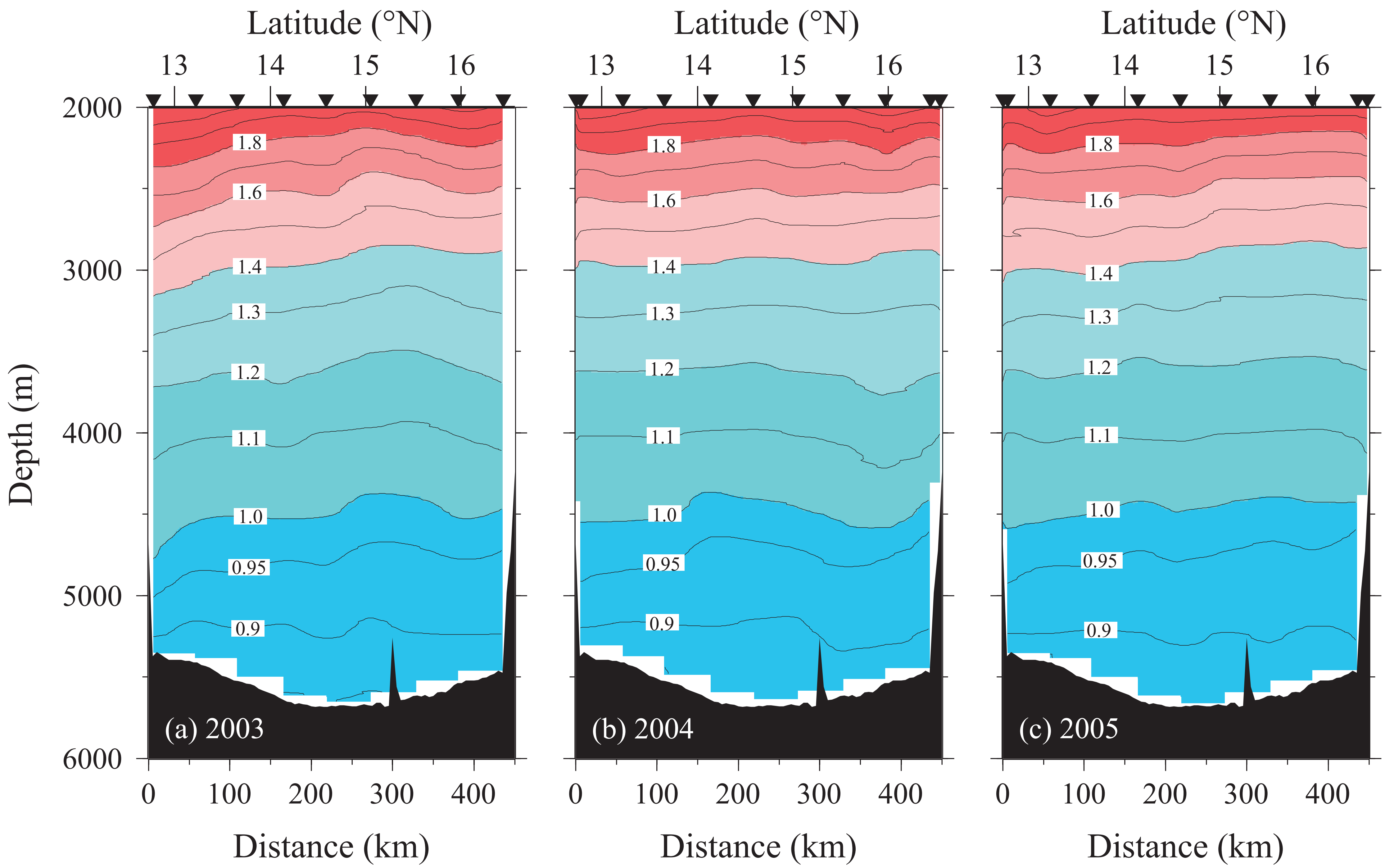

Figure 4
CTD salinity

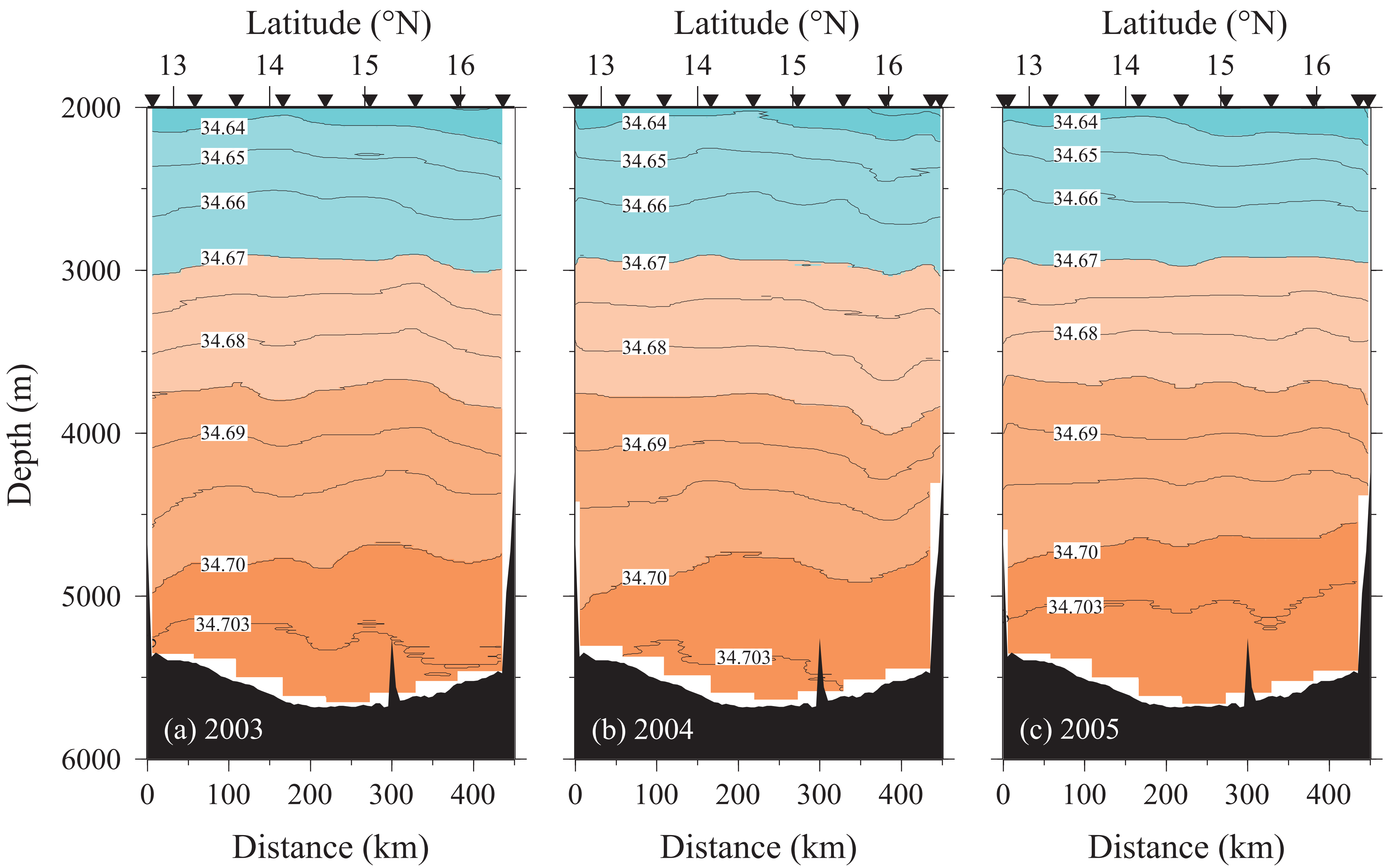

Figure 5
Density (σ_4) (kg m^{-3})

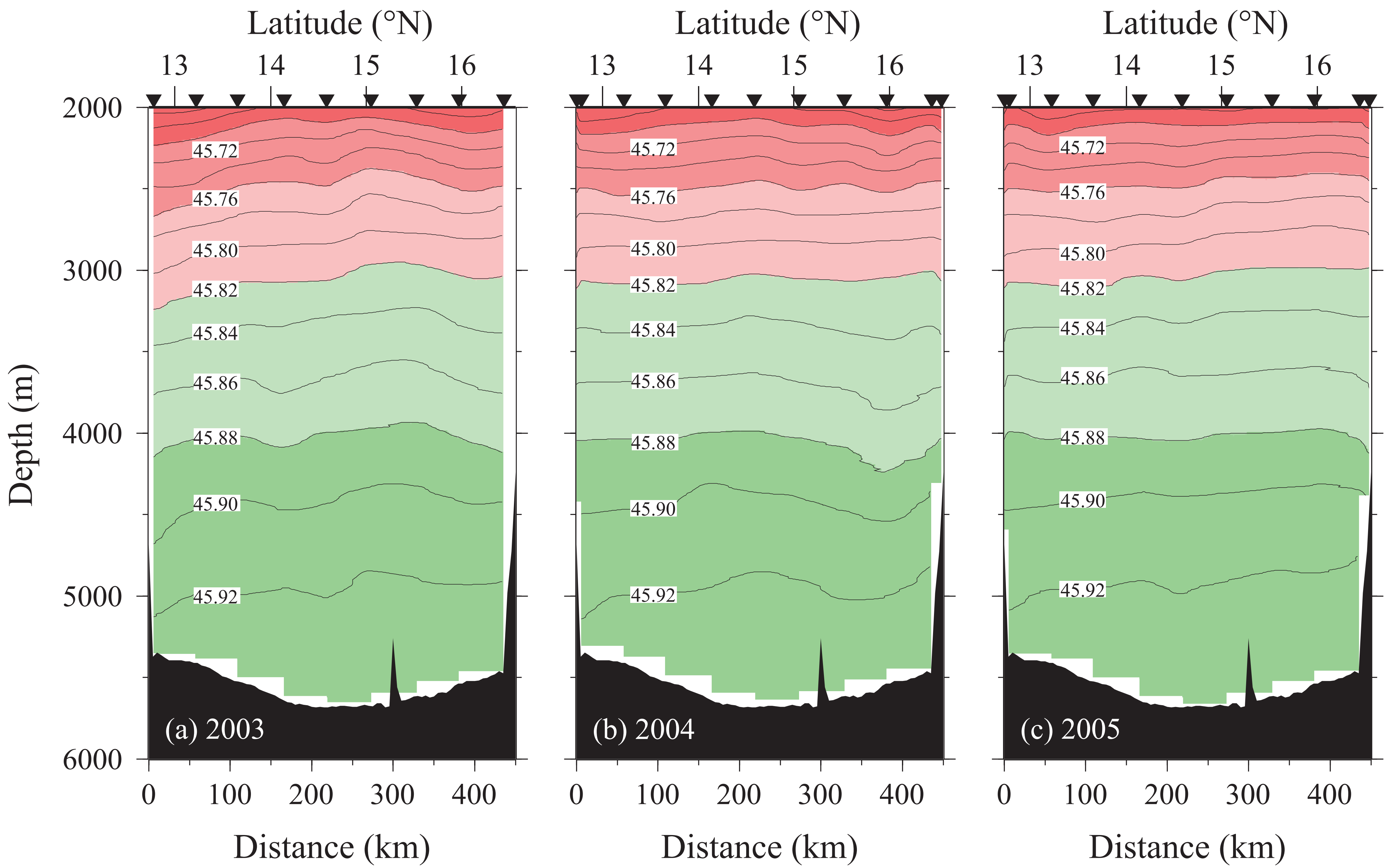

Figure 6
Dissolved oxygen (μmol kg^{-1})

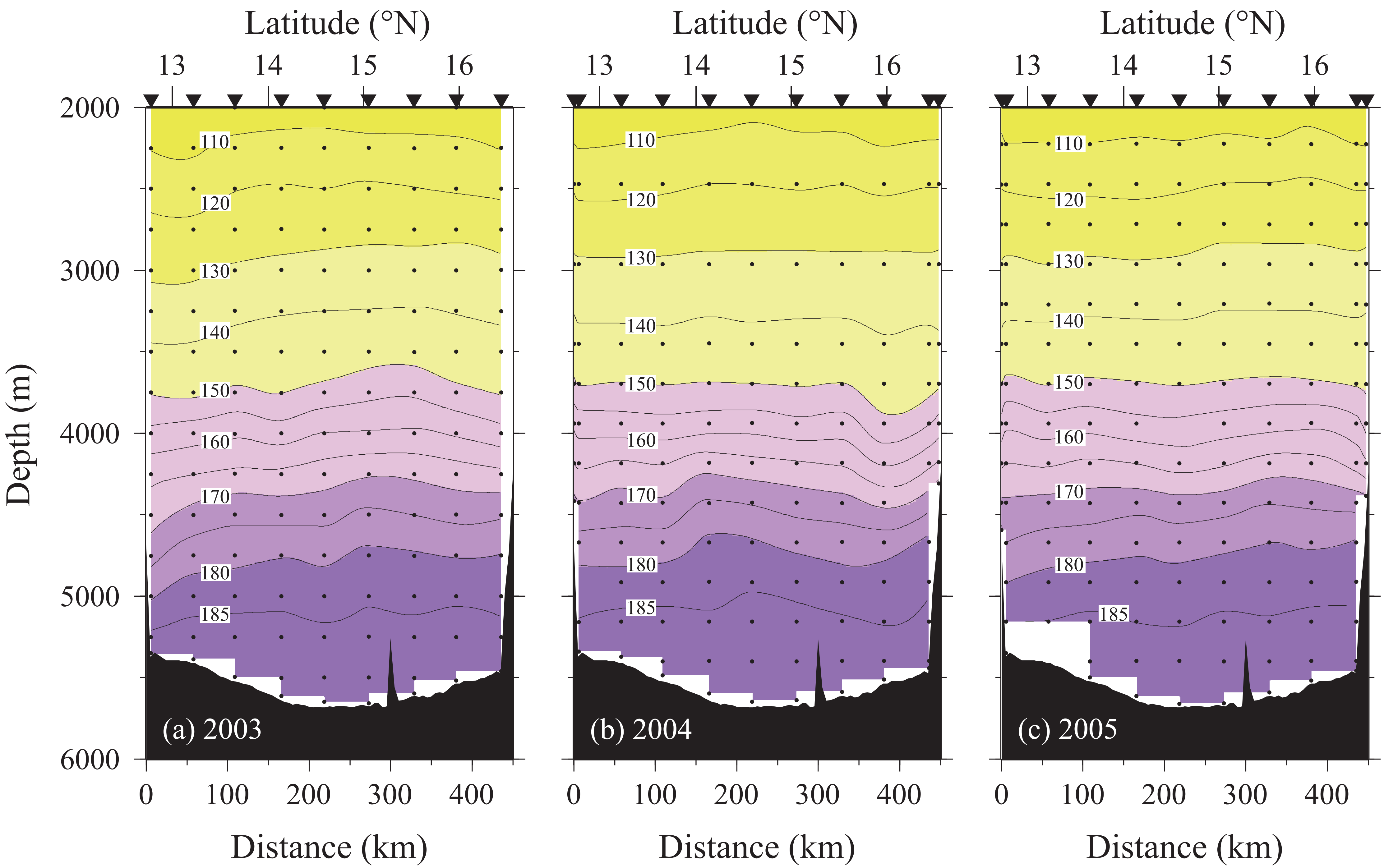

Figure 7
Silicate (μmol kg⁻¹)

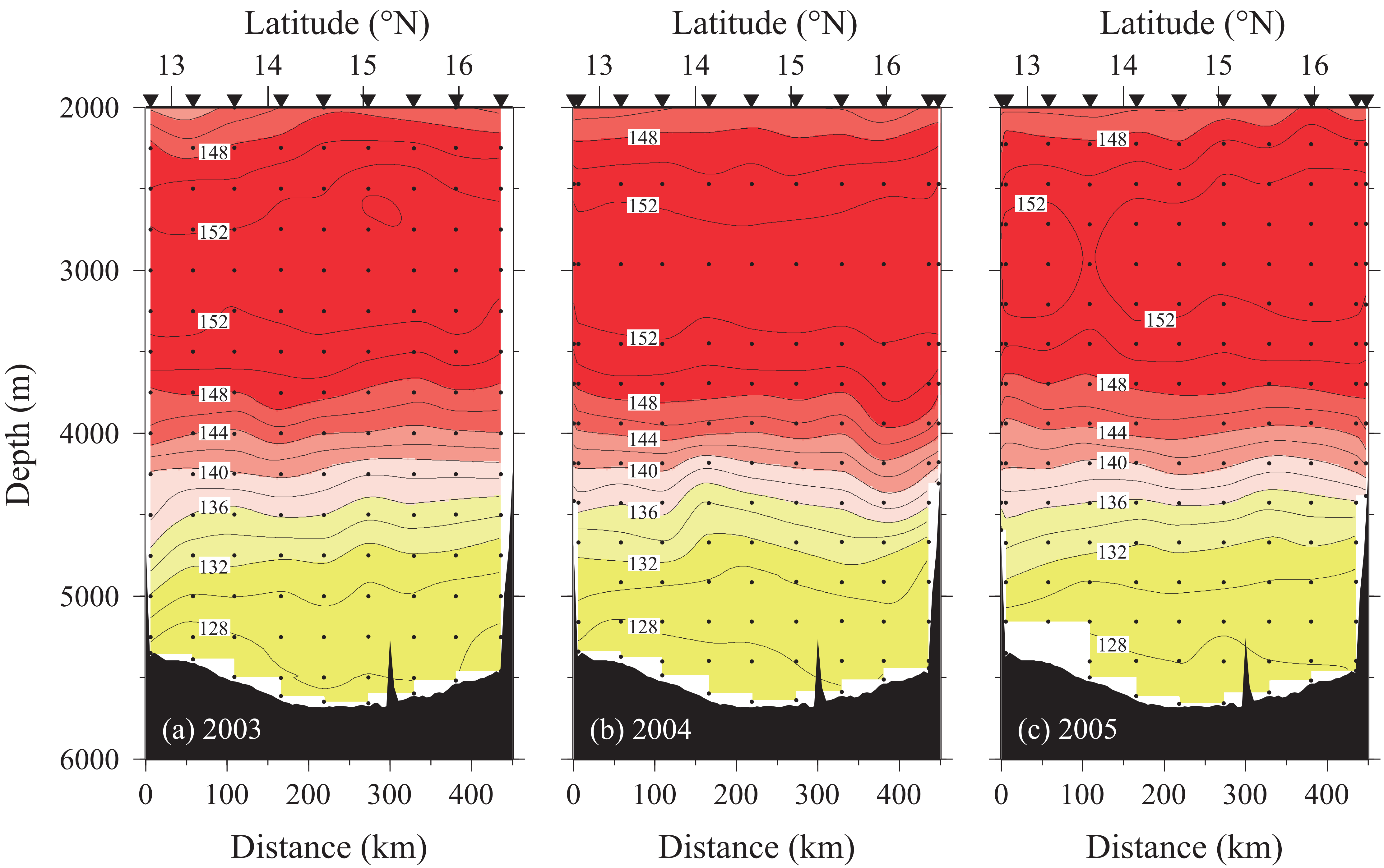

Figure 8
Nitrate (μmol kg^{-1})

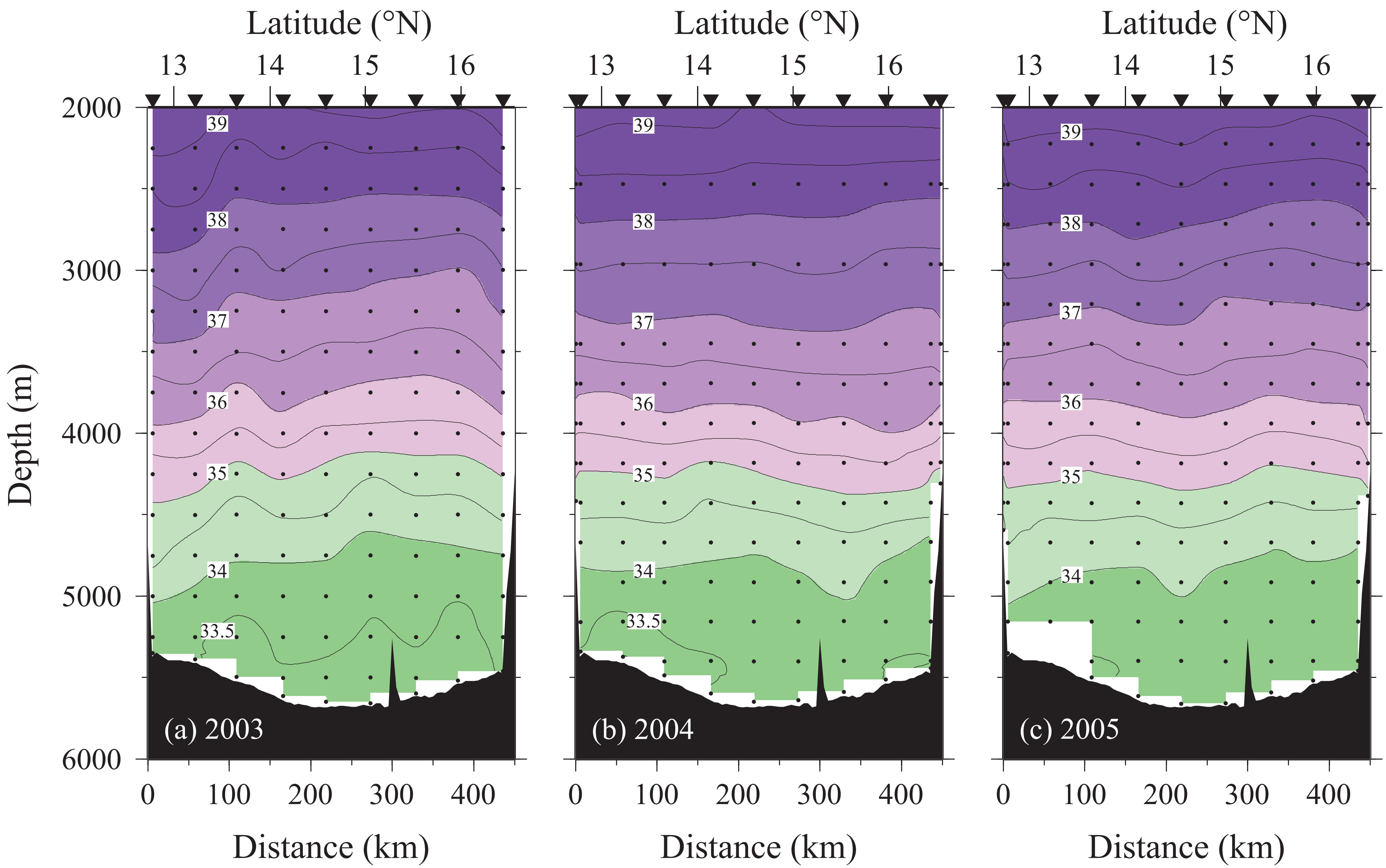

Figure 9

Phosphate (μmol kg^{-1})

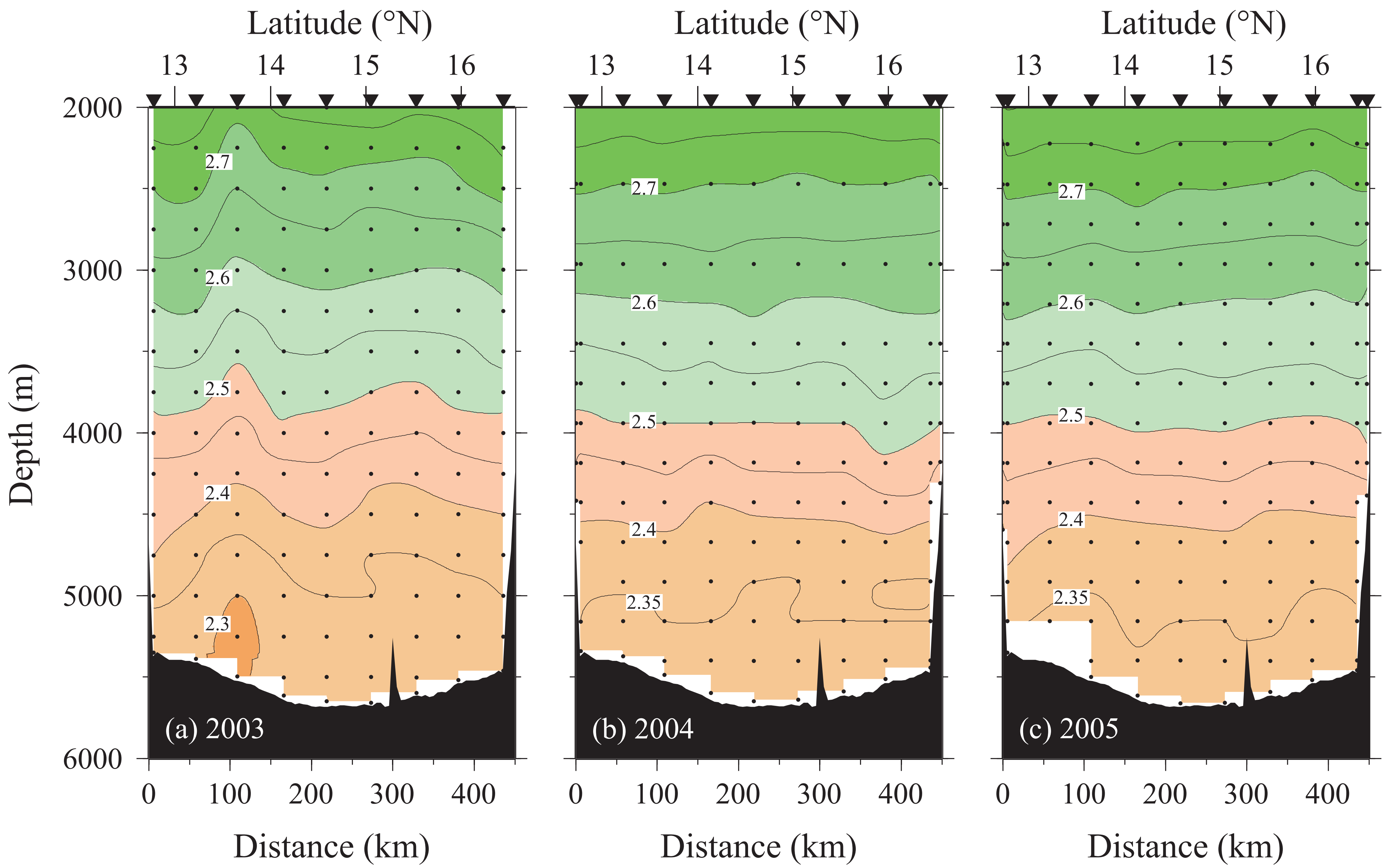

Figure 10
(a) DIC (μmol kg^{-1}), (b) Total alkalinity (μmol kg^{-1}), (c) pH

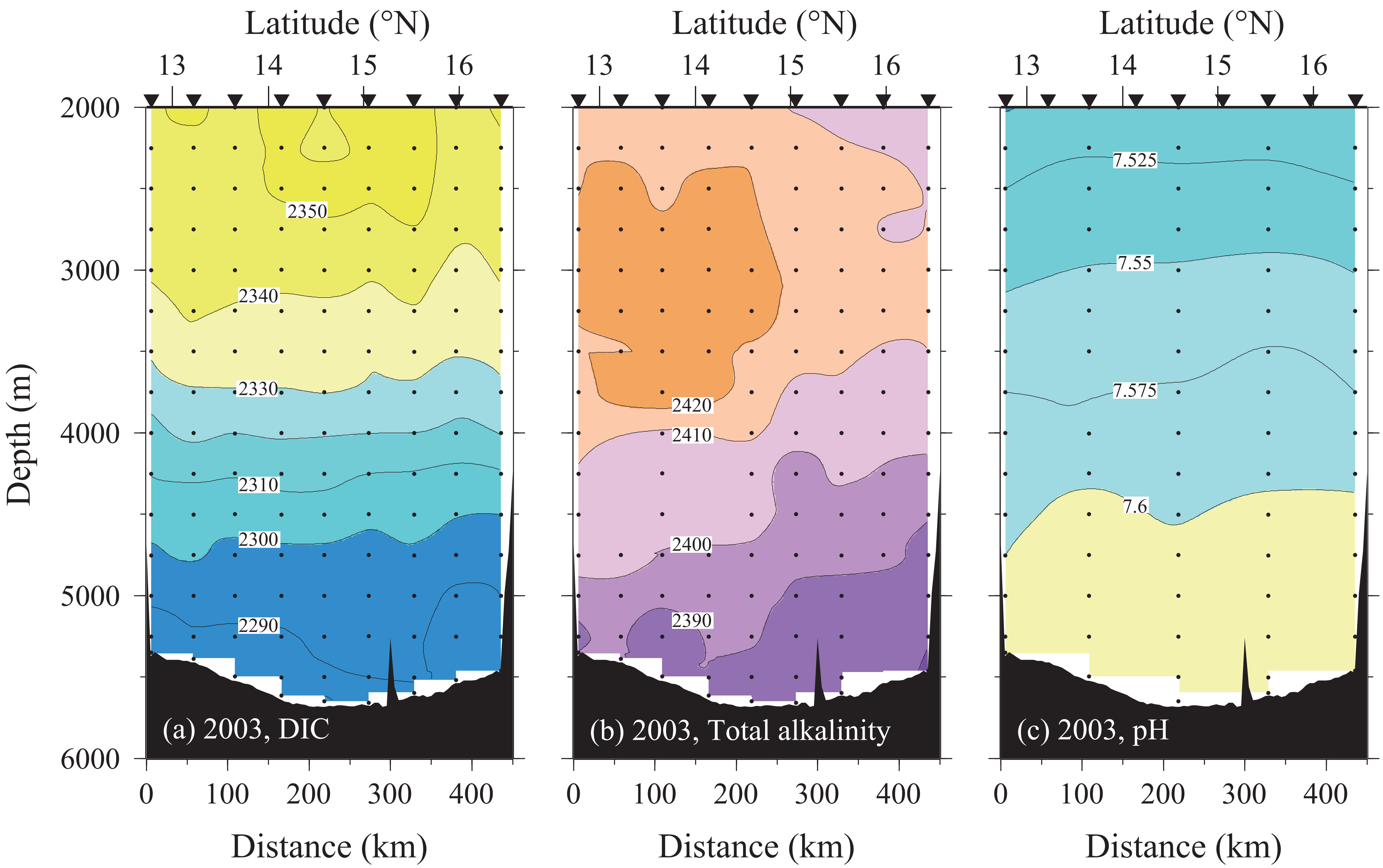

Figure 11
(a) $\delta^{13}C$ (‰), (b) $\Delta^{14}C$ (‰)

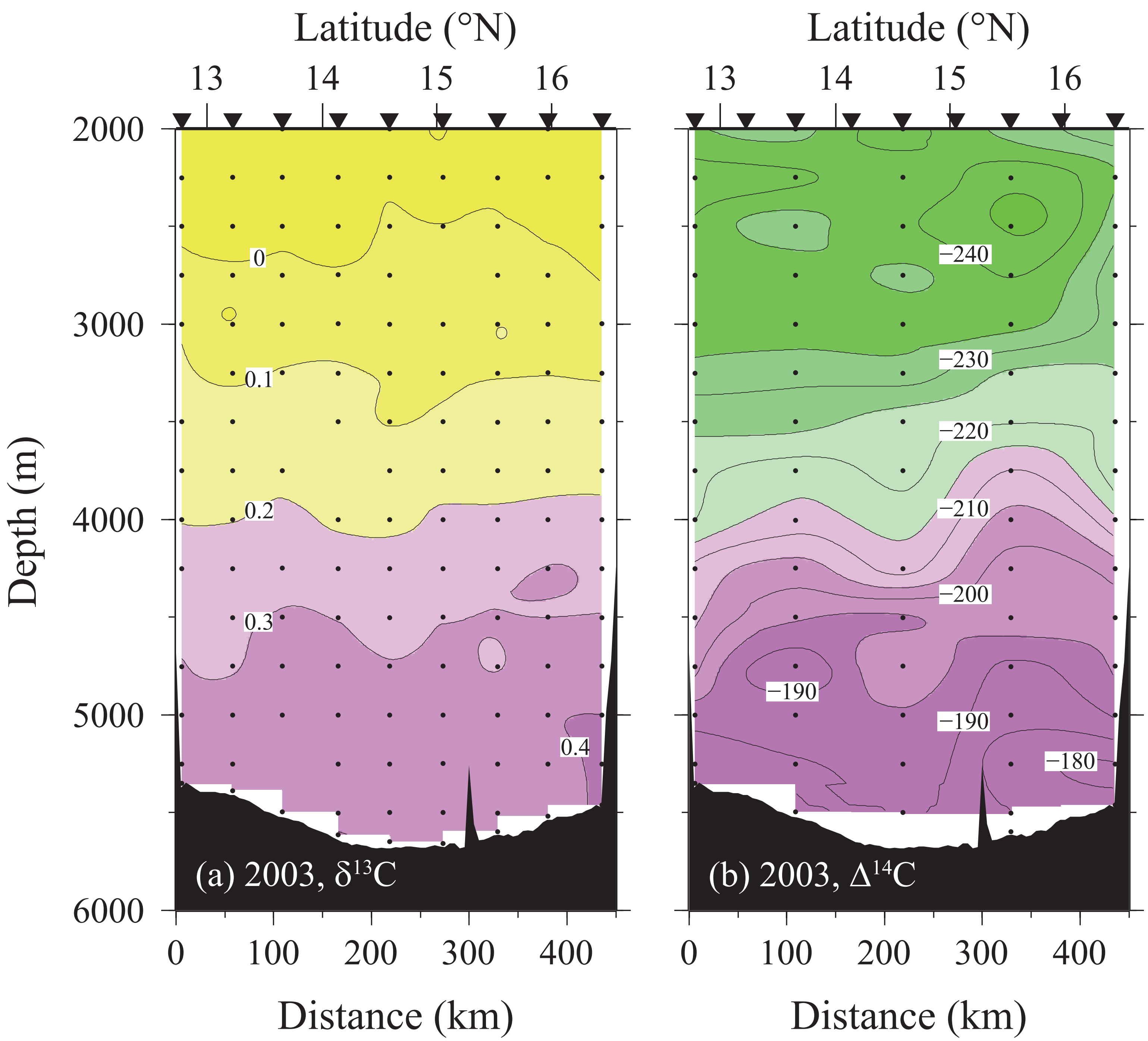

Figure 12
Locations of moored instruments

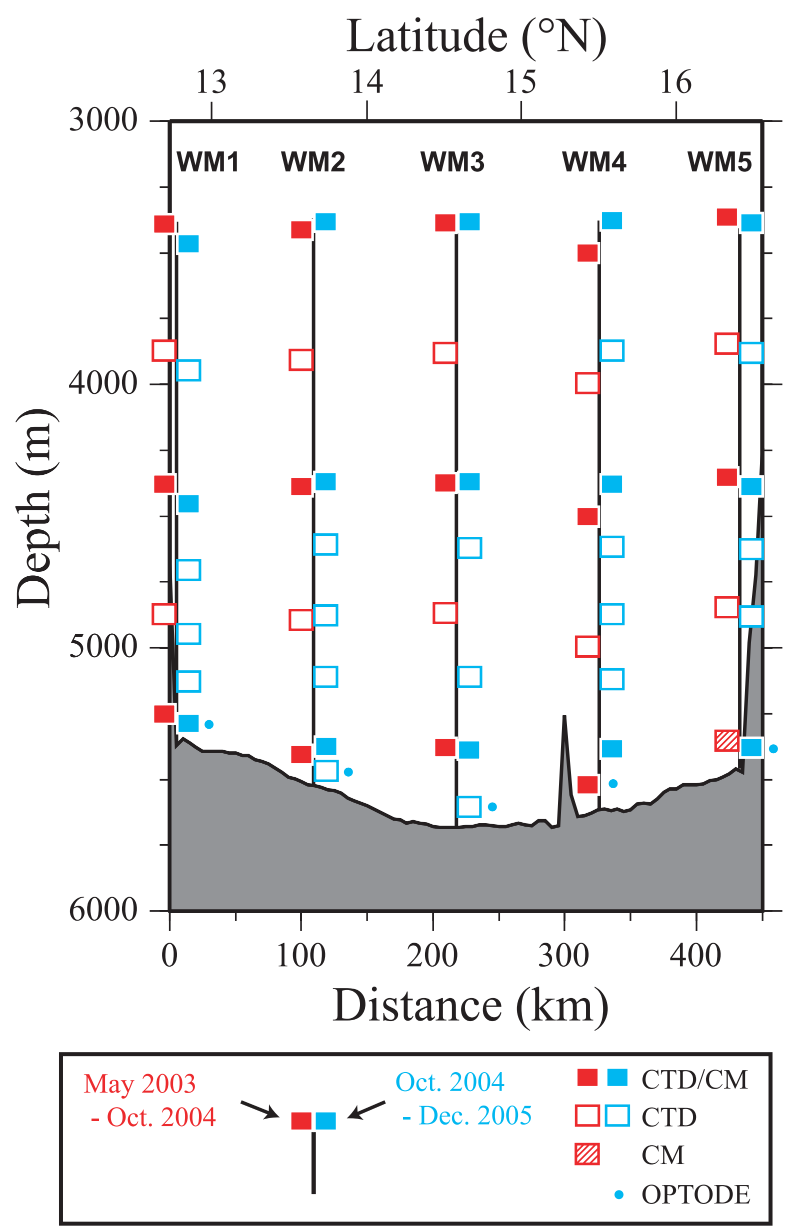

Figure 13
Velocity stick vector for WM1

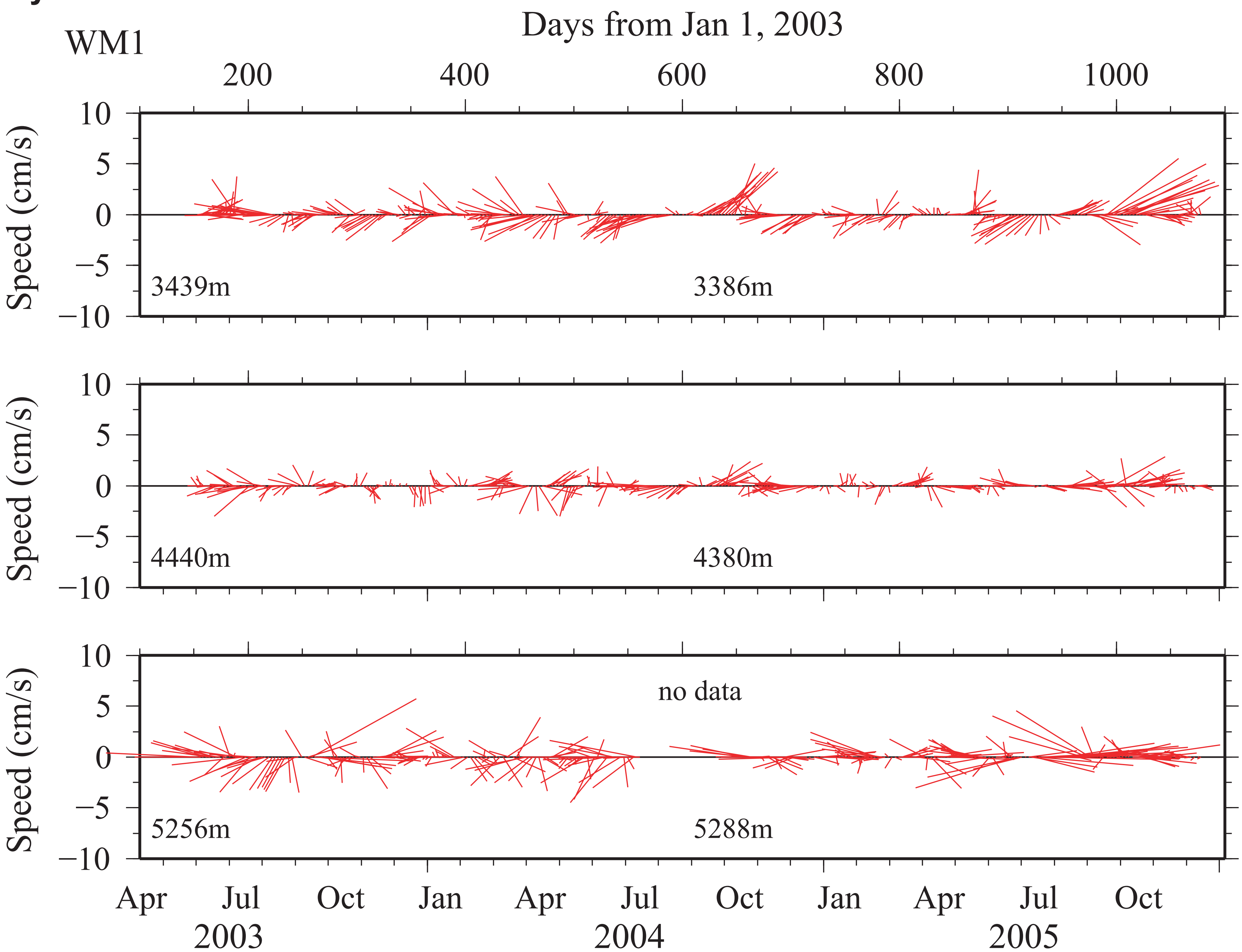

Figure 13
Continued (WM2)

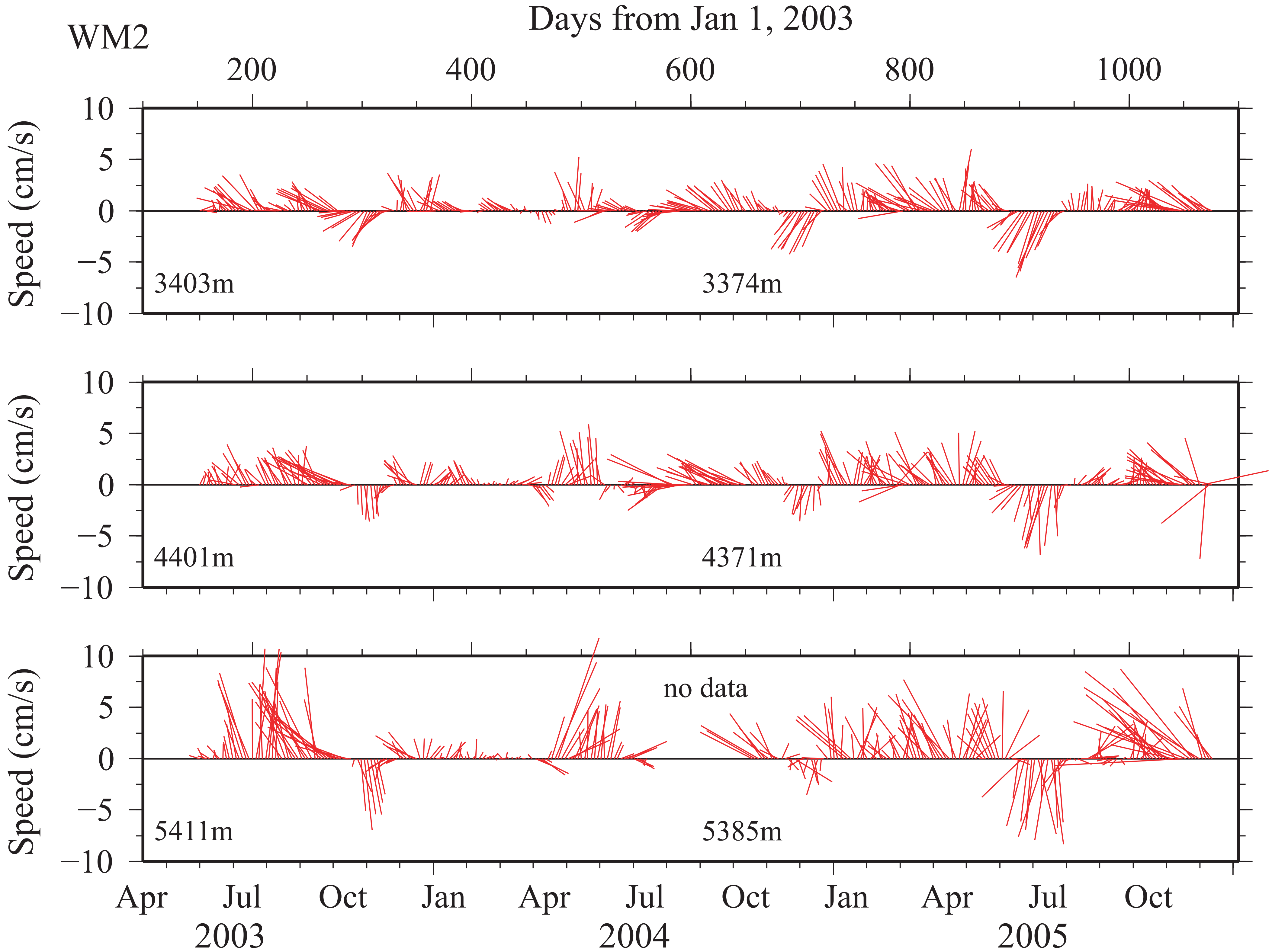

Figure 13
Continued (WM3)

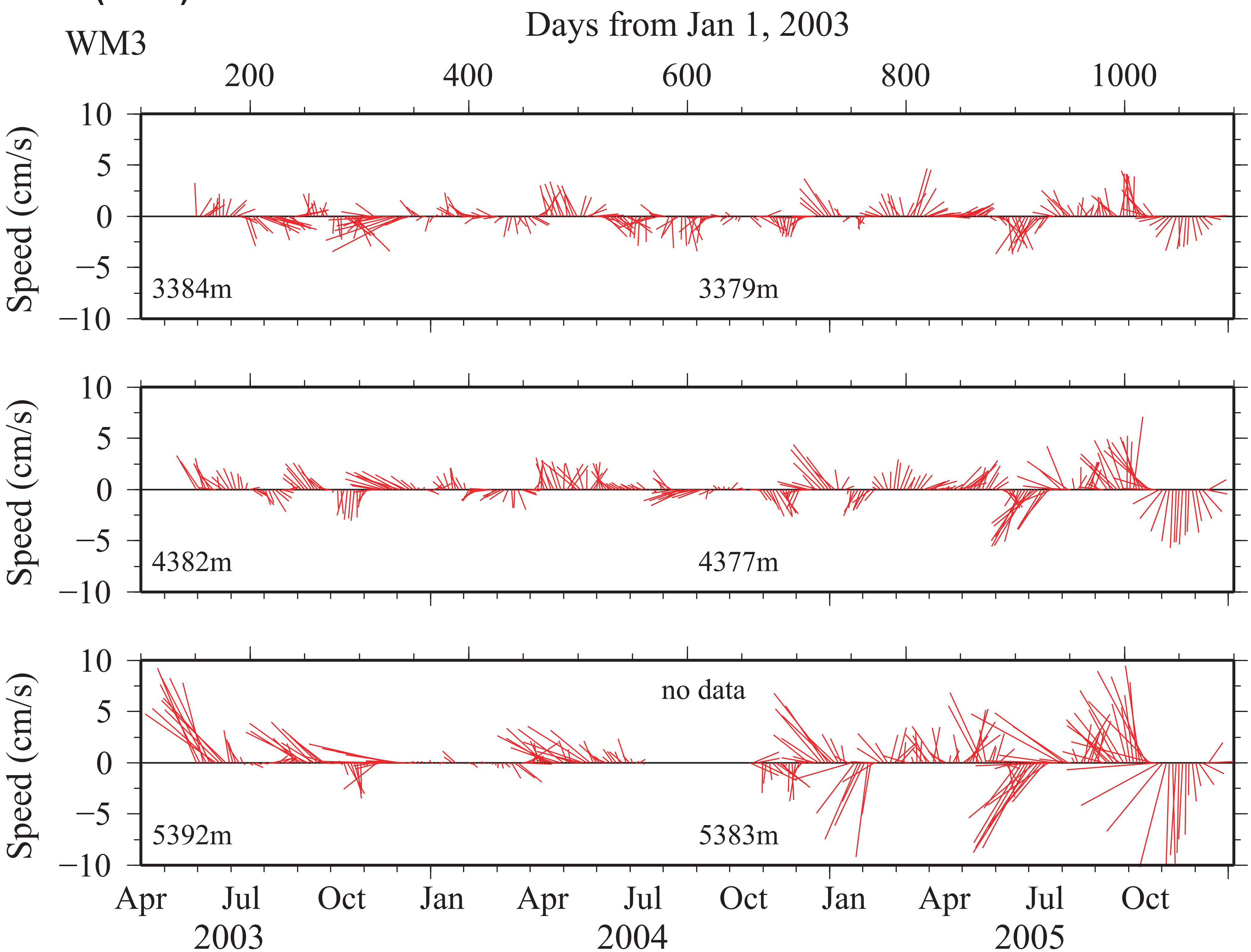

Figure 13
Continued (WM4)

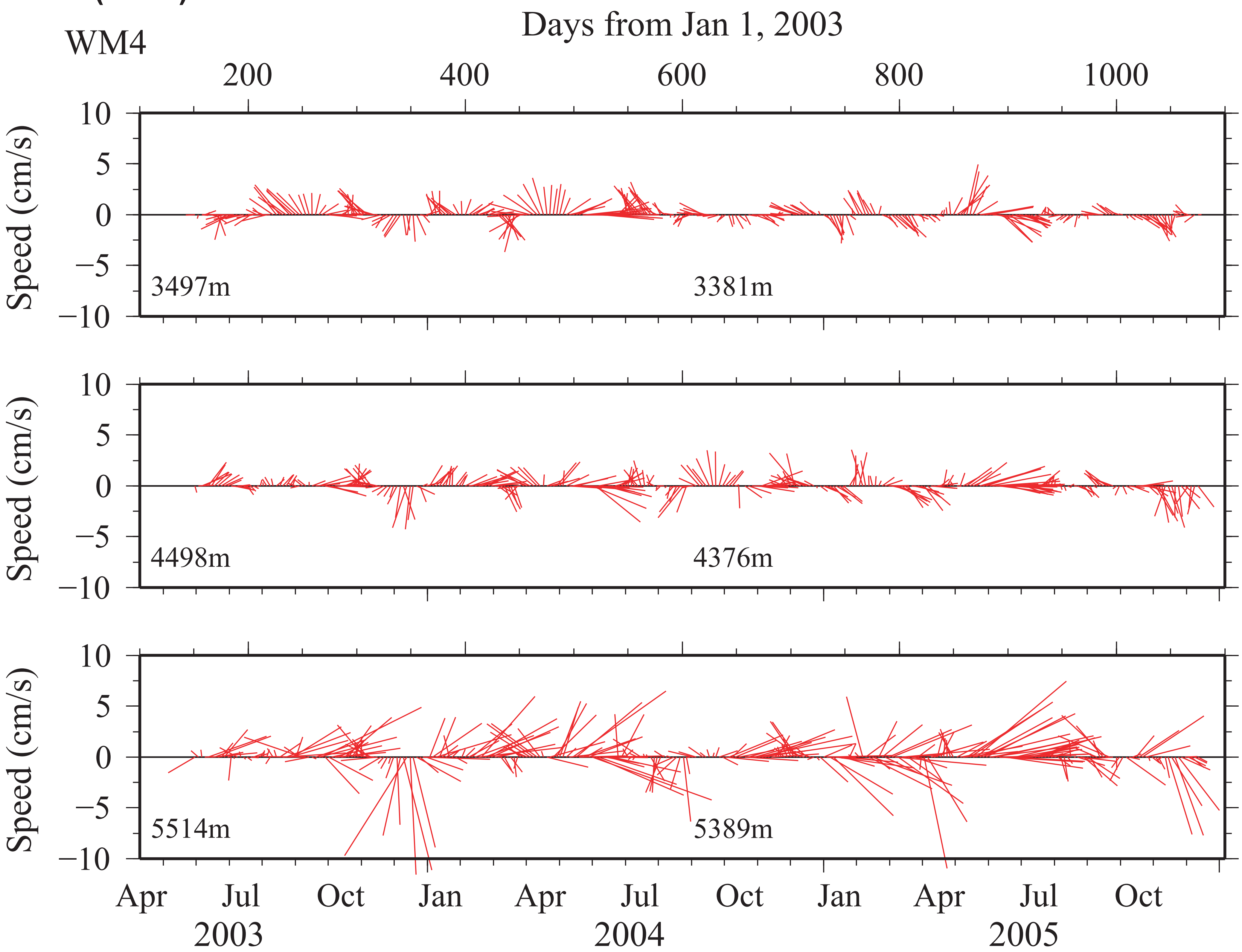

Figure 13
Continued (WM5)

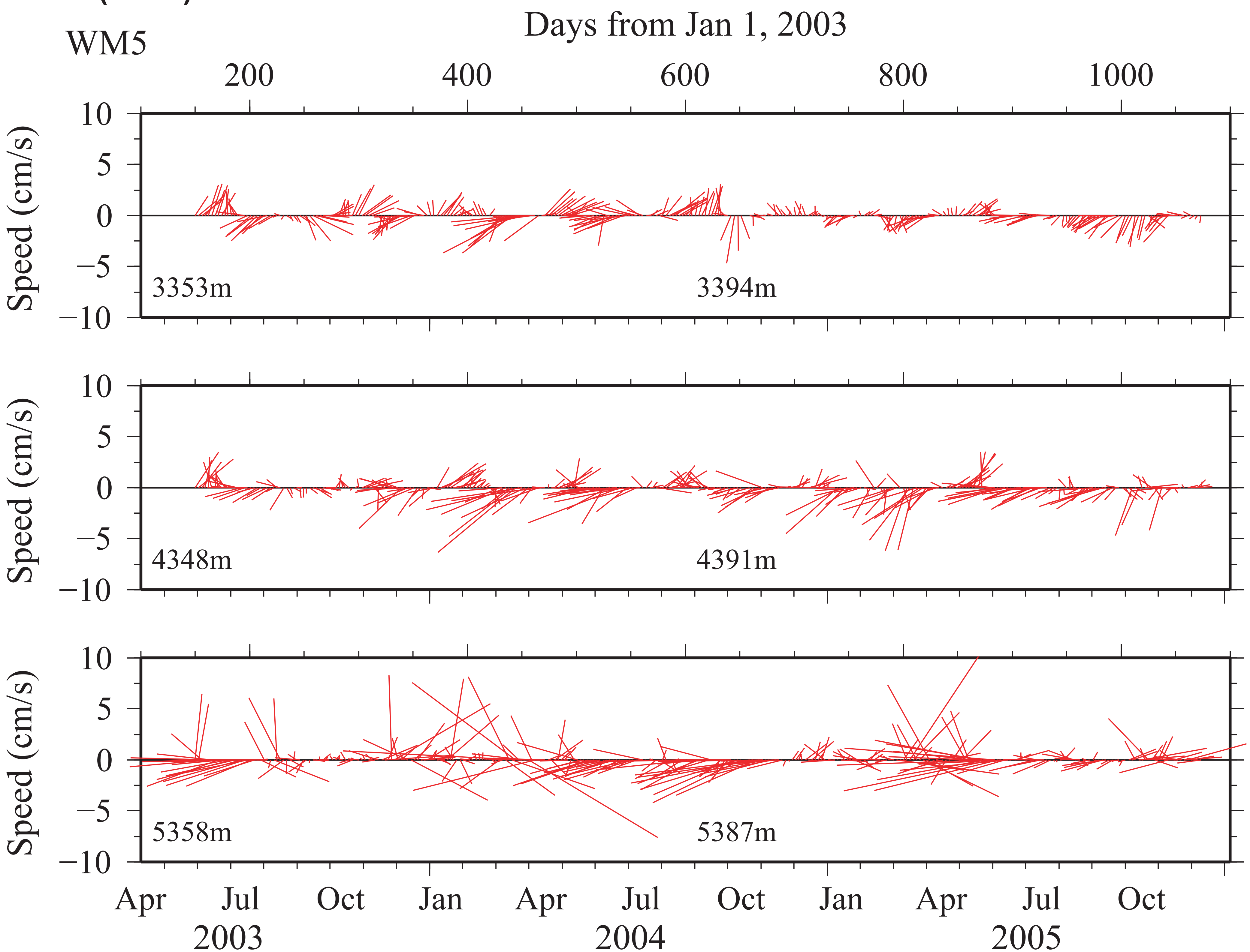

Figure 14
T–S diagrams

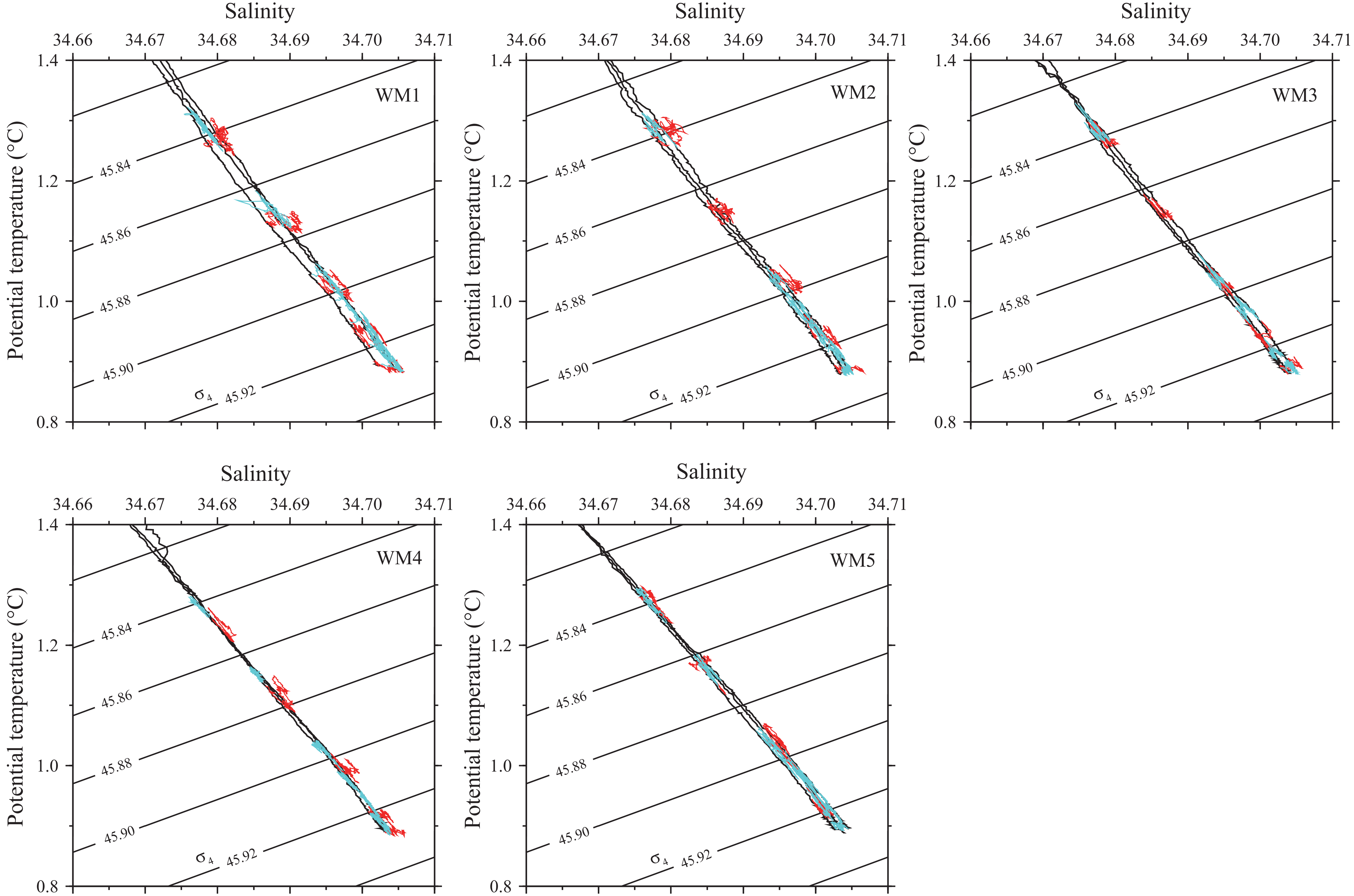

Figure 15
Daily mean (a) potential temperature (°C) and (b) salinity for WM1

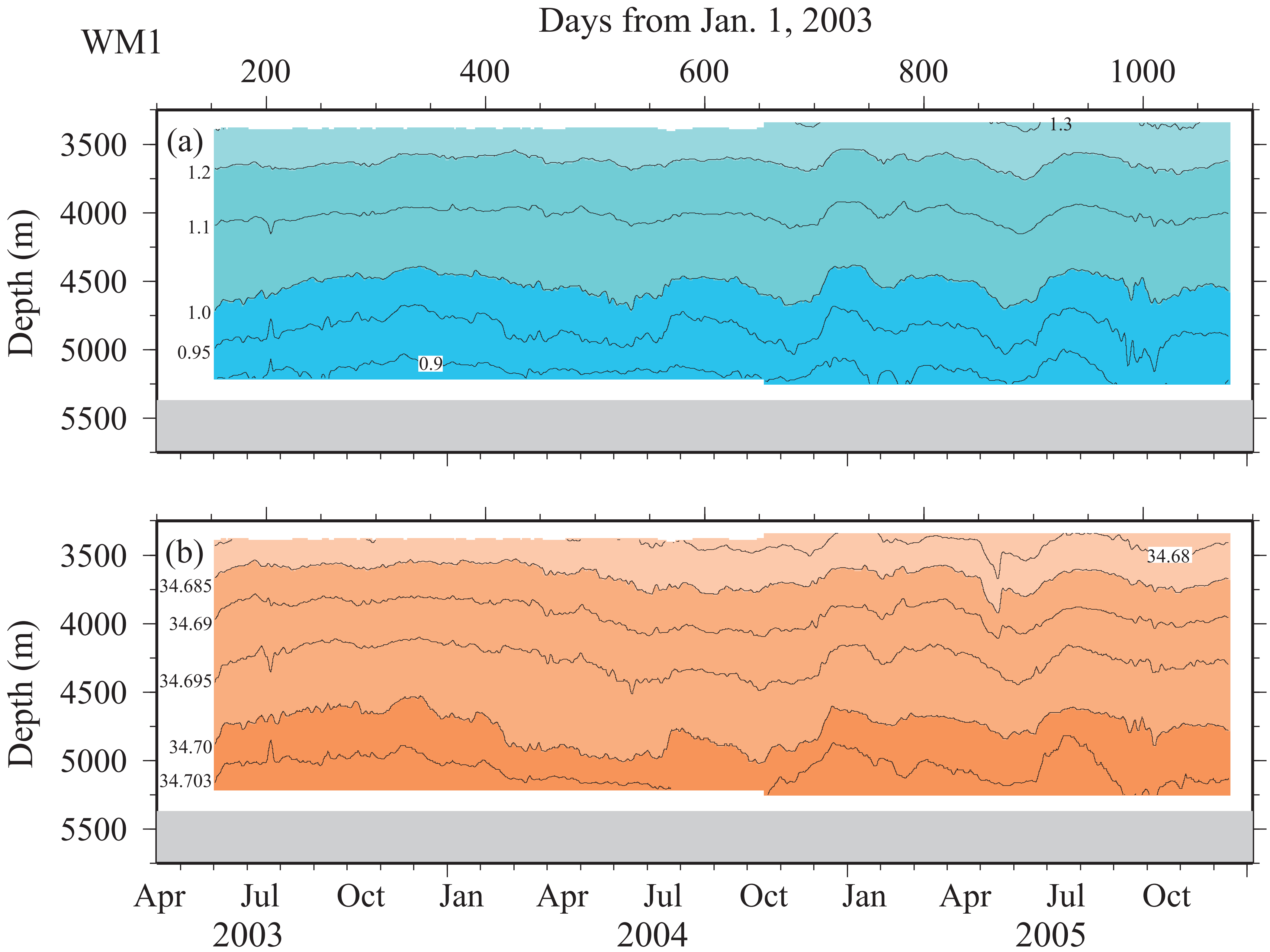

Figure 15
Continued (WM2)

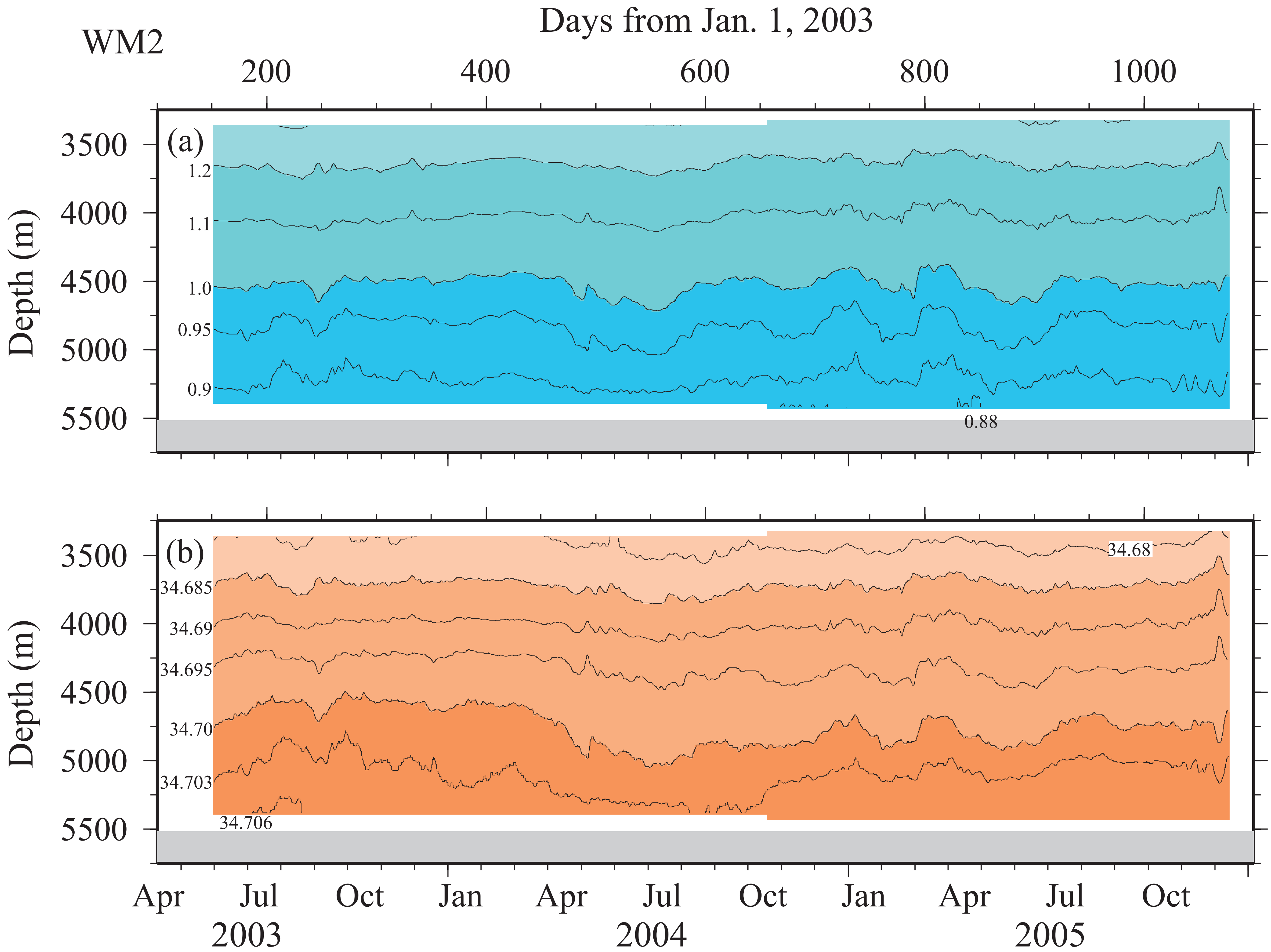

Figure 15
Continued (WM3)

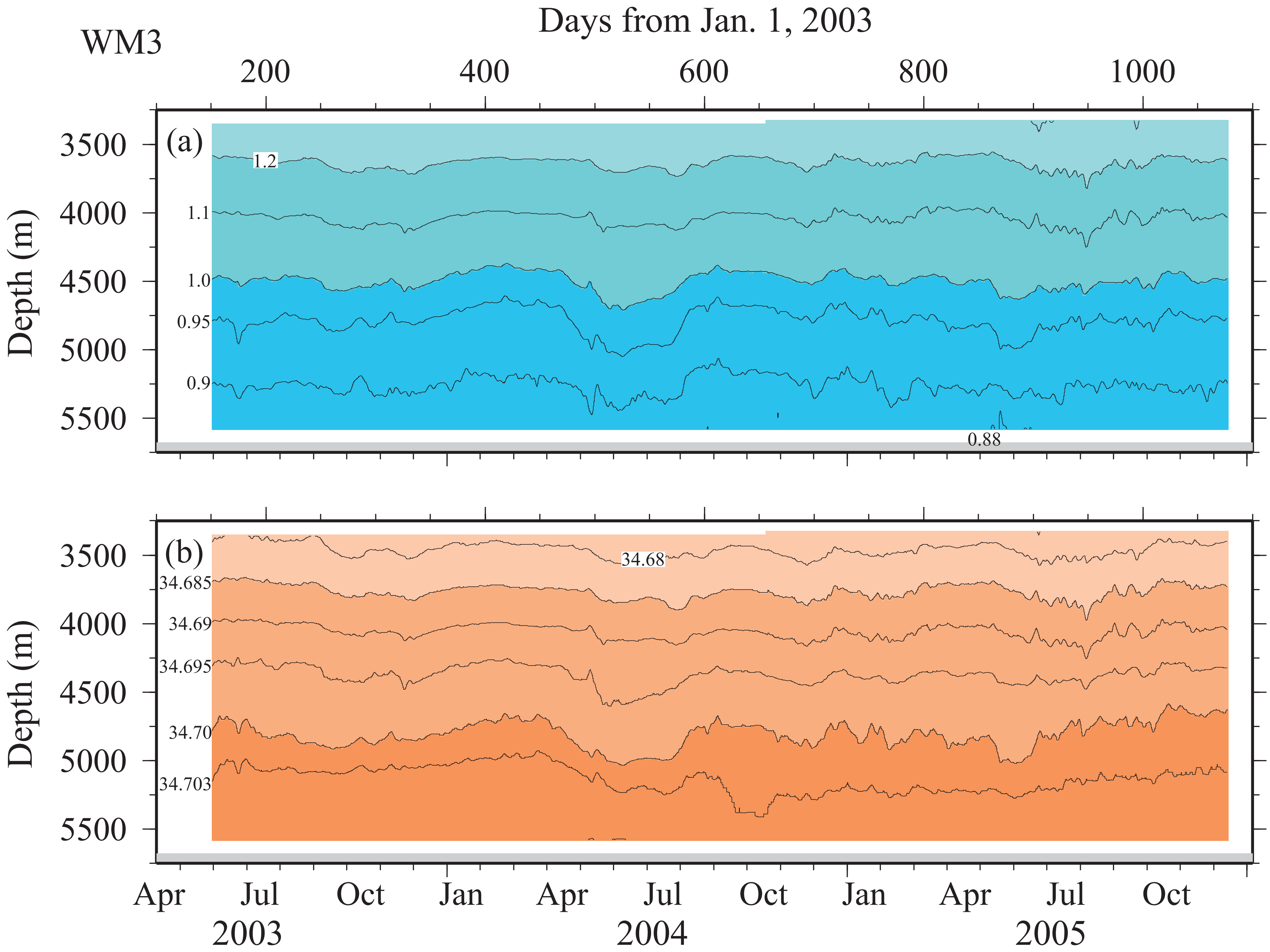

Figure 15
Continued (WM4)

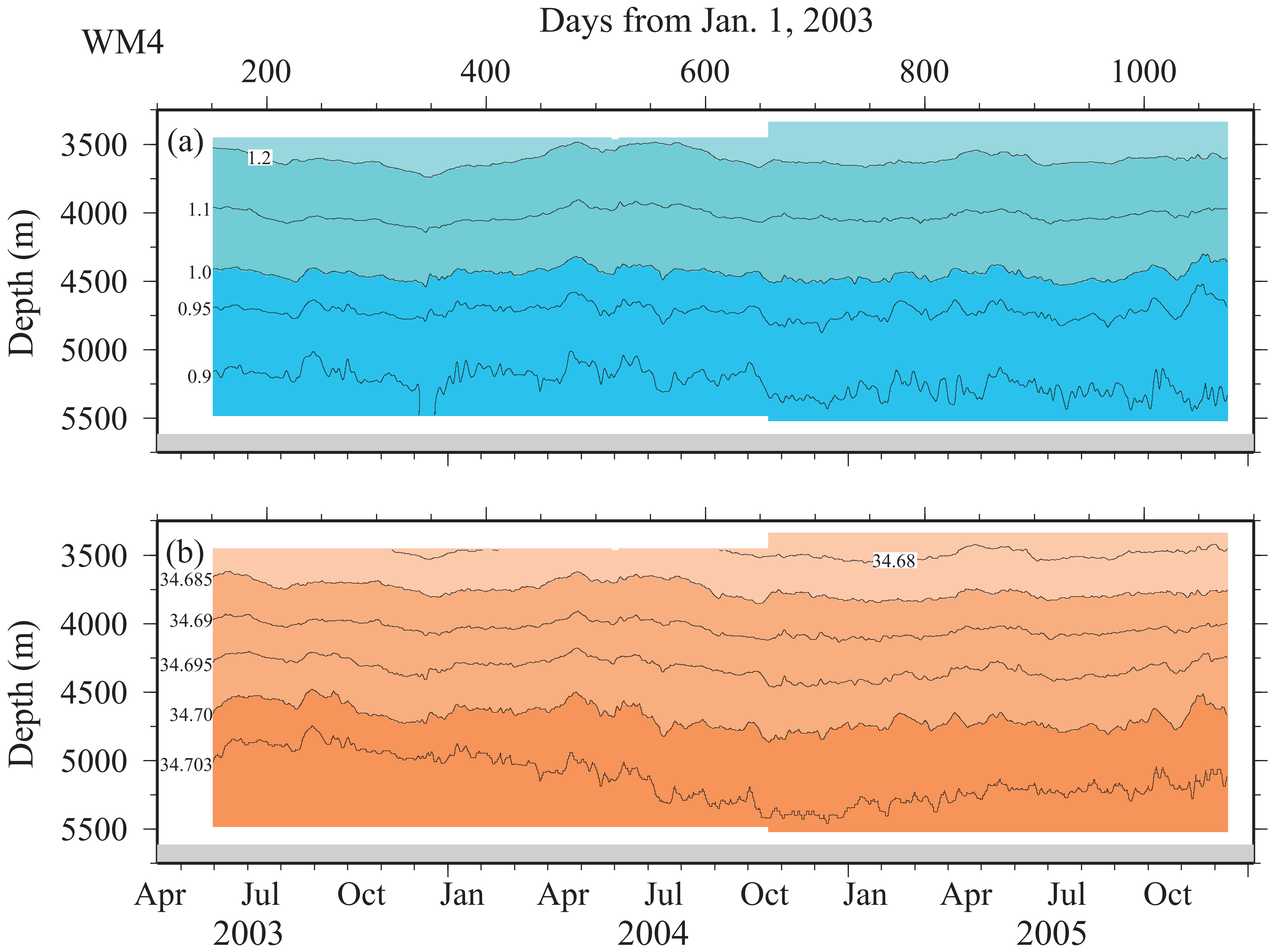

Figure 15
Continued (WM5)

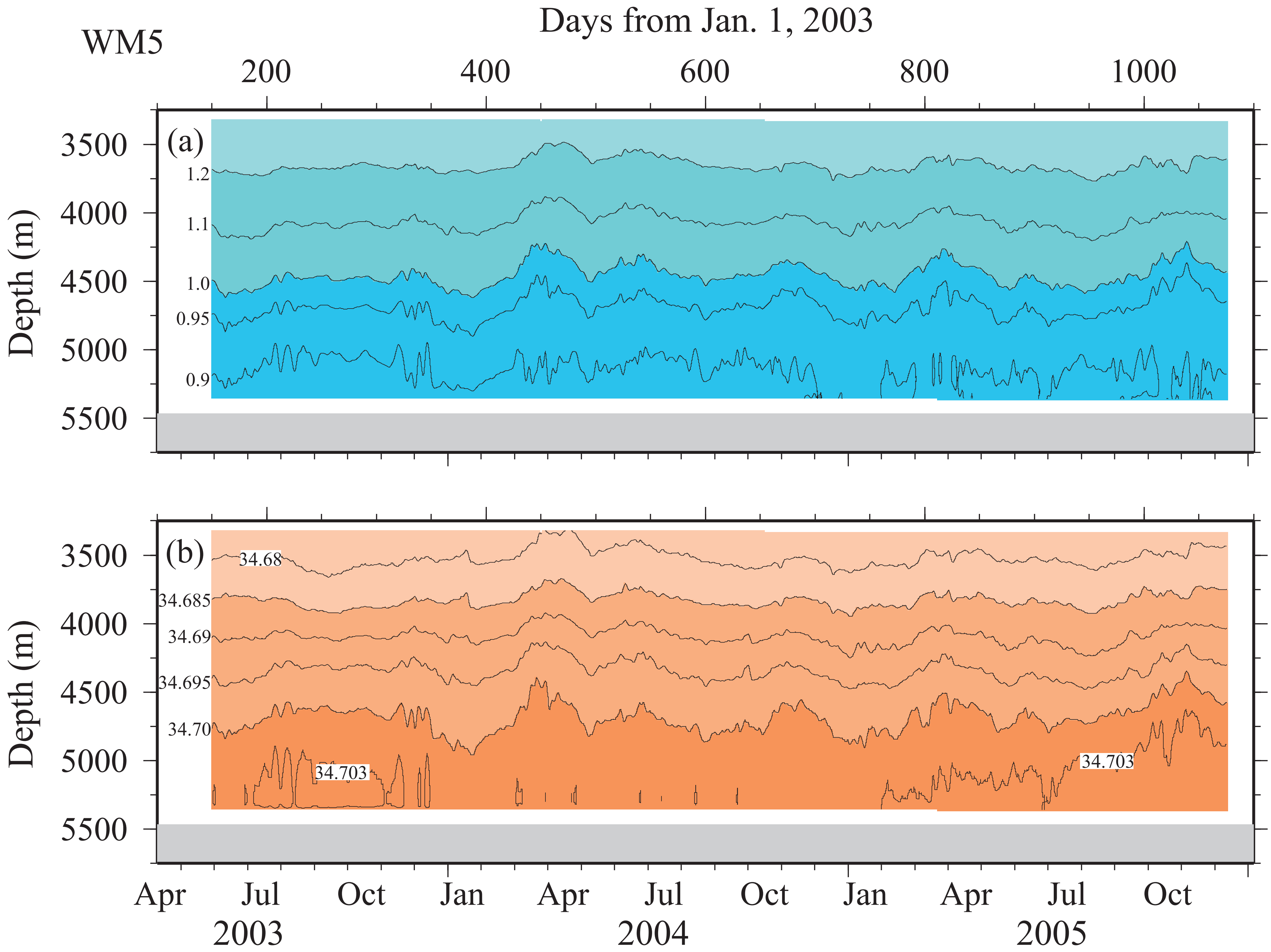

Figure 16

Daily mean velocity anomary components (cm s^{-1}) (a) along and (b) normal to the line at 3600 dbar

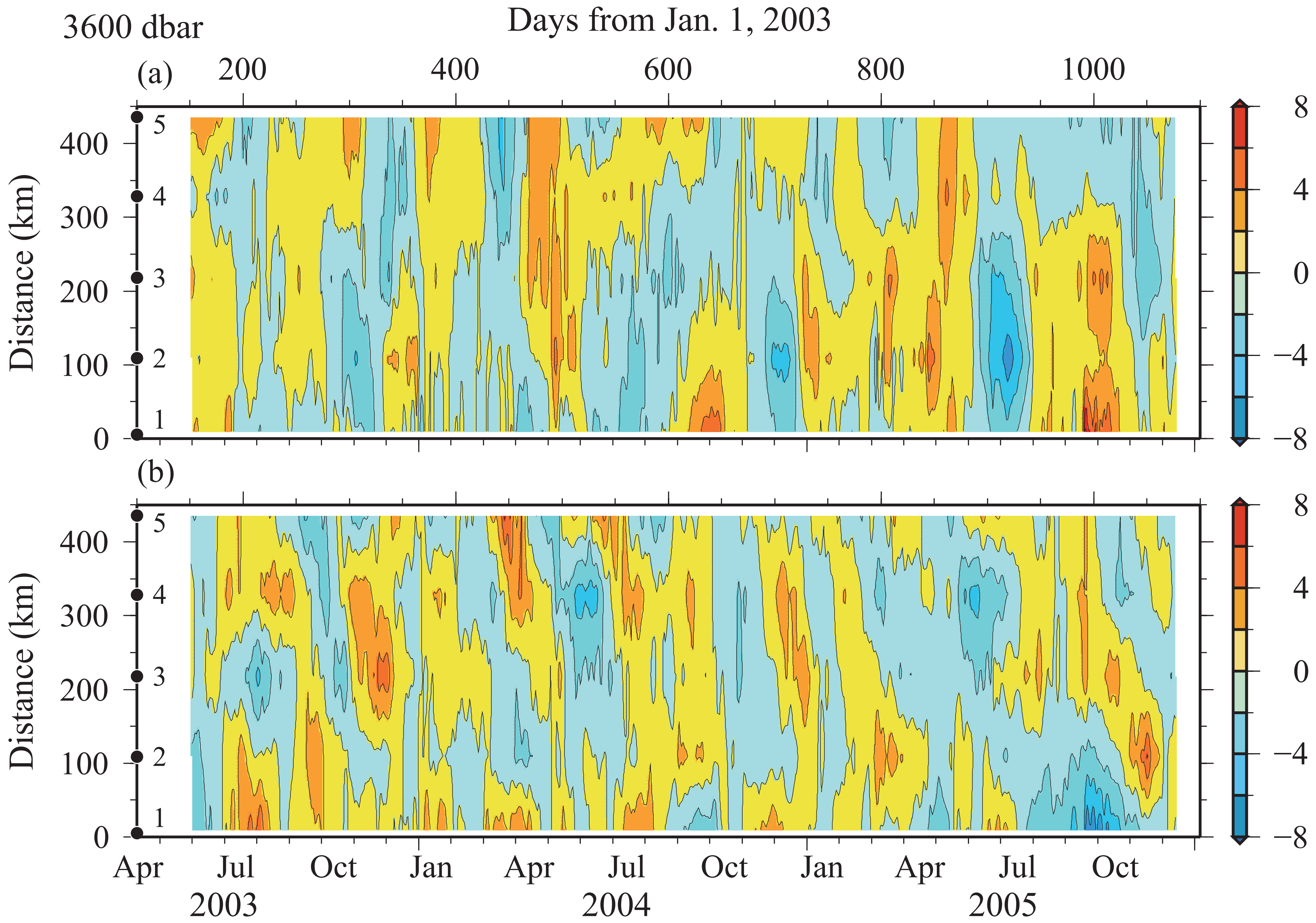

Figure 16
Continued (4400 dbar)

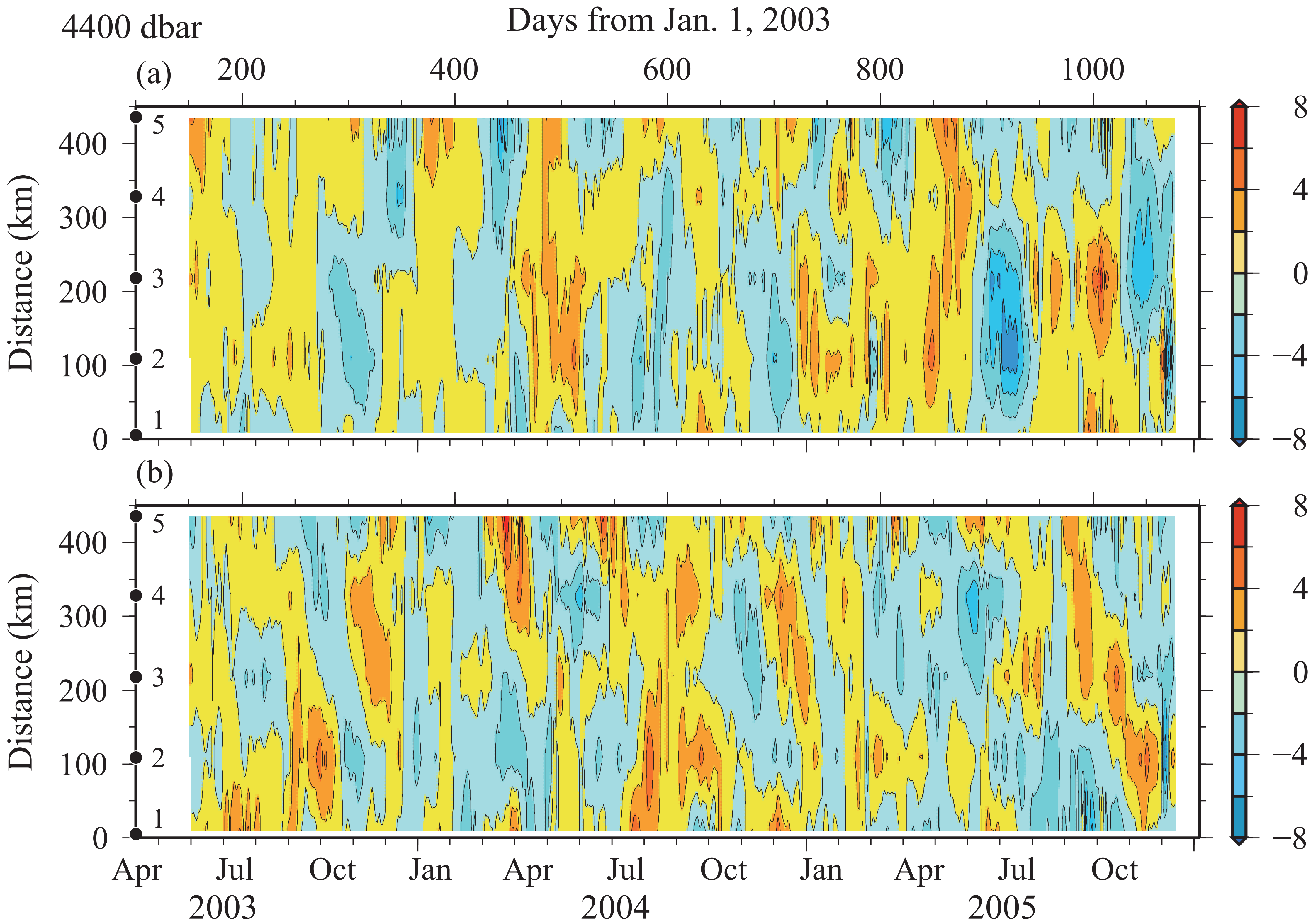

Figure 16
Continued (5300 dbar)

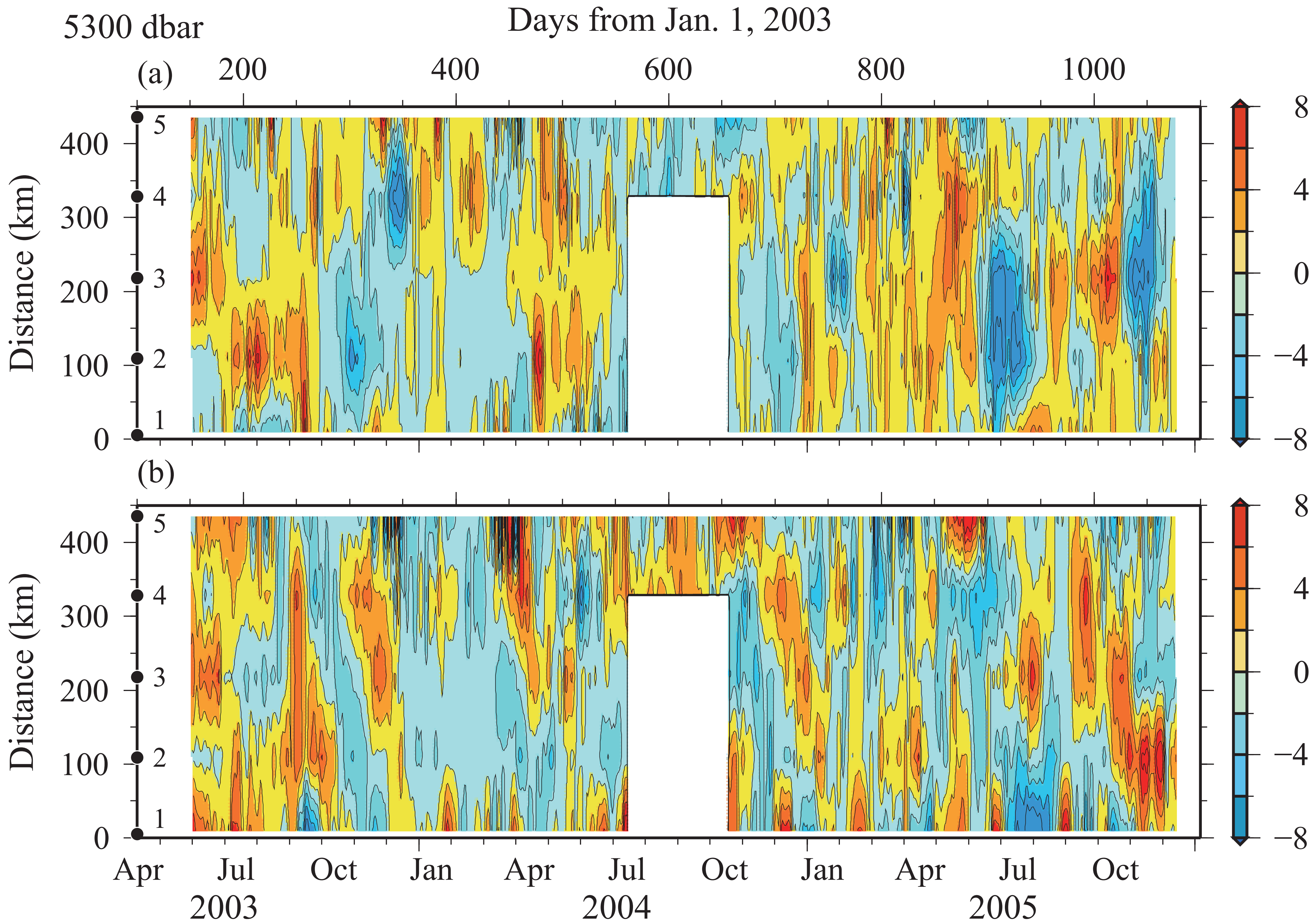

Figure 17
Daily mean (a) potential temperature (°C) and (b) salinity anomaries at 3600 dbar

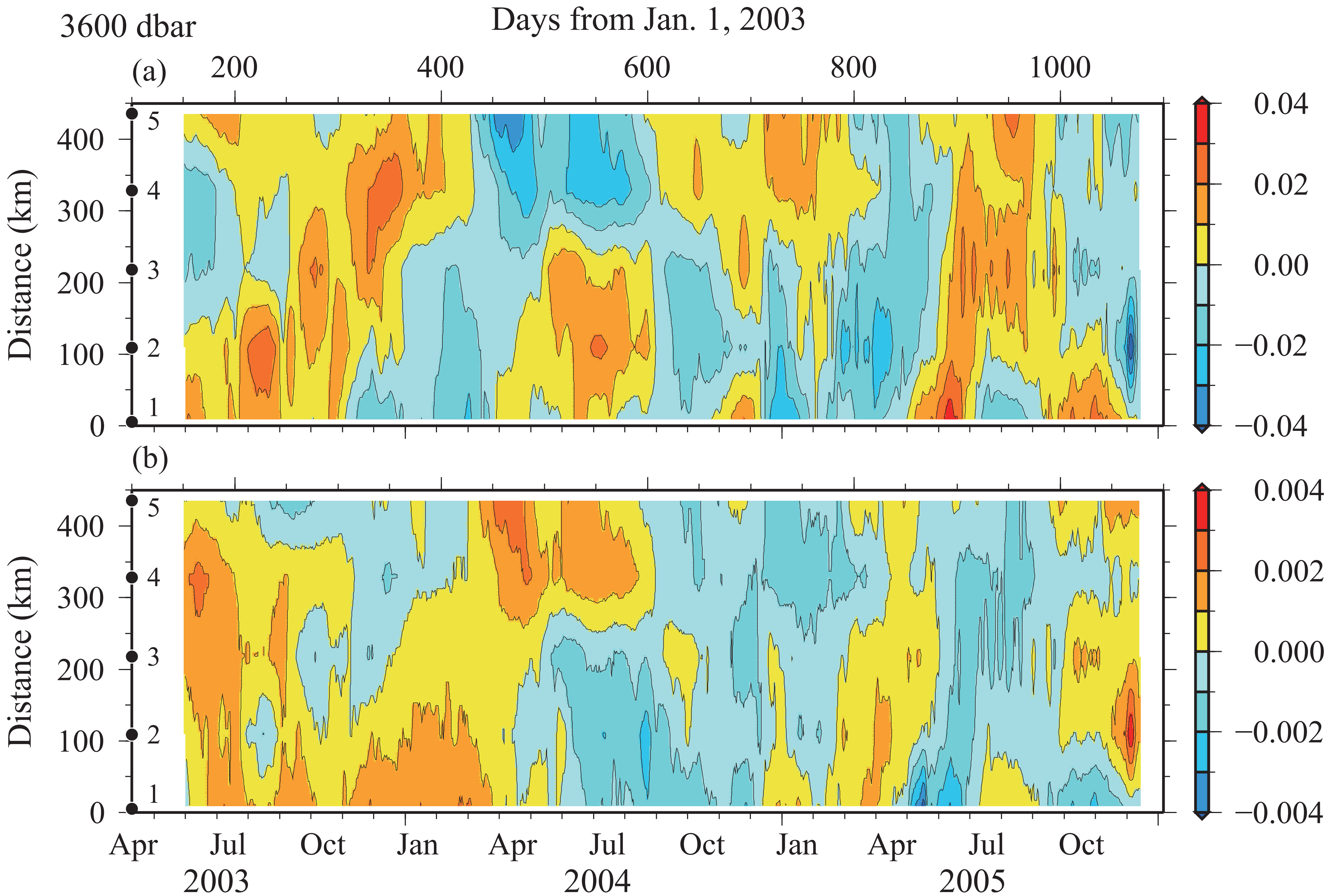

Figure 17
Continued (4400 dbar)

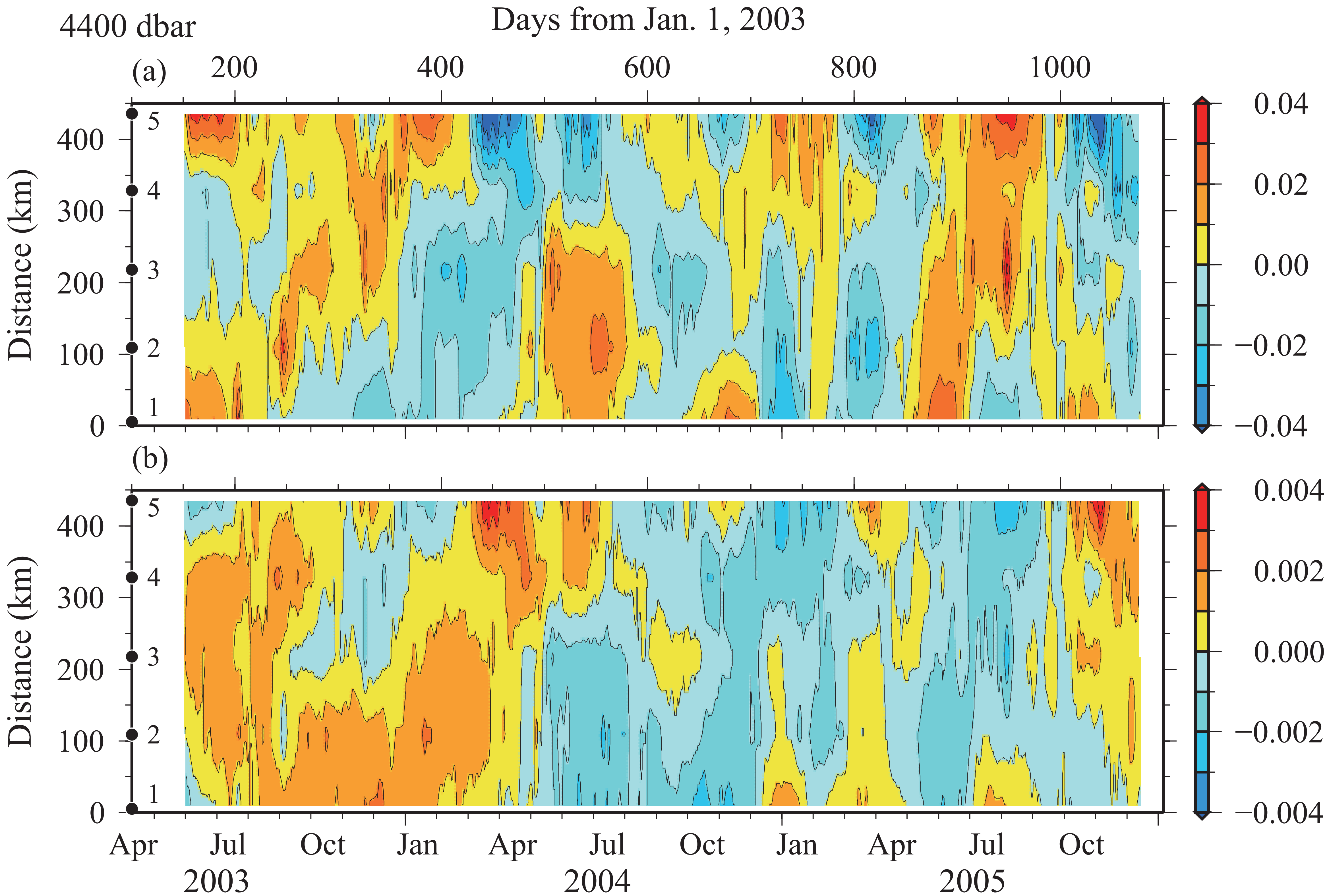

Figure 17
Continued (5300 dbar)

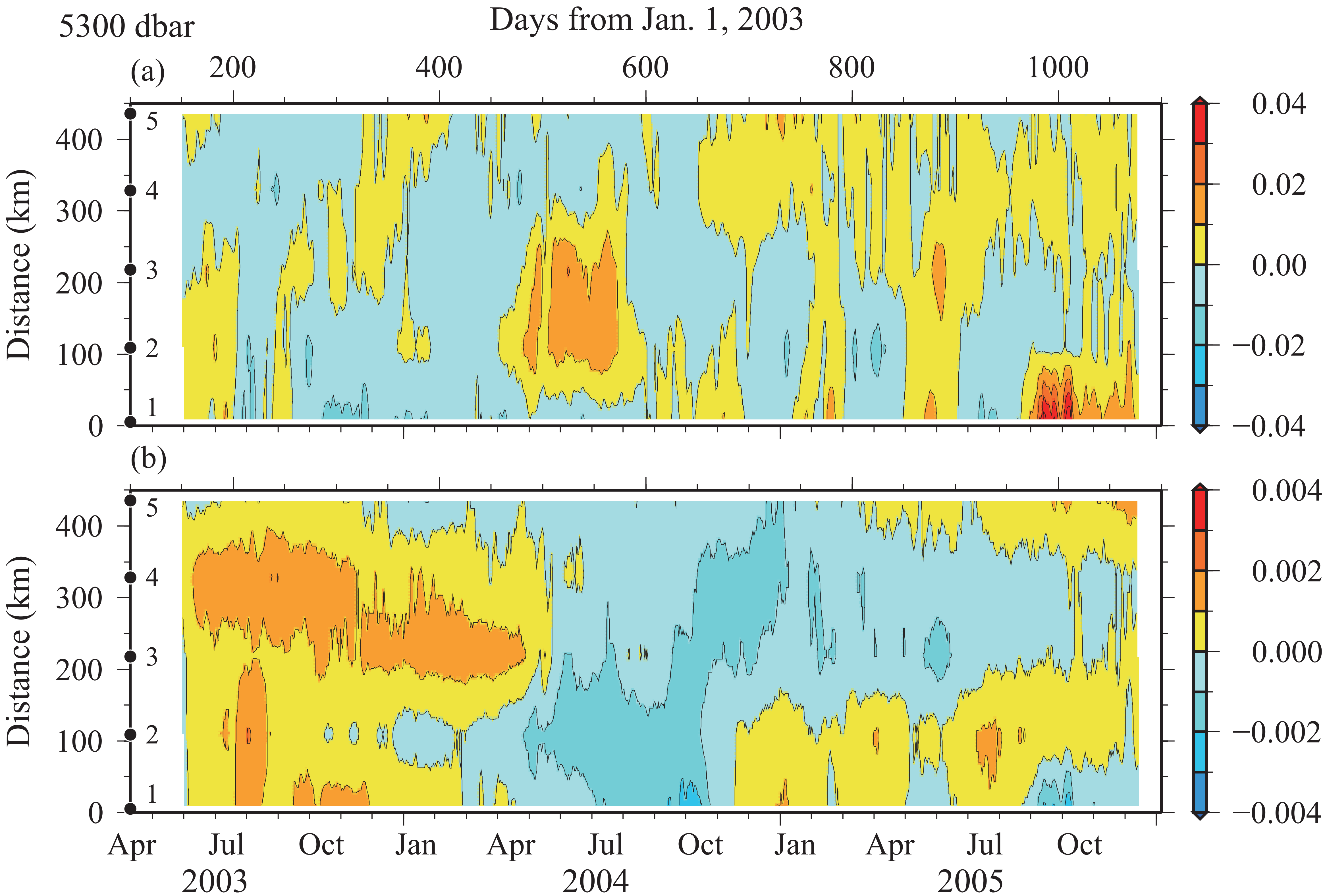

Figure 18
Mean velocity vectors

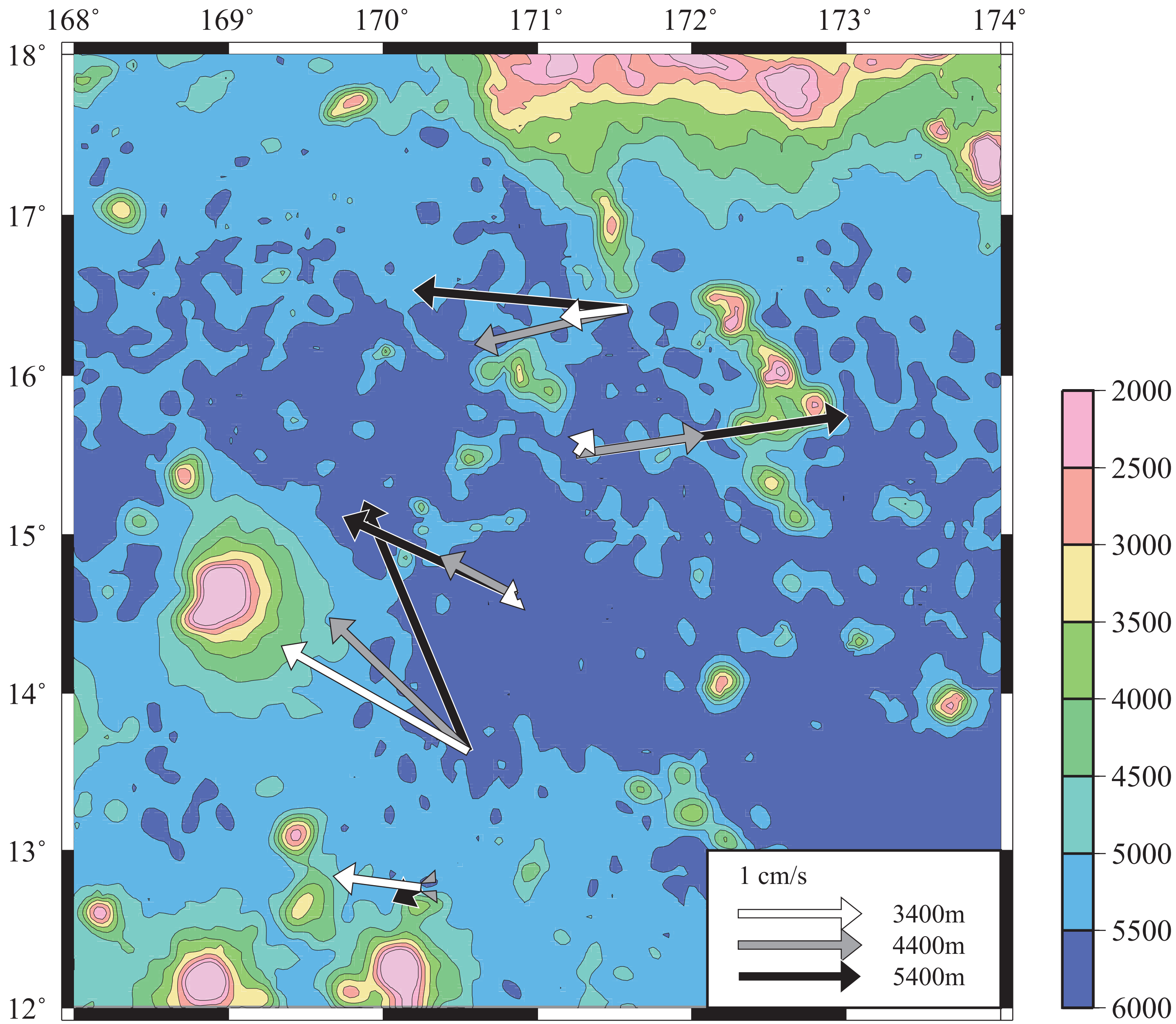

Figure 19
Mean and SD of velocity component along (U) and normal (V) to the line

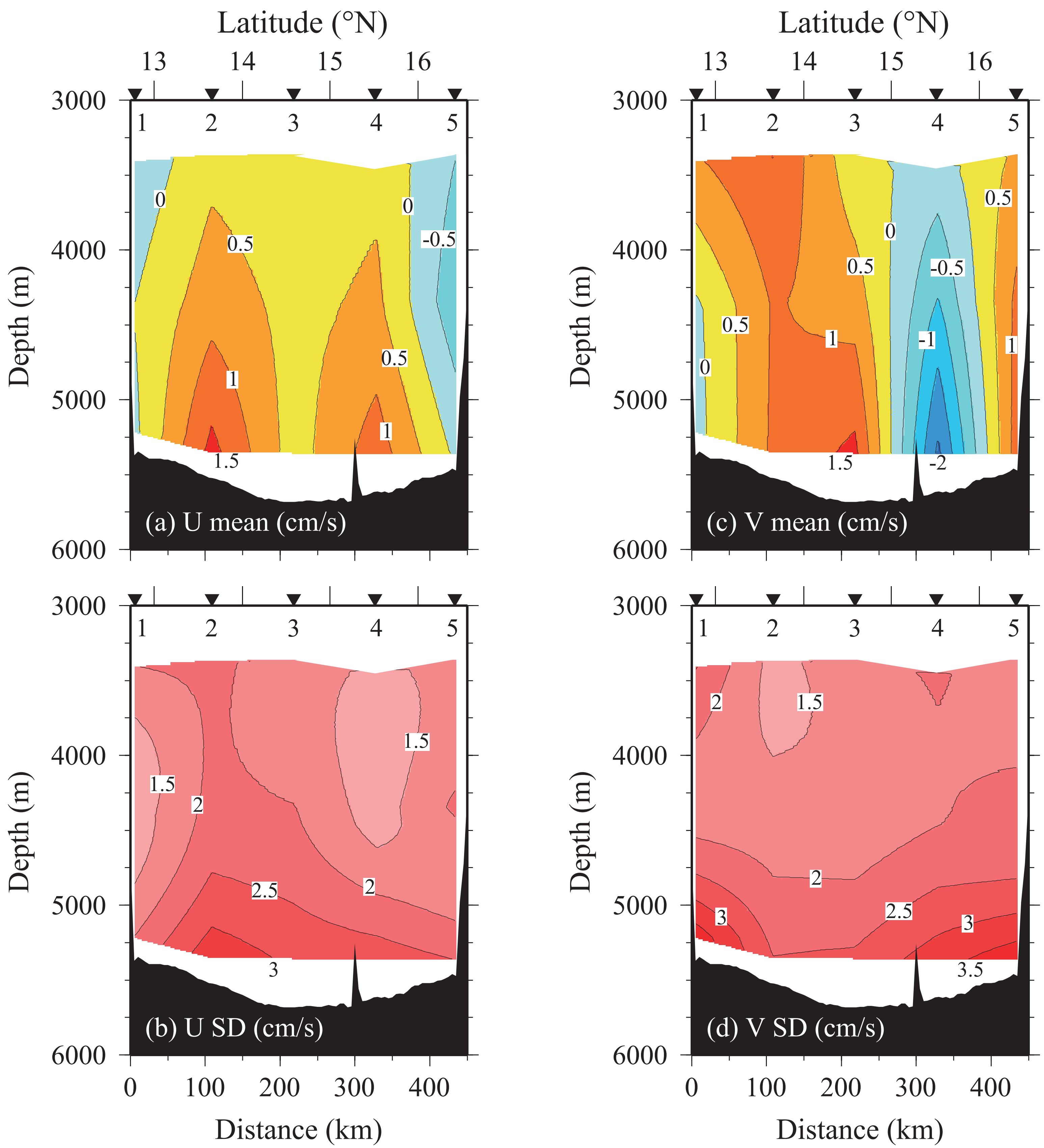

Figure 20
Mean and SD of potential temperature (°C) and salinity